UNIVERSITAT ROVIRA I VIRGILI

CATALYSER PRODUCTION WITH MICROSTRUCTURED COMPONENTS
Diana Cristina Dubert

Dipòsit Legal: T. 272-2012

ADVERTIMENT. L'accés als continguts d'aquesta tesi doctoral i la seva utilització ha de respectar els drets de la persona autora. Pot ser utilitzada per a consulta o estudi personal, així com en activitats o materials d'investigació i docència en els termes establerts a l'art. 32 del Text Refós de la Llei de Propietat Intel·lectual (RDL 1/1996). Per altres utilitzacions es requereix l'autorització prèvia i expressa de la persona autora. En qualsevol cas, en la utilització dels seus continguts caldrà indicar de forma clara el nom i cognoms de la persona autora i el títol de la tesi doctoral. No s'autoritza la seva reproducció o altres formes d'explotació efectuades amb finalitats de lucre ni la seva comunicació pública des d'un lloc aliè al servei TDX. Tampoc s'autoritza la presentació del seu contingut en una finestra o marc aliè a TDX (framing). Aquesta reserva de drets afecta tant als continguts de la tesi com als seus resums i índexs.

ADVERTENCIA. El acceso al contenido de esta tesis doctoral y su utilización ha de respetar los derechos de la persona autora. Puede ser utilizada para la consulta o estudio personal, así como en actividades o materiales de investigación y docencia en los términos establecidos en el art. 32 del Texto refundido de la Ley de Propiedad Intelectual (RDL 1/1996). Para otras utilizaciones se requiere la autorización previa y expresa de la persona autora. En cualquier caso, en la utilización de sus contenidos habrá que indicar de forma clara el nombre y apellidos de la persona autora y el título de la tesis doctoral. No se autoriza su reproducción u otras formas de explotación efectuadas con finalidades de lucro ni su comunicación pública desde un sitio ajeno al servicio TDX. Tampoco se autoriza la presentación de su contenido en una ventana o marco ajeno a TDX (framing). Esta reserva de derechos afecta tanto a los contenidos de la tesis como a sus resúmenes o índices.

Diana Cristina Dubert

CATALYSER PRODUCTION WITH MICROSTRUCTURED COMPONENTS

DOCTORAL THESIS

Supervised by Prof. Dr. Ricard Garcia-Valls

Department of Chemical Engineering

UNIVERSITAT ROVIRA I VIRGILI
Tarragona
2011

I, Prof. Dr. **Ricard Garcia-Valls**, Director of the Technical School of Chemical Engineering (ETSEQ), Director of METEOR - a member of the network of innovation centres of the Catalan Regional Government (XIT)

CERTIFY:

That the present work entitled "Catalyser production with microstructured components", presented by Diana Cristina Dubert to obtain the degree of doctor by the University Rovira i Virgili, has been carried out under my supervision at the Chemical Engineering Department, and that it fulfils the requirements to obtain the Doctor European Mention.

Tarragona, …………… of …………

Dr. Ricard Garcia-Valls

Acknowledgments

I would like to thank my supervisor, Dr. Ricard Garcia-Valls, for all the support and trust that he gave me during these three years of working together. His way of supervising gave me the opportunity to see and to live the meaning of the research environment and for that I appreciate him very much. I would like to thank all my lab mates: Brisa Peña, Cinta Panisello and not last, Hany Hassan for being there for me for better and for worst.

Special thanks for Pepa, without her I would have had a lot of unknown parts of my administrative, ISO and environment doctorate program.

I would like to thank Rovira I Virgili University, IMPULSE (Integrated Multiscale Process Units with Locally Structured Elements) project with the support of European Commission DG Research for financial support. Greetings for research support units in ICIQ: Eduardo Escudero (X-ray diffraction), Susana Delgado (Thermal Analysis) and special acknowledgements for Dr. Francesc Gispert (X-ray diffraction, Thermogravimetric analyses - Servei de Recursos Científics i Tècnics (Universitat Rovira i Virgili) for his guidance through these techniques and advices for their appliance. Also, many thanks for the Microscopy unit from Servei de Recursos Científics i Tècnics (Universitat Rovira i Virgili) for helping me understand the interesting substance morphology. Thank you for your patience.

I would also like to thank my personal friends from all over the world: thank you for all the good moments. To my Romanian flat mates who have made the life in Tarragona pleasant and friendly.

Finally, but not least, I would like to thank my parents that supported me in the best way they could to go on with my carrier and my brother and his fiancé, for beautiful time spent together.

Diana Cristina Dubert,

Tarragona, 19.12.2011

List of abbreviations

$NH_4Al(OH)_2CO_3$	Ammonium aluminum carbonate hydroxide (ammonium dawsonite),
UV/VIS	Ultraviolet/Visible Spectroscopy
IR	Infrared Spectroscopy
NMR	Nuclear Magnetic Resonance Spectroscopy
MS	Mass Spectroscopy
LIGA process	Lithography, Electroplating, Molding Process
IMM	Institute of Microtechnology from Mainz, Germany
Re	Reynolds number
e.g.	(exempli gratia) for example
SIMM	Slit Interdigital Micromixe
HPIMM	High Pressure Micromixer
SIMHEX	Heat exchanger
CPMM	Caterpillar Split-Recombine Micromixer
HPLC	High Performance Liquid-Chromatography
l/l	Liquid/Liquid
g/l	Gas/Liquid
m, mm	Meter, millimeter
cm	Centimeter
mL	Milliliter
HCl	Chloride Acid
NaOH	Sodium Hydroxide
rpm	Revolution per minute
t_r	Average residence time
t_m	Diffusive mixing time

s	second
et al.	(*et alia*) and others
l, µl	litter, micro-litter
$\vec{u}$	velocity vector
p	pressure
ρ	mass density
ν	kinematic viscosity
c	local concentration
D	diffusion constant
MEMS	micro-electro-mechanical systems
$\vec{V}$	velocity field
$\overrightarrow{F_e}$, $\vec{E}$	electrical field
q	density of the free electrical charges
T	temperature
MEMS	Micro-Electro-Mechanical Systems
PDI	polydispersity index
PDMS	polydimethylsiloxane
$Al(OH)_3$	aluminum hydroxide (alumina hydrated)
CaO	calcium oxide (carbonate of lime)
$NaAl(OH)_2CO_3$	sodium dawsonite (sodium aluminum carbonate hydroxide)
$CO3^{2-}$	carbonate ions
Al	aluminum
Na	sodium
$AM(CO3)x(OH)y$	hydroxyl carbonate based compounds
$NH4^+$	ammonium ions
Mg^{2+}, Ca^{2+}, Ba^{2+}	magnesium, calcium, barium ions
Ni^{2+} ,Cu^{2+}	nickel, copper ions
XRD	X-ray Diffraction Technique
TGA	Thermo-Gravimetric Analysis
SEM	Scanning Electron Microscopy
TEM	Transition Electron Microscopy
M	molar concentration
K	Kelvin

h	hour
λ	wavelength
ml/min	milliliter per minute
µl/s	micro-liter per second
α-Al_2O_3	alpha alumina
SAR	split and recombine
Pa mm^{-1}	Pascal per millimeter
BET	Brunauer, Emmett, and Teller theory
$Al(NO_3)_3x9H_2O$	Aluminum Nitrate Nonahydrated
$(NH_4)_2CO_3$	Ammonium Carbonate
L_{vol}	volume-weighted size
B	Bragg angle
k	unit cell geometry dependent constant (0.85; 0.99)
$B_{½}$	full-width-half-max of the peak
B_{obs}	measured peak width
B_m	peak broadening due to the machine
ca.	approximately
V_{pore}	pore volume (cm^3g^{-1})
V_{micro}	volume of micropores (cm^3g^{-1})
S_{meso}	mesopores area (m^2g^{-1})
S_{BET}	specific surface area (Brunauer, Emmett, and Teller area)
PMMA	Poly(methyl methacrylate)
Pd	Palladium
TR-FTIR	Time resolved Fourier transform Infrared Spectroscopy
PDMS	poly (dimethylsiloxane)
ILDP	In-Line dispersion-precipitation
ICIQ	Institut Català d´Investigació Química

Table of contents

Chapter 1: Introduction 1

Chapter 2: NH_4-Dawsonite production within a caterpillar microreactor 39

Chapter 3: Continuous synthesis of ammonium dawsonite within a new microstructured system 57

Chapter 4: Influence of pressure over ammonium dawsonite continuous precipitation at microscale 77

Chapter 5: Influence of imperfect mixing on NH_4-dawsonite particles formation within new types of micromixers 97

Chapter 6: Summary and Outlook 123

Chapter 1

Introduction

This chapter describes a brief introduction regarding microreactor´s technology and its importance in developing safer, cleaner and environmentally friendlier processes. In recent years, their most important characteristics and applications were implemented in the chemical, biochemical or pharmaceutical industry. Based on the microtechnology advantages discovered in last decades a novel application of the microscale processes, dealing with solids production in catalysis field, is presented. Ammonium dawsonite ($NH_4Al(OH)_2CO_3$) was selected as solid product with application in catalysis industry. Further the characteristics of this mineral have been correlated with its different type of synthesis (both conventional and new approaches). The importance of this mineral on industrial field and the need of developing new processes for its synthesis are lettered in the section “Aim of the thesis”.

Chapter 1

Introduction

1. Microreactor technology

Majority of organic and inorganic reactions depend on different physical/chemical factors that determine the outcome of the transformation needed. Based on this, searching for optimal reaction conditions to achieve a particular transformation is time consuming, requires great efforts and large amount of valuable raw materials. Theoretically, the optimization of the process conditions in an efficient and rapid manner has a major impact on pharmaceutical and chemical engineering industry development. Practically though, the complexity of systems used often requires a complete redesign of the synthesis to allow for scale-up. To overcome this drawback new technologies are desired. Microtechnology, based on micro-fluidic devices (microreactors) gain an important interest in applied industry worldwide because of its great advantages compare to conventional technologies. Micrometers range devices are capable of performing a range of single or multi-phase reactions and are able to amenable to automation of reaction optimization[1]. The common benefits of this micrometer scale technology: small quantities of reagent needed, precise control of the reaction variable: flow rate, mixing, reaction time and heat and mass transfer, easy scalable and able to integrated different monitoring devices (UV/VIS, IR, NMR, Mass Spectrometry (MS))[1] will modify significantly the industrial production approach.

1.1 Microreactors – state of the art

A micro-fluidic device (microreactor) is a chemical engineering unit process device that is designed on the micrometer scale. Also, they are defined as miniaturized reaction systems composed of microstructures or channels which are the smallest units of miniaturized continuous flow, elements which can be single or multiple flow channel configuration of a distinct geometric nature, units which are a combination between an element concentrating fluid lines and supporting base material, devices which are units embedded either in a housing or between two end caps, system represents an integration of units in one housing[2] (See Fig. 1.1). Ehrfeld et al. 2000 classify the microreactors by: function of application in analysis: - biochemistry and biology; - chemistry and chemical engineering, and by: function of operation mode: - continuous flow; - batch type. Their book review also the fundamental advantages of these microdevices divided in five categories. First category includes the advantages of miniaturization of analysis systems which was proved to need less space, material and energy, to have shorter response time, the cost could be kept low and it enhance the system performance.

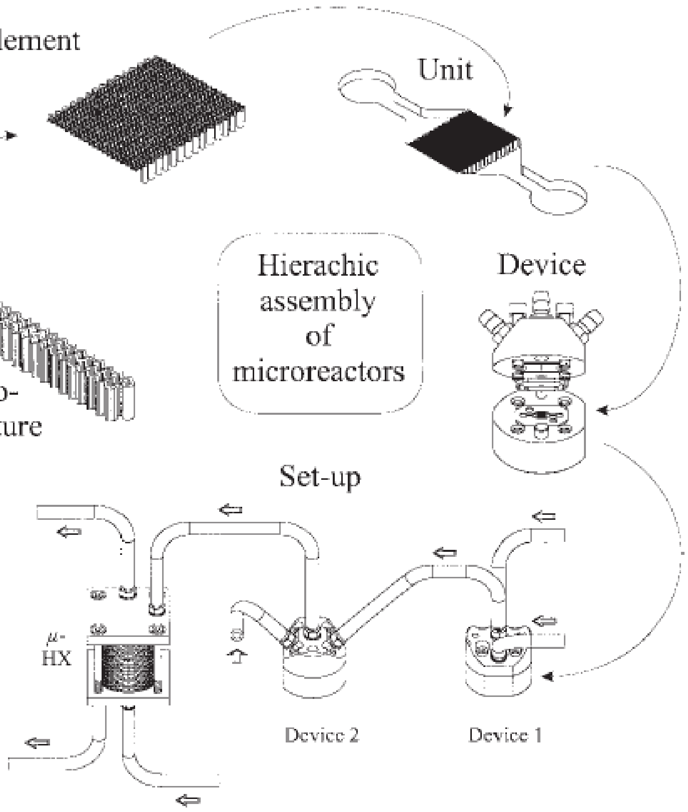

Fig. 1.1: Hierarchical assembly of microreactors, as evidenced for micromixer components. Source*: Ehrfeld et al. 2000.*

The second category represents the nano-scale reactors advantages which deals with supramolecular assembly reaction unit (e.g. molecular tweezers, zeolites, micelles, liposome and Langmuir-Blodgett thin films), interaction by means of molecular forces and modify the electronic structure of reactant (e.g. steric interaction), are changing chemistry in an active mode and influence transport properties. The advantages of microreactors due to decrease of physical size form the third category and describes the main impact focuses on intensifying mass and heat transport, also improving flow patterns, decreasing the linear dimensions increases properties such as temperature, concentration, density, pressure, also driving force for heat and mass transfer/transport or diffusion flux /volume unit or area unit. Other fundamental advantages of microreactors technology are referring to the increased number of units that gives a complex knowledge on scaling-up systems for industry application and lower cost and size of the plant design. The most important of these categories is taking of the numbering-up approach which lately increased the interest worldwide for its simplicity, less expensive reproduction and assembly (See Fig. 1.2).

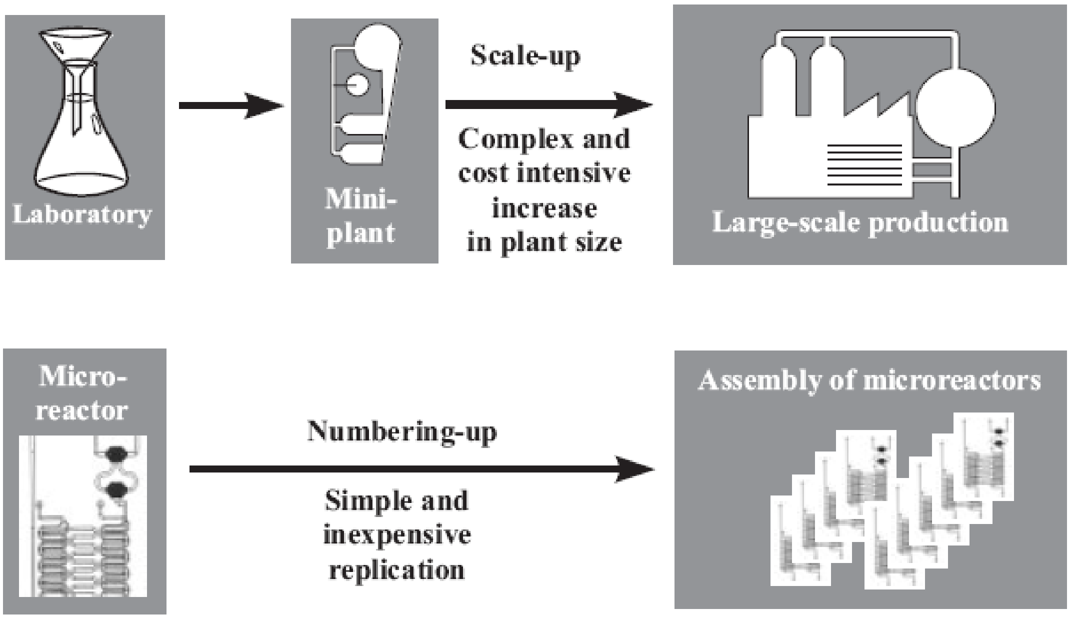

Fig. 1.2: Simplified scheme illustrating scale-up versus numbering-up strategies. Source: Ehrfeld et al. 2000.

The potential benefits of microreactors application are also presented: fast transfer of research results into production, earlier start of production at lower costs, earlier scale-up of production capacity, smaller plant size for distributed production , lower costs for transportation, materials and energy and more flexible response to market demands[2].

1.1.1. Microreactors – fabrication technique

The microreactor technology has increased in the last few decades and for this reason suitable fabrication techniques had to be developed. The most used techniques in the microtechnology field are described as: bulk micromachining of microcrystalline materials, dry etching processes using pressure plasma or ion beams, combination of deep lithography, electroforming and molding micromachining with laser radiation – LIGA process, micromolding, wet chemical etching of glass including anisotropic etching of photosensitive glass, advance mechanical milling, turning, sawing, embossing, punching and drilling processes based on precision engineering, isotropic wet chemical etching, micro electro discharge machining and laser ablation[2,3]. One of the most used techniques to produce mixers (microreactors) represents LIGA process which is based on X-ray microfabrication and electroplating and was adapted and optimized for fabrication of mixer slit plates for micro reactors. For X-ray microfabrication was used a low-cost X-ray mask based on graphite membrane and for electroplating was used Ni-Fe alloy. In comparison with conventionally used agitators, micro-mixers allow especially fast mixing as well as the generation of dispersions with very small drop sizes and especially narrow drop size distributions at a significantly lower energy input. A completely demountable micro-mixer based on the multilamination principle was developed and improved[3] (See Fig.1.3).

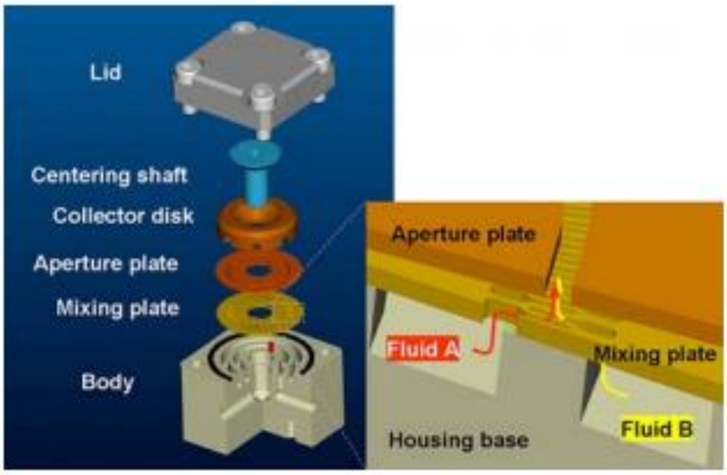

Fig. 1.3: Exploded assembly drawing of a mixer unit LH25 and detailed view of micro parts. Source: Bednarzik M et al. 2008.

Based on the same technique the Institute of Microtechnology from Mainz, Germany (IMM) created different type of micromixers applicable for all kind of processes becoming one of the greatest and known suppliers worldwide. Some of the commercial types of micromixers built are shown in Fig. 1.4. Microreactors made from a series of different materials have been described in the literature: stainless steel, etched silicon, glass, and others[1] which have advantages and limitations. Etched silicon for example, holds a great interest to the chemists because of its inert properties to almost all reagents, stable under a wide range of temperatures and pressures, and cab adapted to specific tasks such as: filled with catalyst in order to conduct heterogeneous reactions[1].

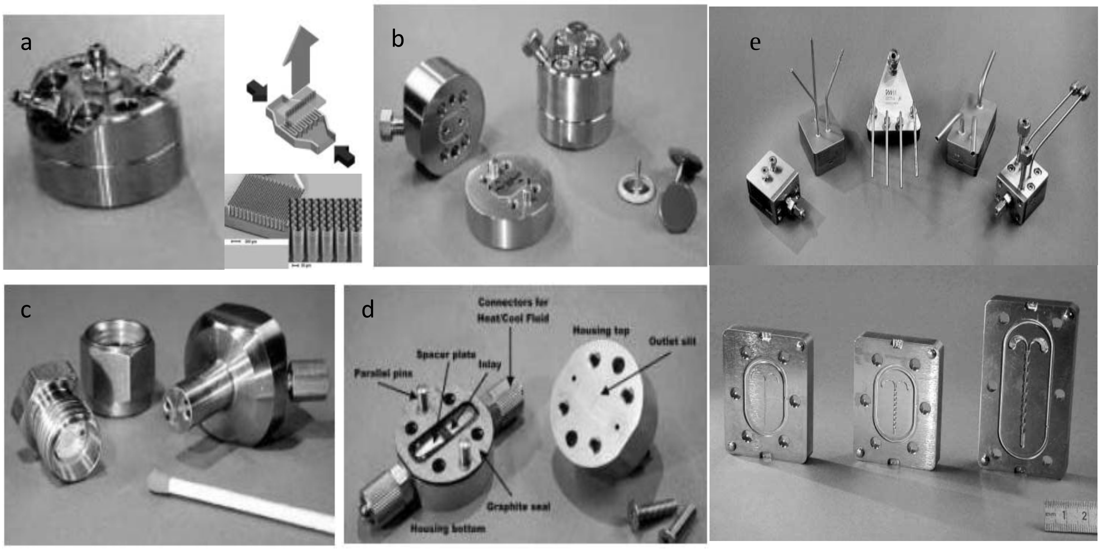

Fig. 1.4: Types of microreactors designed by IMM: a. **SSIMM class**: *combine the regular flow pattern created by multi-lamination with geometric focusing which speeds up liquid mixing - double-step mixing. b.* **SIMM-V2 class**: *mixing using multi-lamination and focusing only. c.* **HPIMM class**: *the mixer comprises expansion-free outlet channel geometry and was optimized using a metal sealing for tightening the two parts of the housing. d.* **SIMHEX class:** *was optimized considering a heat exchange function within the mixer, using graphite sealing for tightening the two parts of the housing. e.* **CPMM group class**: *called also, Caterpillar micromixers, are particularly suitable for applications where fast mixing at higher throughput is desired. Are based on split –and-recombine mixing principle; standard version 1.2 of the Caterpillar Micro Mixers is provided with welded-in tubing or HPLC-connectors enabling 50 – 100 bar system pressure for l/l-mixing or for g/l-, l/ldispersing. Operation temperatures are limited through the used gasket materials to -40 – +220°C but can be extended by use of graphite gaskets to 500°C.*Source*:http://www.imm-mainz.de/fileadmin/upload_daten/Flyerbroschueren/IMM_TheCatalogue09_low.pdf*

A tangible effect of this small dimension is that fluid properties become increasingly controlled by viscous forces rather than inertia. Reducing the dimensions of the microfluidic system leads to a large surface-to-volume ratio which increases heat and mass transfer efficiencies. With dimensions reduced, viscous forces dominate the flow and Reynolds number, *Re*, decreases with the decrease of cross-sectional area of the channels[6] (inner surface areas of several tens of thousands m^{2}m^{-3})[1]. Microreactor technology already adopted as a new concept in chemical engineering has demonstrated the advantages over the conventional process[4,5] through improved surface-area-to-volume ratio which in a typical microreactor, this ratio is about 200 cm^2 cm^{-3} compared with 1 cm^2 cm^{-3} for a 100 mL glass flask and 0.06 cm^{2}cm^{-3} for a 1m^3 batch reactor[1], temperature control (See Fig.1.5) and progression of concentrations (See Fig.1.6), *i.e.*

by comparing a neutralization reaction (chloride acid (HCl) and sodium hydroxide (NaOH) in a 5 m^3 vessel (stirring 500 rpm) and in a microstructured surface[1] (See Fig.1.5 a, b). The experiment showed high heat exchanging rates in case of microcreator which permits exothermic reactions to be performed successfully. Moreover, mass transport is also improved in microreactors (See Fig.1.6)[1].

1.1.2. Microreactors – mixing

Mixing in microfluidic systems is governed by molecular diffusion which generates contact surface between mixed materials (the concentration gradient being kept at high values) but also can effectively decrease concentration modifications in the system. The fluids involved in the micro-scale process are somehow deformed with a rate of deformation which depends on the local rate of energy dissipation, the orientation of a contact surface in the local flow field, physical properties of mixed materials, and scaling of microfluidic devices[6].

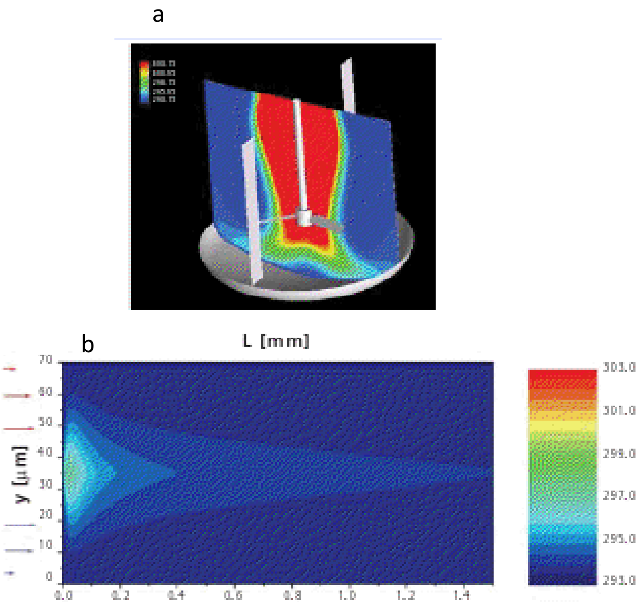

Fig.1.5: a. Batch Synthesis: Levels of temperature ranging from 293.15 K (blue) to 303.15 K (red) according to the color scale top left. b. Figure 2 (b): Microreactor Technology: HCl (red arrows on the left); NaOH (blue arrows on the left). Local temperatures are given according to the scale (right) in K (y represents the cell thickness; L represents the channel length). Source: www.sigma-aldrich.com/chemical synthesis. Source: www.sigma-aldrich.com/chemical synthesis.

Starting with the present microreactor´s classification in the literature[2], some researchers adopted a new terminology for microfluidic devices based on the type of mixing involved, such as active and passive micromixers[6]. Each type develops specific mixing, capacity, mixing speed, and operating conditions which lead at two step mixing process characterized by heterogeneous mixing (by convection) and homogeneous one (by diffusion) at the molecular level[6].

An example of mixing which occur through diffusion between laminar flow layers is visualized in Figure 1.6 for the same neutralization reaction (Fig. 1.5)[1].

Elmabru et al. 2008 suggested that diffusive mixing efficiencies are calculated by using the Fourier number (defined as t_r/t_m, where t_r is the average residence time and t_m is the diffusive mixing time) and furthermore, demonstrated that time of mixing increases directly with the dimensions of the reactor. However, fast reactions with two or more reagents involved are hardly characterized by irregular mixing throughout the whole volume. The reaction rate, in present case, cannot be characterized by kinetics but by diffusion rates[6]. Further, the relationship between reaction and mixing rates is restricted to chemical, diffusional, and mixed chemical/diffusional regimes.

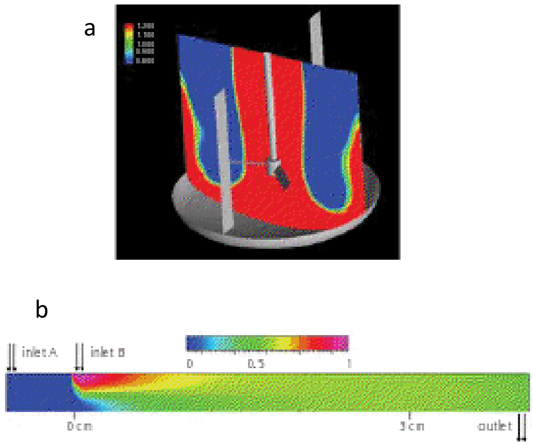

Fig.1.6: a. Batch Synthesis: Concentration equivalents (ranging from 0.8 (blue) to 1.2 (red) according to the color scale top left. b. Microreactor Technology: Compound B is injected (inlet) to a flow of compound A (blue). The green color indicates the 1:1 mixture. Source: www.sigma-aldrich.com/chemical *synthesis.*

Each of these regimes are characterized as follows: chemical regime presents enhanced mixing comparing with the reaction rate generating less amount of product, in diffusional regime, reaction is fast and the rate is limited by the mixing speed which will generate the production of secondary product, and in the mixed regime, both above situations are involved, the product is generated base on interaction between chemical reaction (reaction rate) and fluid dynamics (mixing degree)[6].

Regarding the specificity of mixing within a microdevice an empirical classification was presented in the literature, dividing the micromixers (microreactors) in active and passive types (See Fig. 1.7). The active mixer requires external forces (pneumatic or mechanical vibration) to improve the mixing efficiency but complex fabrication processes are used for their fabrication which makes it difficult to be integrated with other mixing components, whereas passive mixers have longer mixing length than active mixers, require no external force, easy to fabricate and incorporate with other fluidic components. By external perturbation the active mixers introduce vorticity into laminar flow by viscous forces, making it more stable with a Re equal with 1 or smaller. Two common ways of achieving active mixing are presented further: by using electrokinetics instabilities or ultrasonic vibration which can be generated from piezoelectric materials[6].

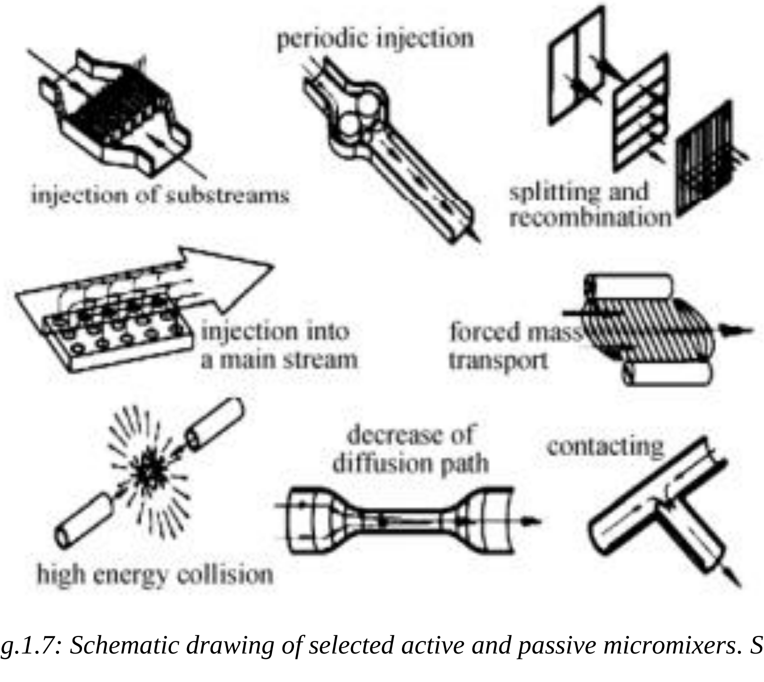

Fig.1.7: Schematic drawing of selected active and passive micromixers. Source: Elmabruk et al. 2008

Mixing in passive micromixers usually is induced by driving fluids through channels with cleaved geometries. For increasing the interfacial area and respectively the mixing quality repeated lamination and splitting of flows were introduced in microfluidic channels[6].

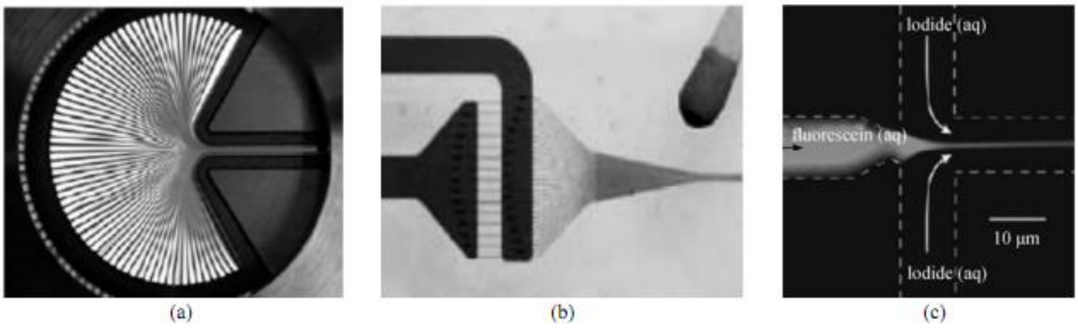

Fig.1.8: Passive mixers: multi-lamination micromixer (a) SuperFocus mixer; (b) Triangular interdigital micromixer;(c) Hydrodynamic focusing mixer. Source: Elmabruk et al. 2008.

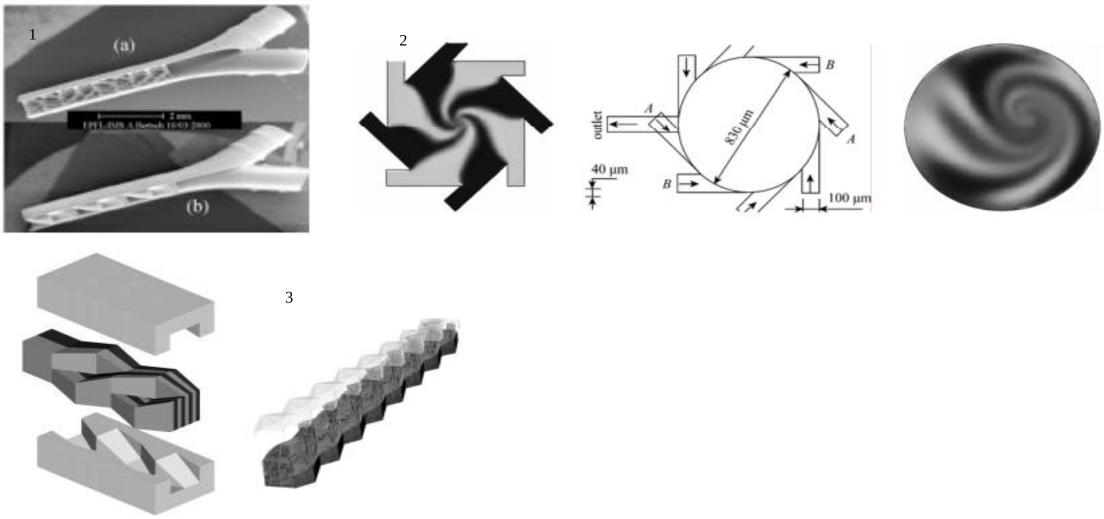

Fig.1.9: Passive mixers: (1) Split-recombine micromixers: Cut-out view of the micromixer structures built by microstereolithography: (a) Micromixer made of intersecting channels; (b) Micromixer made of helical elements; (2) circular micromixer; (3) Split-recombine micromixers – mixing principle shown for two of eight mixing steps (left)and simulated "real" flow profiles at high flow rates in caterpillar mixers (right). Source: Elmabruk et al. 2008.

Examples of passive and active micromixers are presented: multi-lamination micromixer, split-and-recombine micromixer and chaotic one (Fig.1.8, 1.9), periodic injection, forced mass transport or high energy collision micromixers (Fig.1.7), respectively.

Taking into account the information gathered all process parameters such as pressure, temperature, residence time, and flow rate are easily better controlled if the reactions that take place in small volumes. The exothermic or explosive reactions, the toxicity of the reagents can also be drastically reduced[1] inducing higher safety and more economical processes. Higher operating pressures can be used additionally.

The novelty of this level of technology is related to the flow phenomena and mixing characteristics in active and passive micromixers[6]. Further in this chapter are detailed the common factors that influence the mixing within a microfluidic device.

1.1.3. Microreactors (micromixers) – operating and design parameters effect of mixing quality

1.1.3.1. The effect of flow velocity

It was found that varying the flow velocity different stationary flow regimes can occur: laminar, vortex, and engulfment flow (See Fig.1.10)[6]. Therefore, at low Re numbers (0-150) which characterize the so called stratified and vortex regimes, the quality of the mixing still need greater improvement. Increasing considerably the Re number thus the high flow velocity, a new regime was determined, engulfment regime, which was demonstrated to greatly enhance the quality of the mixing[6].

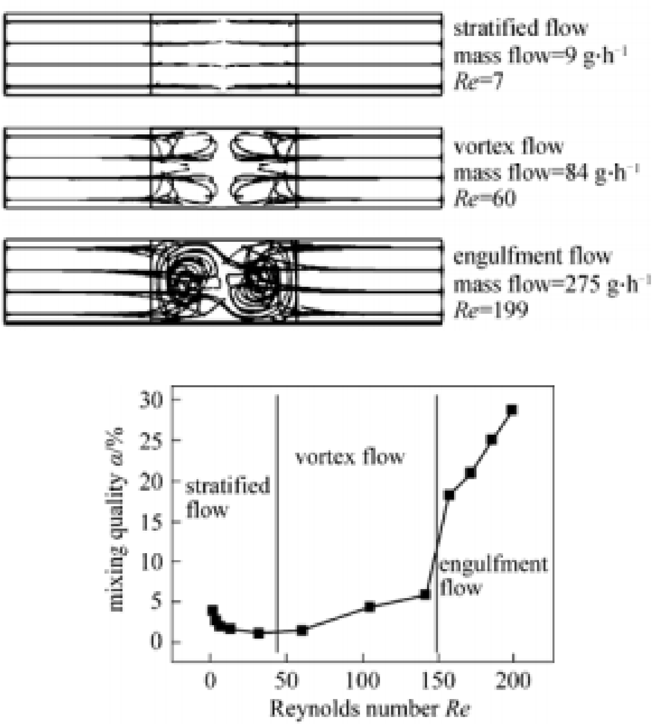

Fig.1.10: The three different stationary flow regimes inside a T-mixer. Elmabruk et al. 2008.

Another way to induce mixing in microfluidic channels is to varying the flow rates in the inlet channels periodically with time. Theoretically the low values of the flow rate induce smaller residence time within the mixing channel and higher mixing length respectively. As Fig. 1.11 shows, in practice, for low values of the flow rates the mixing starts in logger time and the liquid streams flow parallel to each other, thus increasing periodically the flow rates with time, the inlets streams are sent inside the channel by pulsation which was demonstrated to be more efficient if were combined with geometries that induce secondary flow (Fig. 1.12) and mixing was accomplished in less volume and time[6].

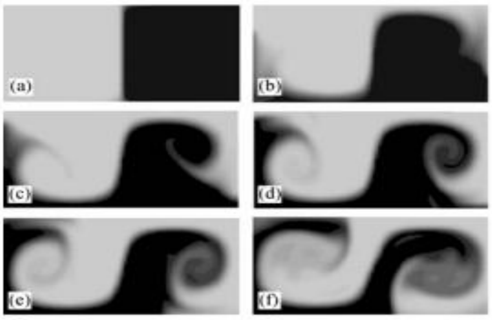

Fig.1.11: Tracer profiles on the cross section of the mixing channel 300 µm behind its entrance for mean velocities of (a) 0.9 m·s^{-1}, (b) 1.05 m·s^{-1}, (c) 1.1 m·s^{-1}, (d) 1.15 m·s^{-1},(e) 1.2 m·s^{-1} and (f) 1.4 m·s^{-1}. Elmabruk et al. 2008.

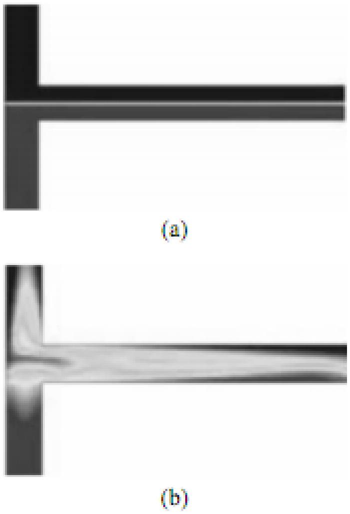

Fig.1.12: The effect of pulsing in mixing quality: (a) No pulsing nor ribs; (b) There is pulsing and ribs along the floor of the main channel. Source: Elmabruk et al. 2008

1.1.3.2. The effect of geometrical setup

Taking into account the flow velocity influence presented in section 1.1.3.1, viscous forces and pressure gradients govern the flow in microfluidic channels giving as result a laminar regime. Although, within this regime, if Re is in order of unity, secondary flow could be implemented and discontinuities in the entire fluid flow appear. Different geometry with additional obstacles such as a sharp bend slanted wall, or a junction can lead to discontinuity of fluid flow. When a liquid is sent over a sharp bend, the direction of the flow is changing and secondary flow is formed. This could be used to improve mixing performance in a micromixer where mixing is turbulence free[6]. Depending on this concept several numerical and experimental studies on mixing in different intersection geometries of microreactor´s channels (See Fig. 1.13) were carried out. For numerical study the fluids were considered Newtonian and incompressible, so the equations of motion are Navier-Stokes and continuity equations:

$$\frac{\partial \vec{u}}{\partial t} + \left(\vec{u} \cdot \Delta\right) \vec{u} = -\frac{1}{\rho} \Delta p + \nu \Delta^2 \vec{u} \tag{1}$$

$$\Delta \cdot \vec{u} = 0 \tag{2}$$

where $\vec{u}$, the velocity vector, p, the pressure, ρ, the mass density, and ν, the kinematic viscosity. For computing the concentration modification the diffusion-advection equation is used:

$\frac{\partial c}{\partial t} + \left(\vec{u} \cdot \Delta\right) c = D\Delta^2 c$, where c is the local concentration.

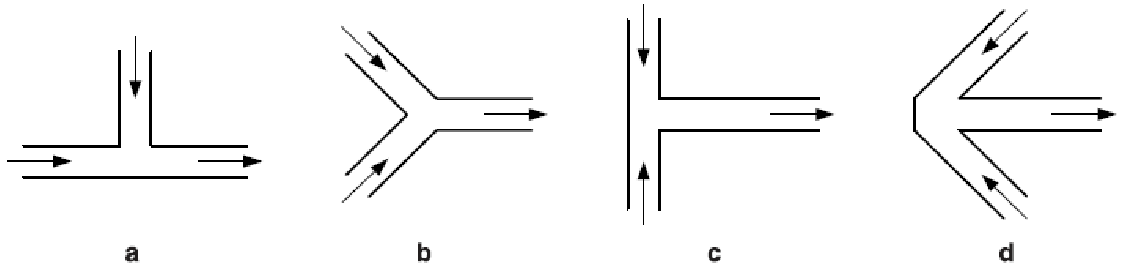

Fig.1.13: Four intersection geometries consisting of two inlets channels and one outlet channel. Source: Goullet et al. 2006.

The simulation can analyze further how the pulsing induces mixing and the effect of pulsing combined with possible obstacles present inside the mirochannel that cause secondary flow[7]. The slanted walls inside the channel induced a high degree of lateral transport across the channel, secondary flow and discontinuities in it occurred, as the transport is not limited by diffusion[6]. Furthermore, several works were reported regarding numerical investigation of obstacles at high Re. The numerical simulations of mixing in a cross-shaped micromixer with static mixing elements incorporated in the outlet channel show that significant improvement in mixing performance can be achieved compared to a micromixer without static mixing elements. Increasing the number of static mixing elements and incorporating the elements at the junction further improve the mixing performance of the micromixer. When the fluid encounters a static mixing element, the stream will separate because of the boundary layer separation around it provoking vortexes which will depend on the flow Re numbers by changing its length and size. At this moment a backflow occurs in the separation region enhancing the mass transfer rate there[8].This is demonstrated in Fig.1.14 based on velocity vectors encountered near the static element.

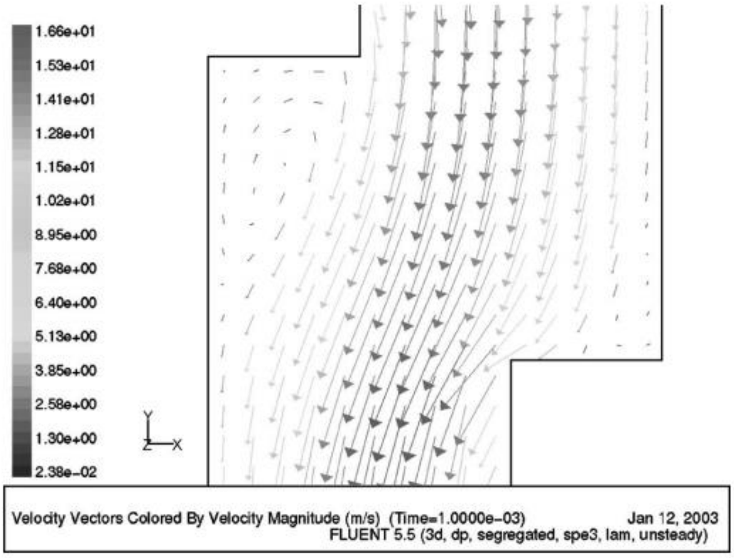

Fig. 1.14: The velocity vector plot shows the rotational flow of liquid caused by the static mixing elements. The static mixing elements cause the swirling effect on the liquid flowing past them and also creating lateral velocity component that assists in the mixing process. Source Wong et al 2003.

It has also been found that asymmetrical conditions in the geometry of T-shaped micromixer lead to an improvement in mixing quality. A few investigations have been done on the effect of mixing channel length on mixing quality but reducing the channel length this will lead to increasing energy dissipation and therefore decreasing the mixing time. So mixers with small channel dimensions seem to have a better mixing performance[6].

Studies regarding the influence of multilamelae flow showed an improvement in mixing within a microchannel. Dividing the inlet streams into n substreams increases the contact surface between the fluids and the diffusion occurs earlier. This is demonstrated in Fig 1.15 which shows an increase from 1 to 3 of contact areas between the fluids both for the T-shape mixer and double-T-shaped micromixer[6].

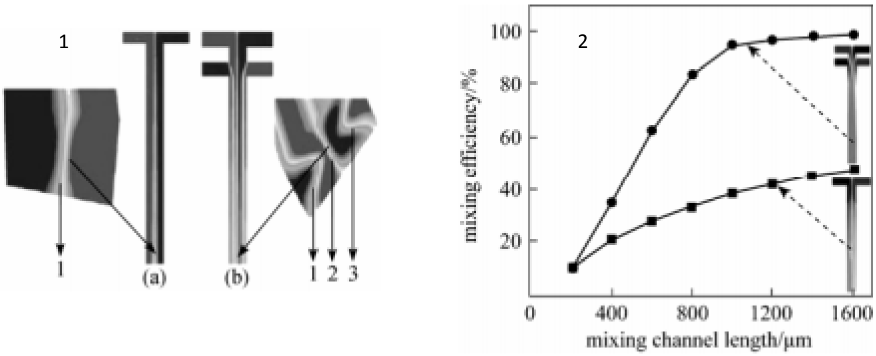

Fig.1.15: 1- Number of effective contact areas between the two sample fluids: (a) T-shaped microfluidic mixer, and (b) double-T-shaped microfluidic mixer; 2 - Mixing efficiency over the length of mixing channel ■ T-shaped mixer; ● double-T-shaped mixer. Elmabruk et al.2008.

1.1.3.3 The effect of external geometry

Mixing can also be accomplished by the action of fluctuating electric fields that causes the two fluids with different electrical properties (conductivity and/or permittivity) to stretch and fold rapidly thus increasing mixing efficiency[9]. As mentioned by the authors[9], one of the advantages of micro-electro-mechanical systems (MEMS) is that electric fields of large magnitude can be obtained by means of low voltages. Mathematically, the mass (continuity) conservation law of an incompressible flow in presence of an electric field can be written by Navier–Stokes equations:

$$\Delta\vec{V}=0 \qquad (3)$$

$$\rho\left[\frac{\partial\vec{V}}{\partial t}+\vec{V}\cdot\Delta\vec{V}\right]=-\Delta p+\eta\Delta^{2}\vec{V}+\vec{F_e} \qquad (4)$$

where $\vec{V}$ is the velocity field and p refers to the pressure and gravitational force is neglected. The electrical field is expressed by eq. 4 as $\overrightarrow{F_e}$ which follow the expression:

$$\overrightarrow{F_e} = q\vec{E} - \frac{1}{2}E^2\Delta_\varepsilon - \Delta\left(\frac{1}{2}\rho E^2\left(\frac{\partial\varepsilon}{\partial\rho}\right)_T\right) \qquad (5)$$

where $\vec{E}$ denotes the electric field, q the density of the free electrical charges and T the temperature[9].

Experimentally, the influence of the electrical field on mixing was studied also by Elmabruk et al. 2008 and was demonstrated to be significant. Increasing the electrical field´s strength the mixing of two fluids is enhanced (See Fig.1.16)[6].

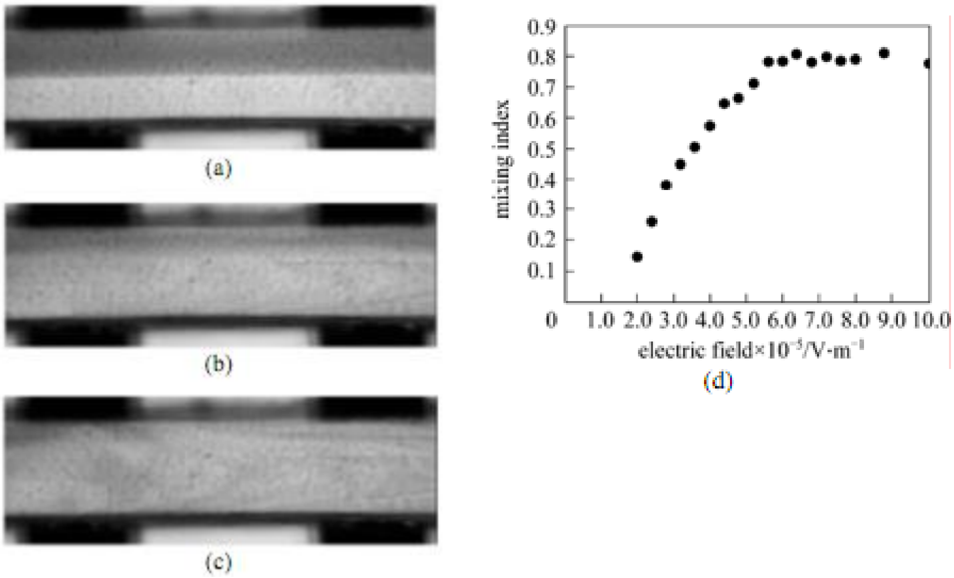

Fig. 1.16: The effect of applied electrical field on performance of T-micromixer: (a) initial condition; (b) after the application of an electric field of intensity $E = 4\times105 V\cdot m^{-1}$*; (c) same as (b) with an electric field intensity of* $E = 6\times105 V\cdot m^{-1}$ *and (d) variation of the mixing index with the intensity of the DC electric field. Elmabruk et al.2008.*

The development of microfluidic systems has been progressing rapidly in recent years but still is considered a very young field of research and a closer look at the flow phenomena in microfluidic systems is missing. Although it is very difficult to attain turbulent flow in microchannels, rapid mixing is still possible by the generation of secondary flow and vortices in the microchannels by applying internal or external forces or changing the geometry of the channel including some obstacles.

1.2. Microfluidics and miniaturization of the systems – state of the art

Microfluidics is the science and engineering of systems in which fluid behavior differs from conventional flow theory due to the small length scale of the systems. It deals with transport phenomena and fluid-based devices at microscopic length scale. Since Richard Feynman´s thought-provoking 1959 speech "There´s plenty of room at the bottom"[10] the technology had developed very quickly – especially regarding the miniaturization of electronic devices. In the late 1970s, silicon technology was developed which later was called MEMS[10]. The main applications of microfluidics are lifescience and chemistry. Microfluidics uses scaling laws, better performance, also, we don´t need to miniaturized all the system we just need to miniaturized the space where the fluid is prepared. Key issue in microfluidics represents microscopic quantity of the fluid used (liquid and gas). The commercial interests are focused on plastic microfabrication for single-use disposal micro fluidic devices. The main applications are: medical diagnostics, genetic sequencing, chemistry production, drug discovery and proteomics (large-scale study – particularly their structures and functions). The main interest in research today is finding the new fluids phenomena possible at the micro-scale. This interest appeared in fluid mechanics domain. This topic refers to the study of how fluids move (fluid properties) and the forces on them (interaction with forces). Fluid mechanics is divided in: fluid statics – the study of fluids at rest and fluid dynamics – the study of fluids in motion. This topic can be sometimes so complicated that it could be solved using only numerical methods[10]. For this reason the fluid mechanical researchers tried to find new approaches regarding the fluid characteristics but at the micro-scale. They demonstrated that these microdevices will not deliver the same power as conventional macro scale devices because of the ratio: surface / volume which are inverse proportional with length scale. If the ratio increases the length scale will decrease and vice versa. Microfluidics devices range from millimeters to few centimeters. In 1990 appeared plastic micromachining with a simple design *i.e.* i-STAT point-of-care blood chemistry diagnostic system. The study of fluid mechanics generally proceeds from the assumption that the fluid can be treated as a continuum. So it can be assumed that density, velocity, pressure are defined everywhere in space and to vary continuously from point to point within the flow. Usually the boundary conditions used have the following assumptions: temperature of the liquid immediately adjacent to the wall is assumed to be the same as that of the wall itself[10]. The most important parameter investigated both in micro- and macro- fluidics is velocity. First liquid-solid boundary condition was exposed by Navier- Stokes in his equation in which he proposed that the relative velocity is directly proportional to the velocity gradient at the wall – and hence the shear stress. The fluids behavior is quite hard to explain because of their molecule interaction but usually liquids behave like a continuum and it can be observed the no-slip and no-temperature-jump boundary conditions[10]. Taking into account this information the microfluidic devices have grown very fast lately and were specialized on fluid processes, especially. The main challenge for worldwide chemical, physics and mechanical engineers represents the application of the fluid dynamic theories on solids handling at microscale. Since, 1900s researchers tried to develop microdevices for multiple applications including solid synthesis, starting with fiber industry development[11].

1.3 Microfluidic devices applications

Beginning with 20th century, synthesis in flow gained significantly more interest for most of the synthetic chemists, because of the benefits of continuous processing at micro-scale: efficient mass and heat transport, small amount of reagents used and flow-alignment attribute[10,11] . The area of microreactors and their impact on chemical and materials synthesis are well reviewed in a wide variety of contexts proving in the same time the importance for science development. Most of these applications were well developed on continuous fluid flow synthesis but very few information were found regarding the continuous solid synthesis at microscale.

1.3.1. Liquid phase reaction

A wide range of liquid phase reactions have been performed in micro reactors devices; some of them are presented further: Grignard-reactions, nitrations, glycosylations, olefinations, peptidecouplings, aldol reactions, epoxidations, multicomponent reactions, Swern-oxidations (See Table 1.1).

Table 1.1: Liquid phase reaction inside microfluidic devises

Type of reaction	Materials used	Microreactors type	Observations
Glycosilation[12]	Reactants: mannoside and galactoside; Product: α-linked product	Jenson silicon microreactor	T = -40^{0}C; Reaction time : 4 min Conversion greater than conventional reactions
Nitration[13]	EOF as microemultion; Surfactant: SDS Cosolvent: butan-1-ol Product: nitrobenzene	Borosilicate glass	Conversion of 65%
Witting reaction[14]	Reactants: phosphonium salt, aldehyde Product: cis-and trans-notrostibene ester	Borosilicate glass	Conversion increased with 10% over the traditional batch synthesis
Cation[11] polymerization	Reactants: N-methoxycarbonyl-N-(trimethylsilymethyl)butylamine Product: cation	IMM microreactor	PDI superior then that from batch reactor
Radical[11] polymerization	Reactants: glutamic acid (NCA), triethylamine Product: homopolymer of NCA	PDMS multilayered system consisting in: PDMS micromixer and poly(tetrafluoroethylene) microtubes	T= 30^{0}C in water bath 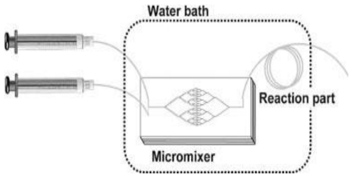
Surface-initiated polymerization[11]	Reactants: monomer of a polymer	Silicon wafer coated with a self-assembled monolayer of an initiator for atom-transfer radical polymerization	Specific polymer morphology is achieved within a microreactor 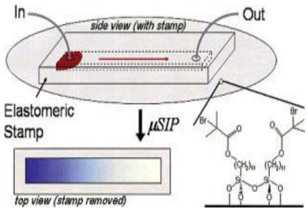

1.3.2. Liquid-solid phase reactions

There are two important liquid-solid phase reaction reported in the literature. They are known as Heck reaction and Suzuki reaction (See Table 1.2). The yields obtained were comparable with Suzuki reactions on a batch scale using homogeneous catalysis but there were negligible levels of the palladium catalyst in the product.

Table 1.2: Liquid-solid phase reactions:

Type of reaction	Materials used	Microreactors type	Observations
Heck reaction (catalytic reaction)	phenyliodide 5 and ethyl acrylate 6	solid-phase cartridge reactor loaded with 10% palladium on charcoal	Residence time was about 30 minutes at 1300C. Conversion was 95%.
Suzuki reaction[16]	arylhalide 36 and phenylboronic acid 37.	Microreactor with flow injection analysis principles	Conversion about 67% Product desired: cyanobiphenyl 35 Temperature: room temperature.

1.3.3. Gas phase reaction

Synthetic transformations using corrosive and toxic gases are generally difficult to perform because of the hazardous and highly reactive nature of the gases. Specially designed liquid-gas microreactors allow for the careful control of gas flow in the reactor and to regulate the contact time between gas and liquid. Integrated gas-liquid separators can be introduced to separate the gaseous phase at the end of the reaction. The utility of microreactors for this chemistry has been well illustrated for fluorination[15], chlorination, nitration[13], and oxygenation[12]. Literature reviews some liquid-gas reactions illustrating in the same time the advantages of applying microreactor technology (See table 1.3)[15]. Micro reactors application in gas and liquid phases had been proved to accomplish faster, safer and cleaner reactions. The miniaturization of the reaction volumes offers better control reaction conditions, including temperature, time, mixing, and less amount of the compounds[12-14]. Microreactors present opportunities to apply conditions that are inaccessible using conventional laboratory equipment, such as super heated solvents, and reactions in “explosive” regimes. The potential of the microreactors to provide the possibility to have a better control over the chemistry environment has enlarged the research interest and new utility of these microdevices was reported. A microchannel system can also act as separation column where the solvents are apart within a non-turbulent environment[15].

Table 1.3: Gas phase reactions:

Type of reaction	Materials used	Microreactors type	Observations
Hydrogenation	1,5-cyclooctadiene 44 to cyclooctene 45	Microreactor with aluminium wafers with mechanically-etched channels	Temperature = 150^0C and residence time ≈ 35 ms. Conversion about 75%. Increasing the time residence of the reaction to 115 ms the conversion increased also to 99.5%.
Fluorination[15]	ethyl acetoacetate 55 Product: ethyl 2-fluoroacetoacetate 56	Copper or nickel micro reactor.	Conversion - about 99% Efficiency improved regarding conventional fluorination process

Integration of a micro reactor device in the world wide industrial market not only is accepted as a better alternative technology for some dangerous processes, fluid flow synthesis, highly sensitive microchannel-based biological assay systems, but also is seen as a potential alternative for solid state production even though, the development of this section is still in its early stage.

1.3.4 Solid materials synthesis

Table 1.4: Solid phase reaction[11]:

Process type	Materials used	Microreactors type	Observations
Beads synthesis 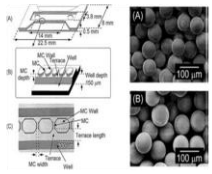 (left) Schematics of the emulsification device made from etched silicon, monodisperse droplets of the monomer snap off because of interfacial tension. (right)	Reagents: aqueous poly(vinyl alcohol) Product: divinylbenzene-containing droplets of different size	Emulsification device made from etched silicon	Monodisperse droplets of the monomer snap off because of interfacial tension. The droplets are later thermally polymerized to form crosslinked beads; Particle sizes were several to tens of micrometers with diameter coefficients of variation (CVs) of less than 5%
Polymer beads synthesis in flow 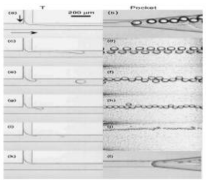	Product: s 1,6-hexanediol diacrylate monomer initiated with Darocur 1173.	T-junction approach.	Droplets were subsequently photopolymerized downstream. Diameter CVs less than 2%

Table 1.4(continuation): Solid phase reaction[11]:

Capsules synthesis 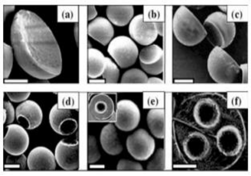 	Reagents: aqueous SDS (liquid C), monomers (liquid B), and silicon oil (liquid A; Product: ethylene glycol dimethacrylate (TPGDA droplet-in- droplet)	microfluidic device that flow-focused three fluids creating droplet-in-droplet structures	They mapped out a ternary phase-like diagram in which the axes reflected the effect of the 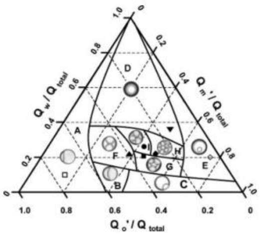 flow rates of the aqueous, monomer, and oil phases on the structure of the formed particle (See fig. above).
Solid disks synthesis 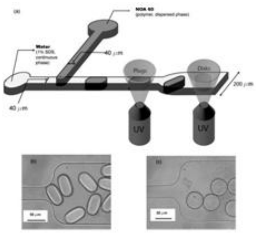 	Reagent: Norland optical adhesive (NOA) 60 - photopolymerizable resin	T-junction approach	The disks were formed by let them laterally expand and then polymerization process

The reaction portfolio of Lonza AG, statistically made by Roberge et al. in Switzerland, for implementation of multipurpose reaction application of microtechnology both in fluids and solids preparation reached the following value: 50% of 84 reactions can benefit from the continuous processing and for less than 20 % of all analyzed reactions the microreactor technology can be applied, due to the presence of solids[16]. Furthermore, solid preparation within microfuidic systems has been developed for some specific applications. Table 1.4 is shown a summarized of content the most known microdevices application in solid preparation.

All the previous examples of preparing solid materials in flow used the droplet pseudophase to template the finit materials. Yet, coflowing laminar streams are also attainable within a microfluidic device, and a number of researchers have created materials shaped by these extended boundaries to form elongated membranes and fibres[11].

Table 1.5: Solid phase reaction: fiber and membrane synthesis[11]:

Type of reaction	Materials used	Microreactors type	Observations
Fiber capture through a precipitation reaction	Solution of polystyrene sulfonate and hexadimethrine bromide are collided under laminar flow conditions	Y shaped microdevice	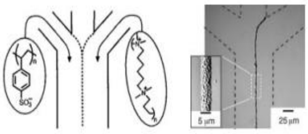 Schematic and optical micrograph of a polymeric structure deposited on glass at the laminar flow interface
Nylon membrane Formation	1,6-diaminohexane into the aqueous phase and adipoyl chloride into the organic phase		Colliding two fluids at a cross-junction formed a nylon membrane at the interface of liquids wetting paths. Membrane pore size was smaller than 200 nm. 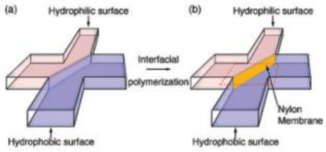

The first examples of applications regarding fiber and membrane preparation published by Whitesides laboratory and Beebe laboratory, respectively, are listed in Table 1.5.

The use of microreactors and microfluidic devices for the production of polymers with controlled properties and morphologies appears to have a bright future. The small dimensions of these microdevices provide benefits for solid, hollow, and multicored, asymmetric and irregularly shaped polymer microparticles as well as membranes and fibers when their synthesis is not accessible through other means. This novel approach may have applications as functional colloids, in photonics, and in the encapsulation of materials for catalysis and controlled delivery[11].

2. Dawsonite type materials

2.1. Dawsonite – state of the art

Dawsonite type materials are crystalline minerals consisting of alumina hydrated ($Al(OH)_3$) mixed with carbonate of lime (Calcium oxide - CaO) and soda (alkaline chlorides). The mineral was discovered in 1862 by Messrs J.H and Gludstone G. and then was collected by John William Dawson, geologist and Principal of McGill University, as 'new mineral specie' called Hovite (double carbonate of alumina and lime) and later named dawsonite, in his honor, by Harrington in 1874[17]. Since its first discovery back in ´62 dawsonite was encountered in many countries worldwide becoming more and more an interest in catalytic industries and not only. Most important abundance can be found in coating vug walls and fractures in hydrothermally altered feldspathic dikes and hornfels associated with nepheline syenite (Mont Saint-Bruno, Canada), in authigenic alkaline shales and coal-bearing rocks (Green River Formation, USA; Sydney Basin, Australia) and in saline soils on nepheline syenite tuffs (Olduvai Gorge, Tanzania)[18].

The natural mineral crystal structure, sodium aluminum carbonate hydroxide ($NaAl(OH)_2CO_3$ *coded* NaAlDw) is orthorhombic-dipyramidal with point group 2/*m* and the space group *Imam*, displaying body-centered symmetry[19].

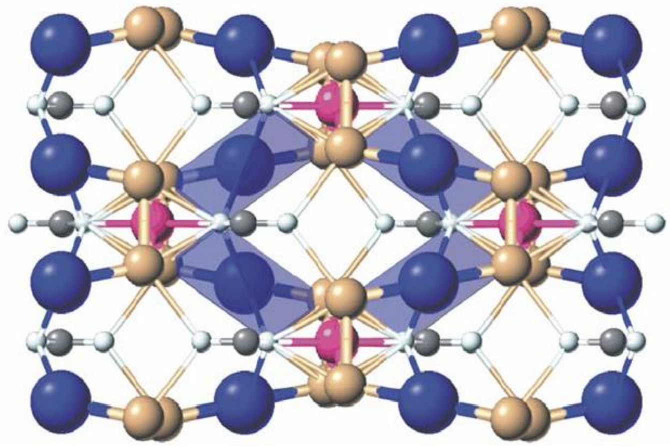

Fig.1.17: Structure of dawsonite, NaAl(OH)2CO3.. Na: blue spheres, Al: purple sticks, C: grey sticks, and O: white sticks. Source: www.webmineral.com

The structure consists of an assemblage of edge-sharing distorted $AlO_2(OH)_4$ and $NaO_4(OH)_2$ octahedra, and $CO3^{2-}$ groups (Fig.1.17). Hydrogen bonding occurs between the Al chain and the CO_3 group, strengthening the Al + Na three-dimensional framework[20]. Multiple bands are observed in both the Raman and infrared spectra in the carbonate stretching and bending modes, indicating a symmetry reduction of the carbonate anion[18,20]. The mineral is formed through low-temperature hydrothermal decomposition of aluminous silicates. Since its discovery varieties, other than sodium dawsonite, had been synthesized. Its recognition and identification by X-ray analysis is difficult because of the mineral's rarity, small size (<20 mm) and brittleness[21]. However, sodium aluminum dawsonite (NaAlDw) is just a member of a large class of analogous (dawsonite-type) synthetic (yttrium and cerium dawsonite)[19] and natural compounds that are nominally described by the general chemical formula $AM(CO3)_x(OH)_y$, where "A" is an alkali (K^+ or $NH4^+$) or alkaline earth (Mg^{2+}, Ca^{2+}, or Ba^{2+}) metal ion and "M" is favorably a trivalent transition or nontransition metal ion, or by $BM(CO3)_x(OH)_y$, where "B" is a divalent transition metal ion (Ni^{2+} or Cu^{2+})[21].

2.2. Dawsonite - applications

Many of these types of naturals/synthetic compounds have the main application as catalyst precursors[20] topic that increased very much in last few years considering that catalytic-grade alumina-based materials are very important from a practical perspective. Recently was demonstrated that these types of minerals (especially natural one) can be used to trap carbon dioxide (CO_2) if the system maintain a high CO_2 pressures and remove greenhouse gases[22]. The most prominent of these are the application as (i) a pollutant gas remover from emissions of coal-fired boiler systems, (ii) flame retardant[23], (iii) a dry extinguisher of in-flight engine fuel leak fires[24], (iv) a stabilizer for chlorine-containing polymers[25], (v) an effective ingredient in antacids[26], (vi) a parent material for transparent spinel and YAG14 ceramics[27]. Also, dawsonite compunds are used in water purification for the removal of alumina species[19].

2.3. Dawsonite – crystal structure

The most studied dawsonite-type materials are ammonium and potassium dawsonite. Further, the attention is focused on ammonium dawsonite (denoted NH_4-dawsonite). It is a unique precursor for alumina with enhanced properties compared to those derived from the conventional Bayer process. The crystal structures of NH_4-dawsonite was found to be isostructural, and is composed of the same $AlO_2(OH)_4$ chains as dawsonite mineral but differs by having a base –centered structure instead of body-centered one (Na-Dw)[28]. The X-ray diffraction (XRD) crystal data of NH_4-dawsonite were found to be a = 6.618 A °, b = 11.944 A ° and c = 5.724 A °, and this makes very probable that the crystal structures of the analog and K-dawsonite (coded K-Dw) (a = 6.3021(3) A°, b = 11.9626(5) A ° and c =5.6456(3) A °) to be closely related[29]. Fernández-Carrasco et al. 2005 published in their work, the difference in structure between natural and the analog mineral that seems to appear at metal-oxygen individual interaction level, which for K-dawsonite the potassium ion (K^+) interacts strongly with three symmetry independent O atom [O(1), O(2) and O(3)], meanwhile for Na-Dw the individual interaction of O(2) with sodium ion (Na^+) is not present[29]. The same interaction listed above could govern the crystal structure of NH_4-dawsonite, as there crystal data were shown to be similar. This could elucidate the real crystal structure of the analog mineral in case. In Figure 1.18 is shown a proposed crystal structure for K-dawsonite.

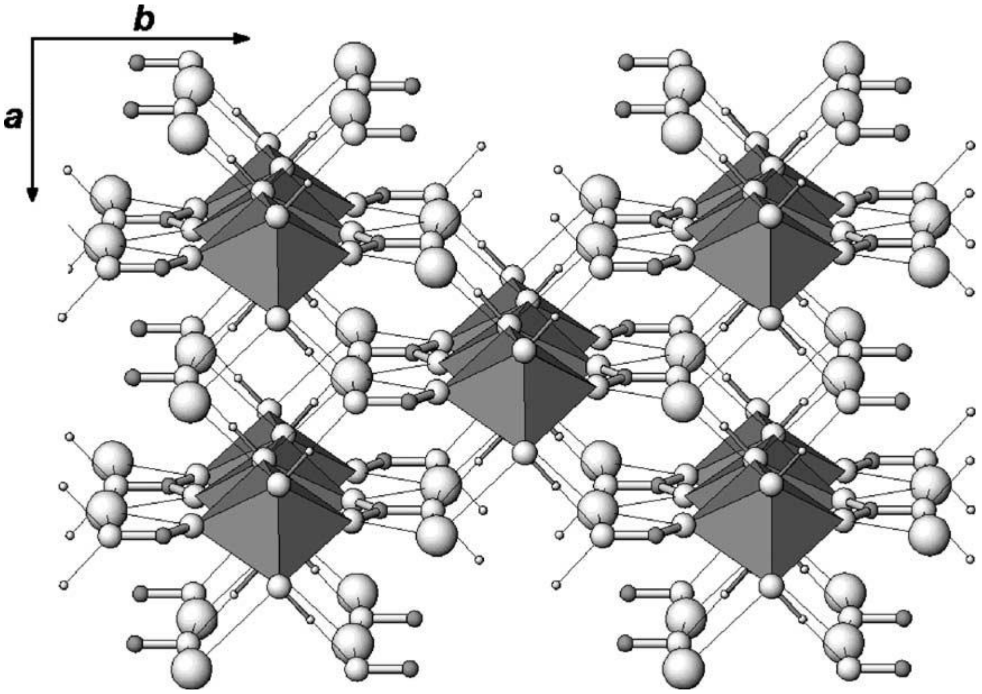

Fig.1.18: Structure of $KAl(CO_3)(OH)_2$ as viewed along the c axis. Source: Fernández-Carrasco et al.2005.

2.4. NH_4-Dawsonite – synthesis and industrial applications

Most of the applications revealed in Section 2.2 are applicable, also, for ammonium dawsonite. Using NH_4-dawsonite as a raw material for very pure alumina (aluminum oxide - Al_2O_3) production by thermal decomposition above 1173K[28] gained more and more ground over the decades and reached an important level in the field of alumina production. Alpha alumina (α-Al_2O_3) based materials (powders, films and fibers) have industrial importance because of their various outstanding properties: high-melting point (2050^0C), chemically inert at high temperature (>1000^0C) in oxidizing and reducing atmospheres, high compatibility with molten light metal and non-oxide ceramics, high-optical transparence, and good mechanical properties[30].

The fibrous α-Al_2O_3-based materials have many important applications in ceramic filters and membranes, strengthening of composites, catalysis, chemisorption of metals, biological and biomedical, and mesoscopic electronic and optical devices[30]. The annual world production of alumina was estimated in 2008 at 80 Mt, giving idea of the relevance of this compound in a number of industries (mining, ceramic, chemical). Giannos et al.[32] obtained NH_4-derived aluminas with specific surface area of 450 m^2 g^{-1} and 145 m^2 g^{-1} after calcination of ammonium mineral at 973 K and 1273 K, respectively. Ali et al.[20] have recently extrapolated the dawsonite route to prepare bulk Cr_2O_3 and Fe_2O_3 by isomorphous substitution of Al by Cr or Fe in the precursor structure, but low-surface area oxides (32 m^2g^{-1}) were obtained. Pitsch et al.[33] prepared bimetallic Fe–Al dawsonites by discontinuous precipitation using $NH_4Fe(SO_4)_2$ as the iron source. Upon calcination at 873 K, Fe_2O_3/Al_2O_3 catalysts (1–10 wt% Fe) with relatively high surface areas (up to 400 m^2 g^{-1}) were attained.

Various methods have been used to synthesize dawsonite for oxide catalyst or precursor of catalyst, which can be classified attending to the phase composition of the reactants (gas-liquid, gas-solid, solid-solid, and liquid-liquid). Synthesis of the mineral analog is typically practiced by *batch* by co/precipitation of aqueous solutions of aluminum salts (NH_4-, $Al(SO_4)_2$, $AlCl_3$, or $Al(NO_3)_3$) or $Al(OH)_3$ suspensions with aqueous solutions of ammonium (bi)carbonate[31]. Recent studies showed a high flexibility in composition of alumina based materials[28] and depending on the metal-content and temperature the products can be different types of alumina: single metal oxides or mixed oxides with spinel, perovskite, and hexaaluminate structure (observed crystalline Al containing phases: α-Al_2O_3, $LaAlO_3$, $LaAl_{11}O_{18}$ by high temperature X-ray diffraction (Fig.1.19)[31]. Moreover, was discovered that presence of pH gradients due to ineffective stirring of the reactor volume in the precipitation process of dawsonite type materials will generate an unwanted by-product[31]. Residence time of the precipitate particles and concentration of reactants which can change throughout the precipitation process have great influence on the degree of nucleation and crystal growth which influence the final product quality[34].

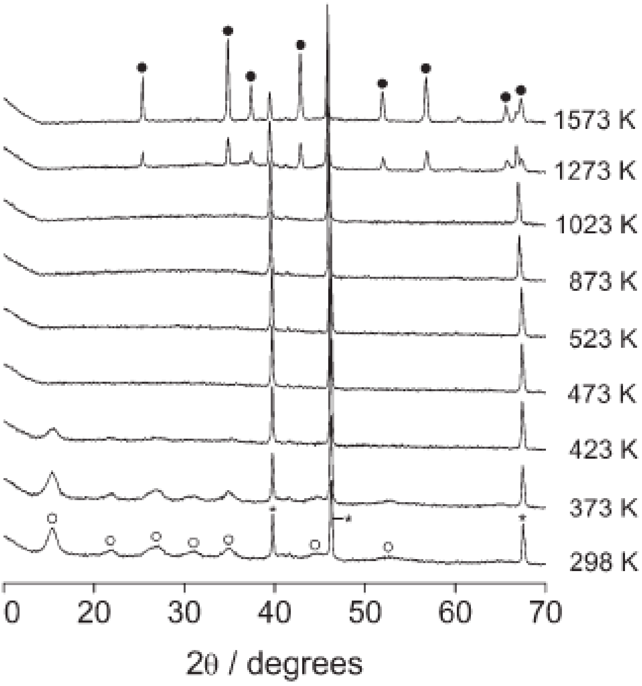

Fig.1.19: In situ X-ray diffraction patterns during decomposition in air of Fe-Al-dawsonite with Fe:Al = 1:11. Symbols: (o) dawsonite, (•) α-Al2O3, and (*) Pt-Rh alloy heater strip (JCPDS 4-802).

A way for preventing the imperfect mixing and generating by-products was published by Santiago et al. 2006[31] and is based on a novel approach, In-Line-Dispersion-Precipitation Method (ILDP), which follows the miniaturization of the precipitation chamber up to milliliter scale inducing better controlled resistance time and highly effective stirring. It is shown that the properties of ILDP-derived metal-substituted dawsonites and the corresponding oxides are superior to those prepared by conventional precipitation as regards element dispersion, porosity, thermal stability, and catalytic performance.

The transition temperature at which NH_4-dawsonite structure collapses (*ca.* 473 K) is independent of the metal composition of the samples[31]. The amorphous nature of the NH_4-dawsonite-derived alumina and its sintering stability, as described before, are very interesting and deserve further investigation. Finally, the acquired knowledge could be extrapolated further for novel technologies of preparing the mineral analogue with enhanced properties for catalytic precursor applications.

3. Aim of the thesis

The thesis presents a new approach regarding the application of microtechnology in production of catalysts, specifically NH_4-dawsonite [$NH_4AlCO_3(OH)_2$], using microreactor technology. The mineral analogue preparation was held within a 78µl volume split-recombine micromixer (CPMM 1200/8 mixer) purchased from the Institut für Mikrotechnik in Mainz, Germany (IMM). As mentioned before the main characteristics of CPMM 1200/8 microreactor: split-recombine approach performing multiple splitting and recombination of liquid compartment, a ramp-like microstructure splits the incoming flow into two parts which are lifted up and down; the new two streams formed are reshaped separately in such a way that two new cross-sections combined restore the original one, were considered the starting point of this thesis work. Miniaturization of the process, at micro scale, was following the same procedure as ILDP (constant temperature and pH) proposed by Santiago et al.[31], but it had to take into account the optimization of the process parameters and the particularity that the precipitation process will take place in a laminar regime and within a non stirring micromixer. Appling the miniaturization advantages the precipitation process will be safer, cleaner, environmentally friendly and economically worthy. The reduced and compact setup will generate more practical utility and space economy. The transferability from laboratory scale to industrial scale for most of the conventional processes adapts the scaling-up step which is time consuming because of the recalculation of the parameters for large scale, meanwhile the microreactor based processes need the numbering-up step which keep the same optimal parameters found and no recalculation is needed. The chemistry of the present precipitation reaction is very hardly present in the literature. The final goal is to determine the kinetics of the NH_4-dawsonite crystallization reaction which could represent a new path evolution of chemistry and chemical engineering field interest. The chemistry is the key to discover more about the mineral analog and its properties and enlarge its applications.

4. Outline of the thesis

An overview regarding microthechnology field is presented in ***Chapter 1*** which is divided in two parts. First is described the current state of the art of microreactor technology, continues with the most important fabrication techniques and a summarized mixing theory applied for these micromixers. Furthermore, is outlined the effect of the operating and designed parameters over mixing quality inside a microreactor. In this subheading is described the most important factors that influence the mixing and could affect the properties of the finite product. Literature named the microreactors the main component of an integrated microfluidic system which is involved in the preparation stage. Further in the chapter are described the general information regarding microfluidics and miniaturization of the system. Part 1 of the ***Chapter 1*** finishes by summarizing the most important applications of microreactors applicable or/and not yet applicable in the worldwide industry. The second part of the first chapter continues with a short overview regarding the dawsonite-type materials exposing to the reader the state of the art since their discovery. This section is more related on one specific dawsonite-type called ammonium dawsonite or ammonium aluminum carbonate hydroxide ($NH_4Al(OH)_2CO_3$) and its general characteristics: physical and structural characteristics, main applications already existing in the industry and not last, relates the most common conventional synthesis methods. The Chapter closes with a short presentation of the advantages of using microreactors over conventional reactors for mineral analog synthesis and how is influencing this microreactor technology the catalytic properties of the product.

Chapter 2 discusses the In-Line Dispersion Precipitation Method (co-precipitation process, coded ILDP) patented by Javier Pérez-Ramírez group in 2007, miniaturized at microscale. Ammonium dawsonite (NH_4-dawsonite) is precipitated within an IMM Caterpillar micromixer following the same procedure used by ILDP method at constant pH and temperature, using as initial solution ammonium carbonate ($(NH_4)_2CO_3$) and aluminum nitrate ($Al(NO_3)_3$) as acid and base, respectively. The precipitation process is taking place under a laminar regime. The experimental section is divided into two parts:

one referring to the optimization of process parameters by modifying the aqueous solutions concentrations and/or flow rates in order to increase the continuity of the production and the second one presenting the experimental work taking into account the aggregation phenomena and crystal growth during and post process. Textural and morphological changes associated with different phases and treatments will be highlighted.

The same procedure as reported in ***Chapter 2*** regarding the co-precipitation of NH_4-dawsonite within microfluidic system is described in ***Chapter 3*** with the particularity that the precipitation process will take place at1 bar of applied pressure. It is known that in the absence of turbulent convection, mixing of larger volumes of fluids in microchannels at low Reynolds numbers is difficult, and often requires resourceful combinations of both convection and diffusion to reduce processing times, path lengths, and pressure drops to within acceptable levels[35]. In this case a reduced pressure drop is needed in order to enhance the mixing governed by laminar flow. A study regarding the influence between the pressure drop and flow rate was needed[15]. A new microsystem set-up will be proposed in order to satisfy the pressure/pressure drop necessity. Some of the trials experimented in ***Chapter 2*** will be used in this pressurized experimental system. The aim of this Chapter is to improve the process continuity with the help of the applied pressure. Structural properties of the product showed traces of ammonium nitrate (NH_4NO_3) in some specific cases (specific initial solution concentrations and their flow rate), fact that restrained the interval of the process parameters which are needed to be optimization and informed us about the sensitivity of this technology when solids are involved. Since the main objective of this thesis is to optimize the precipitation process parameters at microscale and run a continuous unlimited time production with the aim of industrial applications, next chapter, ***Chapter 4***, continues the experiments within the pressurized microsystem. In order to determine the influence of the system pressure over the mixing phenomenon with the result in a better control of the crystal growth, homogeneous particle size distribution at nanometer range, the precipitation process was held at constant pH and temperature but the working pressure was increased step-by-step. Uniform size distribution and nano-sized NH_4-dawsonite particles production was controlled by choosing an optimal flow rate for both initial solutions as fix parameter. Pressure influence over the product morphological and physical properties is study, also. Better porosity properties and smaller particle size were determined comparing with previous work and conventional batch precipitation. The need of pressure within a microreactor technology, especially dealing with solids production inside microchannels, was demonstrated to depend on the aim of the research studied.

The results obtained in the previous experiments (***Chapter 2-4***) showed that microreactor technology can be applied for solids production in a limiting time of synthesis. Even though, the clogging problem was not fully solved, the knowledge gained made us take a step forward in applying microreactor technology for solids synthesis. A new microreactor-based system is presented in ***Chapter 5*** which could be able to overcome the unsolved drawback of microreactor technology. The microscale set-up contains the same components as presented in previous experiments, only with the particularity that the microreactor´s channel is straight which provides a non-homogeneous (chaotic) mixing of the initials solutions. The difference between perfect mixing within the split-recombine micromixer and chaotic one by using straight channel micromixer is lettered in this chapter. The experimental work follows the same conditions as controlled within the split-recombine microreactors reaching the level of pressure 2 bar. The influence of both types of mixing over the product quality will be discovered and compared with the results published in the literature. Moreover, this chapter presents some pre-synthesis experiments of NH_4-dawsonite precipitation process by changing the stainless steel Caterpillar Micromixer with T-junction approach in order to predict the process evolution within a chaotic mixing and engulfment regime. Based on this, the experimental work was continued within a poly(methyl methacrylate) (PMMA) split-recombine Caterpillar micromixer and than Y- shaped straight microchannel mixer purchased from IMM, Germany with the aim of adjusting the optimal process parameters and in the same time to examine the precipitation process by optical visualization.

Textural and morphological properties of NH_4-dawsonite obtained in each of these cases presented above (***Chapter 2-5)*** were investigated by using X-Ray Diffraction Technique for crystal pattern and crystallite size determination, followed by in depth understanding of transitions phases during thermal decomposition (Thermogravimetric Analyses - TGA) with the goal of predicting the purity of the product; oval (rounded), root or rock-like micro/nano particles were measured by using both Scanning Electron Microscopy (SEM) and Transition Electron Microscopy (TEM). The porosity and some catalytic properties of the powder were discovered by applying the N_2-adsorbtion Technique (BET technique and t-method).

Computational fluid dynamics is one of the most important approaches for simulate and model a process at micro and nanometer scale. If solids are involved, the approach gets harder and harder to be solved. One way to overcome the drawback which miniaturized system is facing: the limited interval of solids production, clogging and cleaning repeatedly processes, is to have the best knowledge about the process itself. This implies not only physical, mechanical or engineering knowledge but also chemical ones. A deep study on ammonium mineral precipitation reaction from chemistry point of view regarding the crystallization process is still investigated (as manuscript for publishing) and will give a better understanding regarding the high accumulation of solid inside the microreactor´s channel and also is helping us to learn the way of controlling it in order to have a continuous flow production and enhanced product quality. All these important data will serve further for modeling and simulating the precipitation process by using COMSOL software which can predict the process optimal parameters and the mixing inside microchannel which will help us in numbering up step which had to be included in transferring the system at industrial scale.

Finally, the summary and outlook of the thesis are put in perspective in ***Chapter 6***.

References

[1] Enabling Technologies. Microreactor Technology, ChemFile vol.5, No.7, www.sigma-aldrich.com/chemical synthesis;

[2] Ehrfeld W., Hessel V. and Lowe H., 2000, Microreactors. New Technology for Modern Chemistry, Wiley-VCH Verlag GmbH, D-69469 Weinheim, Germany**;**

[3] Bednarzik M., Waberski C., Rudolph I., Löchel B, Herbstritt F., Ahrens G., 2008, Mixer slit plates fabricated by direct-LIGA, Microsyst Technol 14:1765–1770, DOI 10.1007/s00542-008-0569-4;

[4] Jahnisch, K.; Hessel, V.; Lowe, H.; Baerns, M., 2004, Chemistry in Microstructured Reactors, Angew. Chem. Int. Ed. 43, 406 – 446;

[5] Watts P. and Haswell S. J., 2005, The application of micro reactors for small scale organic synthesis, Chem. Eng. Technol., 28, 290-301;

[6] Elmabruk A. M., Mingxing Y., Yundong W. and Youyuan D., 2008, A State-of-the-Art Review of Mixing in Microfluidic Mixers, Chinese Journal of Chemical Engineering, 16(4) 503—516;

[7] Goullet, A., Glasgow, I., Aubry, N., 2006, Effects of microchannel geometry on pulsed flow mixing, Mech. Res. Commun., 33, 739-746;

[8] Wong S. H., Bryant P., Ward M., Wharton C., 2003, Investigation of mixing in a cross-shaped micromixer with static mixing elements for reaction kinetics studies, Sensors and Actuators B 95, 414–424;

[9] Moctar, A.O.E., Aubry, N., Batton, J., 2003, Electro-hydrodynamic micro-fluidic mixer", Lab Chip, 3, 273-280;

[10] Nguyen N.T., Wereley S.T., 2006, Fundamentals and Applications of Microfluidics, second edition, Artech House integrated microsystems series, Boston, London;

[11] Steinbacher J. L., Mcquade D.T., 2006, Polymer Chemistry in Flow: New Polymers, Beads, Capsules, and Fibers, J. Polym. Sci. Part A: Polym. Chem.: Vol.44 Issue 22, 6505-6533, (Wiley InterScience: doi/10.1002/pola.21630/pdf);

[12] Geyer K. and Seeberger P.H., 2008, Microreactors as the Key to the Chemistry Laboratory of the Future, Systems Chemistry, Proceedings, Bozen, Italy;

[13] Doku G. N., Haswell S. J., McCreedy T. and Greenway G. M., 2001, Electric field-induced mobilisation of multiphase solution systems based on the nitration of benzene in a micro reactor, Analyst, 126, 14–20**,** DOI: 10.1039/B007585J;

[14] Skelton V., Greenway G.M., Haswell S.J., Styring P., Morgan O.D., Warrington B.H. and Stephanie Y. F. W., The generation of concentration gradients using electroosmotic flow in micro reactors allowing stereoselective chemical synthesis, Analyst, 126, 11-13, DOI: 10.1039/B006727J;

[15] Fletcher P.D.I., Haswell S.J., Pombo-Villar E., Warrington B.H., Watts P., Wong S. Y. F. and Zhang X., 2002, Micro reactors: principle and applications in organic synthesis, Tetrahedron 58, 4735-4757;

[16] Kockmann N., 2008, Transport phenomena in micro process engineering, Springer--Verlag Berlin Heidelberg, Germany;

[17] Harrington B. J., 1874, Notes on Dawsonite, A new Carbonate, *Can. Natural.* Vol. 7, 305, (http://rruff.info/uploads/CNQJS7_305.pdf);

[18] Stevenson J.S. and Stevenson L.S, 1977, Dawsonite-fluorite relationships at Montreal-area localities, Can.Mineral. Vol. 15, 117-120;

[19] Frost R. L. and Bouzaid J. M., Raman spectroscopy of dawsonite $NaAl(CO_3)(OH)_2$, 2007, J. Raman Spectrosc., 38: 873–879;

[20] Ali A. A., Hasan M. A., Zaki M. I., Dawsonite-Type Precursors for Catalytic Al, Cr, and Fe Oxides: Synthesis and Characterization, 2005, Chem. Mater., 17, 6797-6804;

[21] Sirbescu M.L., Nabelek P.I., 2003, Dawsonite: An inclusion mineral in quartz from the Tin mountain pegmatite, Black Hills, South Dakota, Am. Mineral., Vol.88, 1055-1060;

[22] Hellevang H., Aagaard P., Oelkers E., Kvamme B., 2005, Can Dawsonite Permanently Trap CO2?, Environ. Sci. Technol. 39, 8281-8287;

[23] Woycheshin E.A., Rigge R.J., Sobolev I., 1975, U. S. Patent 3 878 166;

[24] Altman R. L., Mayer L. A., Ling A. C., 1983, U. S. Patent 4 406 797;

[25] Kuhn K.J., Wehner W., 1998, U.S. Patent 6 136 900;

[26] Kumura T., Imataki N., Hasul K., Yasutomi K., 1972, U.S. Patent 3 650 704;

[27] Li J.G., Ikegami T., Lee J.H., Mori T., 2000, Fabrication of Translucent Magnesium Aluminum Spinel Ceramics, J. Am. Ceram. Soc., 83 [11] 2866 – 68;

[28] Stoica G. and Pérez-Ramírez J., 2007, Reforming Dawsonite by Memory Effect of AACH-Derived Aluminas, Chem. Mater. 19, 4783-4790;

[29] Fernández-Carrasco L., Puertas F., Blanco-Varela M.T., Vázquez T., Rius J., 2005, Synthesis and crystal structure solution of potassium dawsonite: An intermediate compound in the alkaline hydrolysis of calcium aluminate cements, Cement and Concrete Research, 35, 641-646;

[30] Jing C., Xu X., Hou J., 2008, Synthesis of sub-micro-sized solid alpha alumina fibers with smooth surfaces by sol–gel method, J.Sol-Gel Sci. Technol. 45:109-113; DOI 10.1007/s10971-007-1644-5;

[31] Santiago M., Yalfani M. S., Pérez-Ramírez J., 2006, In-line dispersion–precipitation method for the synthesis of metal-substituted dawsonites. Genesis of oxide materials with superior properties, J. Mater. Chem.16, 2886–2889; DOI: 10.1039/b607031k;

[32] Giannos, M., Hoang, M., Turney, T.W., 1998. Thermally stable aluminas for high temperature applications. Chem. Lett. 8, 793–794;

[33] Pitsch I., Gabner W., Brückner A., Mehner H., Möhmel S., Uecker D.C., Pohl M. M., 2001, Synthesis and characterization of Fe2O3 containing aluminas by thermal decomposition of modified ammonium dawsonite, J. Mater. Chem. 11, 2498–2503; DOI: 10.1039/b101466h;

[34] Abelló S. and Pérez-Ramírez J., 2006, Tuning Nanomaterials' Characteristics by a Miniaturized In-Line Dispersion–Precipitation Method: Application to Hydrotalcite Synthesis, Adv. Mater. 18, 2436–2439;

[35] Ou J., Moss G. R., Rothstein J. P., 2007, Enhanced mixing in laminar flows using ultrahydrophobic surfaces, Physical Review, 76, 016304;

Chapter 1

Introduction

Chapter 2

NH_4-Dawsonite production within a Caterpillar microreactor

Co-precipitation is one of the most frequently applied methods in preparing precursors of catalysts and support materials with good dispersion of the components, carried out most of the time in a batch mode. The chapter presents co-precipitation of ammonium dawsonite (NH_4-dawsonite) catalyst precursor within the channel of an IMM Caterpillar micromixer. Aluminium nitrate nonahydrate ($Al(NO_3)_3x9H_2O$) and ammonium carbonate ($(NH_4)_2CO_3$) were used as reagents for precipitating the catalyst within a microreactor set-up proposed by our group. Correlation between reagents flow rate and concentration by changing their values enables the production time to be better controlled and to give certain information about the catalyst properties. NH_4-dawsonite has been characterized by X-Ray Diffraction Technique (XRD) and Thermogravimetric Analysis (TGA) in order to determine the crystallinity and purity of the product and then scanning electron microscopy (SEM) was used for visualizing the morphology. Particle size was measured by J-Image software.

Chapter 2

NH_4-dawsonite production within a Caterpillar microcreactor

1. Introduction

As mentioned before alumina (Al_2O_3) is an important catalyst support in the chemical and petrochemical industries. Two of the most produced structures of alumina type materials are α-Al_2O_3 and γ-Al_2O_3, by decomposition of aluminum hydroxide or aluminum oxy hydroxide but most thermodynamically stable is the version alpha (α) which represents the crystalline form , named commonly corundum. The process represents the second step of entire Bayer process of producing aluminum from bauxite (mixture of gibbsite - $Al_2O_3 \cdot 3H_2O$ and boehmite - $Al_2O_3 \cdot H_2O$). Alumina produced has a purity of 99% and a hardness of 9 on Mohs scale becoming the second hardest natural substance after diamond[1]. As coprecipitation methods are not easy to control and reproduce and impregnation techniques cannot always be made to yield the desired active-phase distribution, it is worthwhile to consider alternative methods[2,3].

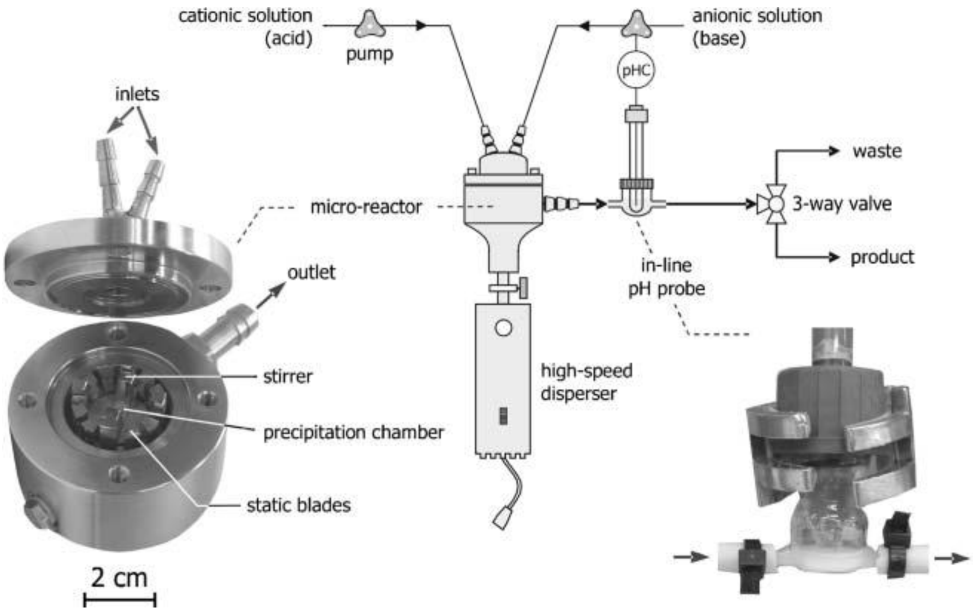

Figure 2.1: ILDP set-up, with photographs of the precipitation micro-reactor and the in-line pH probe. Source: *Santiago et al. 2006*

A new approach in producing pure alumina represents the mineral analogue which was demonstrated to be a unique precursor for alumina with enhanced properties compared to those derived from the conventional Bayer process. Santiago et al. (2006)[4], as mentioned in *Chapter 1*, proposed a novel method of synthesis for ammonium dawsonite (NH_4-dawsonite) by using In-Line-Dispersion-Precipitation Method (ILDP), based on miniaturization of the precipitation chamber down to milliliter scale, higher controlled resistance time and effective stirring. The principle of the ILDP method was explained by Santiago et al. 2006[4] (Figure 2.1).

The acid (aluminum nitrate) and base (ammonium carbonate) solutions used for ammonium dawsonite precipitation were continuously pumped by use of peristaltic pumps into a home-made micro-reactor with an precipitation volume of ca. 6 ml. The micro-reactor holds inside a rotating element attached to a high speed disperser (up to 24 000 rpm), and static blades (Fig.2.1). This provoke a high degree of mixing inside the precipitation chamber, inducing a turbulent regime ($Re \approx 10^5$). The pH of the precipitation resulting aqueous slurry is measured directly at the milliliter reactor outlet being connected to one of the pumps to maintain the preset pH constant[4]. Santiago et al.[4] have proved that the miniaturization of processes to milliliter scale brought important discoveries regarding the mineral analog synthesis. The results showed better control of crystal and particle distribution formation with enhanced properties of the finite product comparing with the conventional ones. Furthermore, these extraordinary results constrained the development research to go deeper in knowledge, forcing the miniaturization to reach the micrometer scale level. No experimental work was found regarding the transfer of ILDP process to micro-scale. Herein, the work is based on a totally novel application of both microreactors and NH_4-dawsonite precipitation reaction. Taking into account the advantages of miniaturization of the systems presented before, the work is focused in precipitating ammonium dawsonite by using an IMM split-recombine Caterpillar microreactor (Figure 1.2, Chapter 1).

2. Experimental section

2.1. Reagents and chemicals

Aluminum nitrate nonahydrated ($Al(NO_3)_3x9H_2O$) purchased from Chem-Lab NV. and ammonium carbonate ($(NH_4)_2CO_3$) from Fluka and J.T.Baker were used as reagents in mineral analog synthesis. A certain amount of $Al(NO_3)_3x9H_2O$ powder, corresponding to a concentration of 1.1M aqueous solution and almost double amount of $(NH_4)_2CO_3$ powder, corresponding to an excess concentration of 2M aqueous solution were first prepared as base and acid solution, respectively by using Milli-Q water. Both aqueous solutions were synthesized in 200ml glass beakers under magnetic stirring (500rpm-1000rpm). The pH was measured by using pH paper and was found to be 2-3 for $Al(NO_3)_3x9H_2O$ and 10 for $(NH_4)_2CO_3$, approximately.

2.2. Methodology and equipment

Miniaturization of the process, at micrometer scale, was adopting the same procedure as ILDP (lattered above), but with respect of microreactor technology the optimization of the parameters and the particularity that the precipitation process will take place in a laminar regime had to be taken into account. A possible set-up is presented further (Figure 2.2a). The acid and base solutions are continuously pumped into Caterpillar split-recombine micromixer with an effective volume of 78 µl and a microchannel width about 0.47mm (ImageJ measurements), 1.47mm approximately within the experimental measurements (Figure 2.2b). As it is shown in Figure 2.2b,c the microreactor presents a very tiny zig-zag channel which is giving the split-recombine approach and a laminar regime of mixing. The two peristaltic pumps (working without pressure) are fixed at different flow rates and are connected to the both inlets of the reactor. The flux is adjusted manually depending on the stroke length and frequency of the pulses. Therefore, the process is not fully continuous but is the closest version for the laboratory scale. The flow rates are managed in such a way that both solution to reach the entrances of the microreactor at the same time. NH_4-dawsonite was first prepared by microsystem using aqueous solutions of 1.1M $Al(NO_3)_3x9H_2O$) and 2M $(NH_4)_2CO_3$ heated at 333K (60^0C) and then sent to the precipitation channel. Syntheses were carried out at constant pH = 7-9 into a laminar regime at the atmosphere pressure. For better adjustment of the process parameters and in the same time for comparative purposes dawsonite synthesis was held further at different value of flow rates and concentrations of acid and base solution. The resulting products were aged at 333 K (60^0C) for 3 h to facilitate the crystal´s control growth, followed by filtration, washing and drying at 333K (60^0C) for more than 12 h (mostly over night). The crystallization process of dawsonite –like materials is different depending on the concentration of ions in each type. For fiber-like crystals the crystallization process occurs as a phenomenon characterized by cannibalizing their own interiors[5]. In general this process is an important factor in overcoming the presence of amorphous phases during the calcinations processes[6] and most of the information was corroborated with natural mineral properties (characterized by fiber, hollow fiber-like crystals) and little knowledge was presented in literature, regarding the mechanism of the analog mineral crystal growth. This could have a great importance in controlling the continuous production of crystalline NH_4-dawsonite inside the Caterpillar microchannel (See more in ***Chapter 5***). For this, the first post-treatment steps of dawsonite slurry including the crystal growth process by stirring followed by the rest of the steps, presented above, was used further in the experimental work.

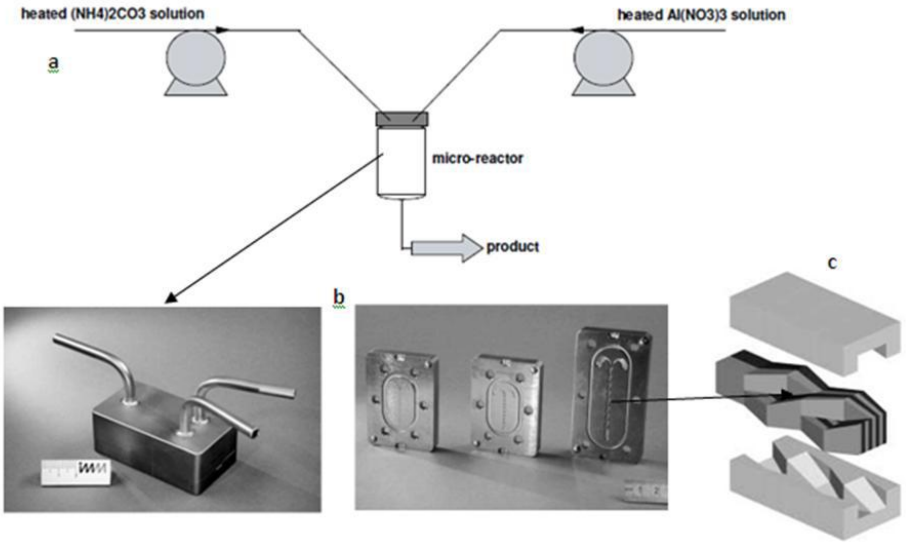

Figure 2.2: a,b,c. Microsystem set-up photo: peristaltic pumps, heaters and the microreactor; b. CPMM1200/8microreactor.Source:http://www.imm-maiz.de/fileadmin/upload_daten/Flyerbrochueren/IMM_TheCatalogue09_low.pdf

2.3. Characterization of NH_4-dawsonite

The crystalline phase of the dawsonite product was investigated by using X-Ray Diffraction Technique (XRD) in a Siemens D5000 diffractometer with Bragg-Brentano geometry and Ni-filtered CuKα radiation ($\lambda = 0.1541$nm). Data were recorded in the range 10-70º 2θ with an angular step size of 0.05^o and a counting time of 5s per step. Thermogravimetric Analysis (TGA) for the only crystalline phase appeared for dawsonite samples ($NH_4Al(OH)2CO_3$) were carried out in a Perkin Elmer model Thermobalance TGA7 device. The analyses were performed in synthetic air with an adjusted flux of 70 ml min^{-1} increasing the temperature from 30^{0}C to 900^{0}C with 5^{0}C min^{-1} temperature step and recording the weight loss function of temperature and its derivative. The morphological properties of NH_4-dawsonite were characterized by scanning electron microscopy (SEM) using a Joel JSM-6400 scanning microscope series with a resolution up to 4nm. The sample particles were deposited on a holder covered with carbon foil and then coated with gold nanoparticles in a very thin film. The gold thin film is used as a conductive material which gives a high secondary electron yield and carries away the charging electrons; this gives better signal and images. The particle size was manually measured by using ImageJ software and the scale was approximated including both hand and software errors.

2.4. Results and discussion

The metal content analysis was necessary for assuring the dawsonite crystalline phase obtained at different parameters (increasing/decreasing specific parameters as flow rate (ml/min) and/or concentration (M). The results of crystalline dawsonite prepared are shown in Table 2.1. The experimental section was following two important issues: one referring to the optimization of process parameters by playing with aqueous solutions concentrations and/or flow rates and the second one was taking into account the aggregation phenomena and crystal growth during and post process.

Table 2.1. Experimental parameters used, time of production and average particles size of dawsonite powder

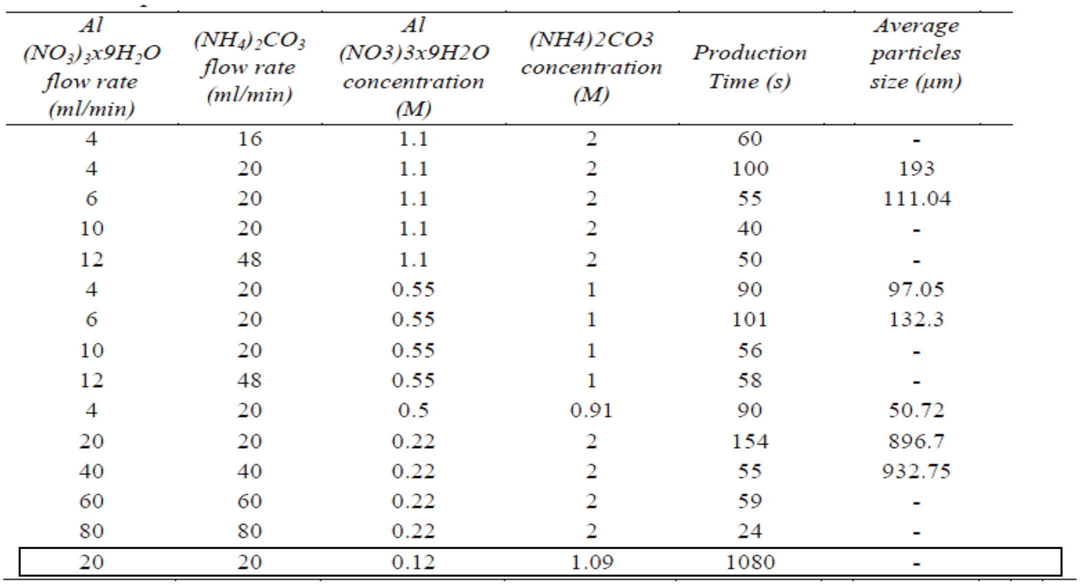

Al $(NO_3)_3x9H_2O$ flow rate (ml/min)	$(NH_4)_2CO_3$ flow rate (ml/min)	Al (NO3)3x9H2O concentration (M)	(NH4)2CO3 concentration (M)	Production Time (s)	Average particles size (μm)
4	16	1.1	2	60	-
4	20	1.1	2	100	193
6	20	1.1	2	55	111.04
10	20	1.1	2	40	-
12	48	1.1	2	50	-
4	20	0.55	1	90	97.05
6	20	0.55	1	101	132.3
10	20	0.55	1	56	-
12	48	0.55	1	58	-
4	20	0.5	0.91	90	50.72
20	20	0.22	2	154	896.7
40	40	0.22	2	55	932.75
60	60	0.22	2	59	-
80	80	0.22	2	24	-
20	20	0.12	1.09	1080	-

Table 2.2. Experimental parameters and process characteristics

Sample Code	Reagent concentration (M)		Reagent flow rate (ml/min)		pH	Total flow rate (µl/s)	Time of production (s)	Residence time* (s)	Comments
	$Al(NO_3)_3$x $9H_2O$	$(NH_4)_2CO_3$	$Al(NO_3)_3$x $9H_2O$	$(NH_4)_2CO_3$					
PD3	1.1	2	4	16	8	333.33	60	0.23	Crystalline
PD4	1.1	2	3	16	8	316.66	46	0.24	Crystalline
PD1	1.1	2	12	16	8	466.66	50	0.17	Amorphous
PD2	1.1	2	12	48	8	1000	60	0.08	Crystalline
S5	1.1	2	3.5	16	8	325	60	0.24	Amorphous
PD6	1.1	2	4	20	9	400	100	0.2	Crystalline
S9	1.1	2	20	24	8	733.33	40	0.1	Amorphous
PD5	1.1	2	8	20	8	466.66	50	0.17	Amorphous
S11	1.1	2	14	26	3	666.66	∞	0.13	Amorphous
PD9	1.1	2	6	20	9-10	433.33	55	0.18	Crystalline
PD8	1.1	2	10	20	7-8	500	40	0.16	Crystalline
PD10	0.55	1	4	20	9	400	90	0.2	Crystalline
PD11	0.55	1	6	20	8	433.33	101	0.18	Crystalline
PD12	0.55	1	10	20	8	500	56	0.16	Crystalline
PD13	0.55	1	12	48	8	1000	58	0.08	Crystalline
S19	0.3	0.55	4	20	9	400	∞	0.2	Uncertain**
S20	0.4	0.73	4	20	8-9	400	∞	0.2	Uncertain**

* Residence time = (total flow rate/effective volume) (78µl); ∞ - channel not clogged or the initial solutions finished; **No sample after filtering.

First, the concentration of 1.1M for aluminum based solution, respectively 2M for carbonate based solution were kept fixed and their flow rates were increased (4-12ml/min for ($Al(NO_3)_3x9H_2O$)), 16-48ml/min for ($(NH_4)_2CO_3$)). A white precipitate was obtained during an interval of some seconds till 18 minute showing both crystalline and amorphous phases (See tables 2.1.,2.2) but also some of the trial presented a non reacting product (clean solution obtained, Table 2.2°).

Second step in process optimization was to equal the flow rate for both initial aqueous solutions and decrease the concentrations (down to 0.12M ($Al(NO_3)_3x9H_2O$)/1.09M $(NH_4)_2CO_3$) reaching the higher ratio (9.08) between the concentrations which is able to produce crystalline product), in order to evaluate entire microsystem performance.

Table 2.2. Experimental parameters and process characteristics

Sample code	Reagent concentration (M)		Reagent flow rate (ml/min)		pH	Total flow rate (µl/s)	Time of production (s)	Residence time* (s)	Comments
	$Al(NO_3)_3x$ $9H_2O$	$(NH_4)_2CO_3$	$Al(NO_3)_3x$ $9H_2O$	$(NH_4)_2CO_3$					
S21	0.48	0.87	4	20	9	400	∞	0.2	Uncertain°
S22	0.5	0.91	4	20	8	400	90	0.2	Crystalline
S23	1.1	2	4	20	8-9	400	94•	0.2	Crystalline
S23u	0.55	1	4	20	8	400	90•	0.2	Crystalline

•Time of production under ultrasound influence; u - ultrasound

Table 2.3. Experimental parameters – new approach – fixed concentration and different fluxes

Sample code	Reagent concentration (M)		Reagent flow rate (ml/min)		pH	Total flow rate (µl/s)	Time of production (s)	Residence time* (s)	Comments
	$Al(NO_3)_3x$ $9H_2O$	$(NH_4)_2CO_3$	$Al(NO_3)_3x$ $9H_2O$	$(NH_4)_2CO_3$					
S24	0.22	2	20	20	8	666.66	109	0.12	Crystalline
S26	0.22	2	20	20	9	666.66	Batch	0.12	Amorphous
S29	0.22	2	40	40	8-9	1333.33	55	0.06	Crystalline
S31	0.22	2	60	60	8-9	2000	50	0.04	Very Crystalline
S34	0.22	2	80	80	9	2666.66	23	0.03	Crystalline

By using lower concentrations of aqueous solutions less amount of substances were introduced in the system, the aggregation phenomenon was reduced, and the time of production was increased (e.g. 1080 seconds, See Table 2.1 and 2.3).

The flow rates were chosen to be equaled with the aim of controlling the pressure drop inside the microchannel. All experiments presented in Table 2.2 showed a strong relationship between physical and chemical process parameters and time of production. Moreover, the product crystallinity is improved for precipitation process characterized by similar values of residence time inside the microchannel. Even though, the concentration ratio between the two solutions presented remained unchanged during all these trials some uncertainties stepped forward and could be explained in terms of crystal growth process influenced more by concentration of the aqueous solutions than residence time of the precipitation process (or flow rate adjusted for each experiment). They are marked in Table 2.2 (°).

Figure 2.3: Microsystem set-up photo: a-mechanic heaters, b- peristaltic pumps and c- the microreactor immersed inside a Bandelin Sonorex ultrasonic bath.

Particle size of the precipitate was determined and was found to be in the range of hundreds of µm which can be related with the aggregates formation. Some of the results are shown in Table 2.1. This range, in passive mixing facilitates the wall attraction forces to increase and in the same time the deposition effect to appear. To avoid the accumulation inside the microchannel and control the aggregation process a new device was added to the set-up with the aim of crush these aggregates into smaller particles. This device was a BANDELIN SONOREX DIGITEC DT 514 BH ultrasonic water bath (sonicator) as is shown in Figure 2.3. The ultrasound phenomenon was applied as one of the three important solutions in overcome the aggregation and wall forces inside the microchannel and induce better mass and heat transfer[7]. Two different experiments were selected for ultrasound trials. First the pumps were adjusted for continuous pumping of 4 ml/min as base solution flux and 20 ml/min as acidic solution flux. The concentration of the aqueous solutions was 1.1M and 2M for acidic and base solutions, respectively. As shown in Table 2.2 these parameters were optimum for producing high quantity of crystalline dawsonite. Under the action of ultrasound waves for a period between 5 to10 minutes no significant changes appeared and the time of production was nearly the same (See table 2.2•). The extra factor applied, in this case had no importance. Furthermore, the second trial under ultrasound conditions was selected from the above experiments with the particularity that the flow rates were fixed at 4 and 20 ml/min for acidic and base solution, but their concentrations were decreased to 0.55M for aluminum aqueous solution and 1M for carbonate one. The same results were obtained as the process performed at normal parameters and no significant changes were found (See table 2.2•).

Adjusting the quantity of moles from each aqueous solutions by fixing the concentration of base solution at 2M and decreasing 5 times the acidic solution concentration (used initial concentration was 1.1M) and equal the flow rates for both aqueous solutions, a new experimental approach has been developed in order to understand better the mixing process and also to reduce de pressure drop inside the microchannel which has a large influence over the precipitation process. The results are presented in Table 2.3 and are showing a tide correlation between the time of production and the flux. The time of production increases proportionally to the decrease of the same flow rate of both solutions (See Figure 2.4). For intermediate values (40 ml/min and 60 ml/min) of the flux no significant influence was reached but the dependency is given by the extremities of the analyzed data (20 ml/min and 80 ml/min, respectively).

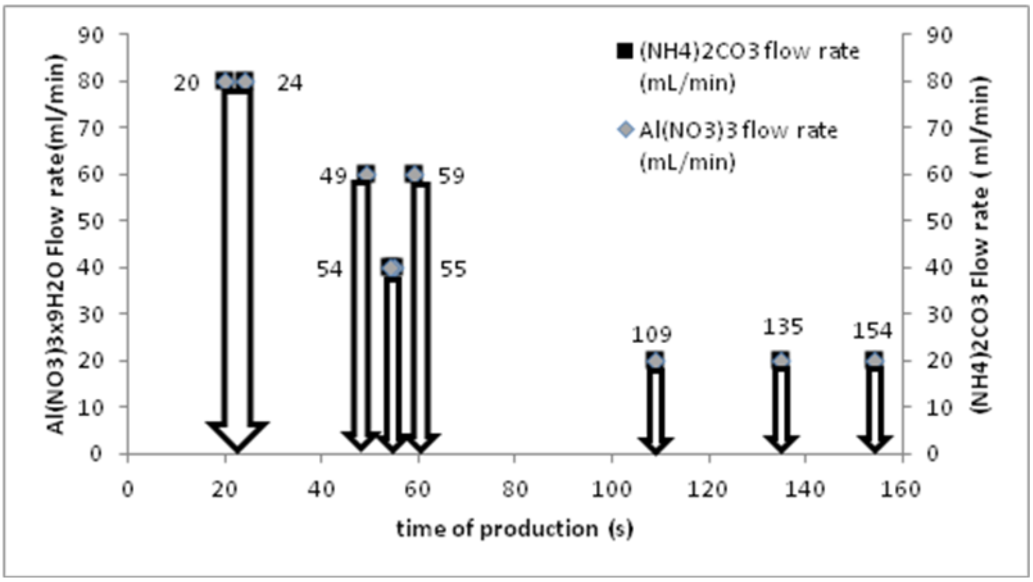

Figure 2.4. Time of production tendency as a function of flow rate modification.

The optimal flow rate for running the experiments in these mentioned conditions was found to be 20 ml/min equal for both aqueous solutions (Fig. 2.4). This information pushed the research further giving the opportunity to explore in deeper level of understanding the microfluidic processes applied for producing solids.

The next step in determining the optimal process parameters in order to have a continuous NH_4-dawsonite production was to adjust the system to run at fixed flow rate and different concentrations of the mother solutions. The fix flux was adjusted for the same value for both pumps (20 ml/min) and the concentrations were decreased step by step (See Table 2.4). The experimental aim for this level of trials was to determine the minimum concentration ratio which can be transformed into crystalline dawsonite. By leveling the flow rates to the same value and keeping this value constant the pressure drop inside the channel was controlled and minimized. Based on this, by decreasing the concentrations of both aqueous solutions the results obtained confirmed the hypothesis this experimental part started with. The time of continuous production exceeded the maximum value of about 18 minutes at lowest values of the concentration. A primary system optimization was achieved, which represents a step forward in development of solids microtechnology production.

Table 2.4. Experimental parameters – fixed flow rate versus different concentration of both aqueous solutions

Sample code	Reagent concentration (M)		Reagent flow rate (ml/min)		pH	Total flow rate (µl/s)	Time of production (s)	Residence time* (s)	Comments
	$Al(NO_3)_3$x $9H_2O$	$(NH_4)_2CO_3$	$Al(NO_3)_3$x $9H_2O$	$(NH_4)_2CO_3$					
S38	0.15	1.36	20	20	9	666.66	96	0.12	Crystalline^{o}
S43	0.13	1.18	20	20	9	666.66	250	0.12	Crystalline•
S46	0.12	1.09	20	20	9	666.66	1080	0.12	Crystalline
S39	0.11	1	20	20	9	666.66	∞	0.12	Amorphous

^{o}crystal´s type: rods (same shape as sodium dawsonite crystals); ∞ - channel not clogged or the initial solutions finished; • very few crystallinity, more amorphous but with some specific reflections;

The metal content in NH_4-dawsonite was determined by X-Ray Diffraction technique (XRD) and matches the pure synthetic analogue reference pattern ($NH_4AlCO_3(OH)_2$, JCPDS 42-250) see Figure 2.5. As shown in the diffractograms the dried precipitate typically exhibited the NH_4-dawsonite crystalline phase only at specific process parameters and known concentrations of the initial solutions (see also Tables 2.3, 2.3, 2.4). No traces of impurities reflection were found. The high crystalline phase was obtained for concentrated aqueous solutions with a ratio of 1.8 and higher ratio between the flow rates used (See table 2.2 and Figure 2.5a, b). Increasing the time of production by adjusting the optimal parameters (see Table 2.3,2.4) the crystalline phase of the dawsonite powder decreased (See figure 2.5c, d) but the size of the crystals increased taking into account the Scherrer equation theory[8]. Thermogravimetric analysis (TGA) confirms the purity of the product (Figure 2.6). The thermal process of ammonium dawsonite in synthetic air shows a one-step weight loss for most of the samples analyzed in the range 30-200^{0}C (Figure 2.6.a) and two-step weight loss(See Figure 2.6 b) appearing at different temperature intervals (30-200^{0}C and 200-300^{0}C). The total weight loss of each sample involved was in the range 40-61%. This indicates that product weight loss obtained is comparable with the ideal value (63%) which indicates high purity product. One-step thermal decomposition process characterizes a higher purity ammonium dawsonite, meanwhile two-steps or more thermal decomposition is reducing the product purity at specified precipitation parameters (See Figure 2.6.b, sample PD13).

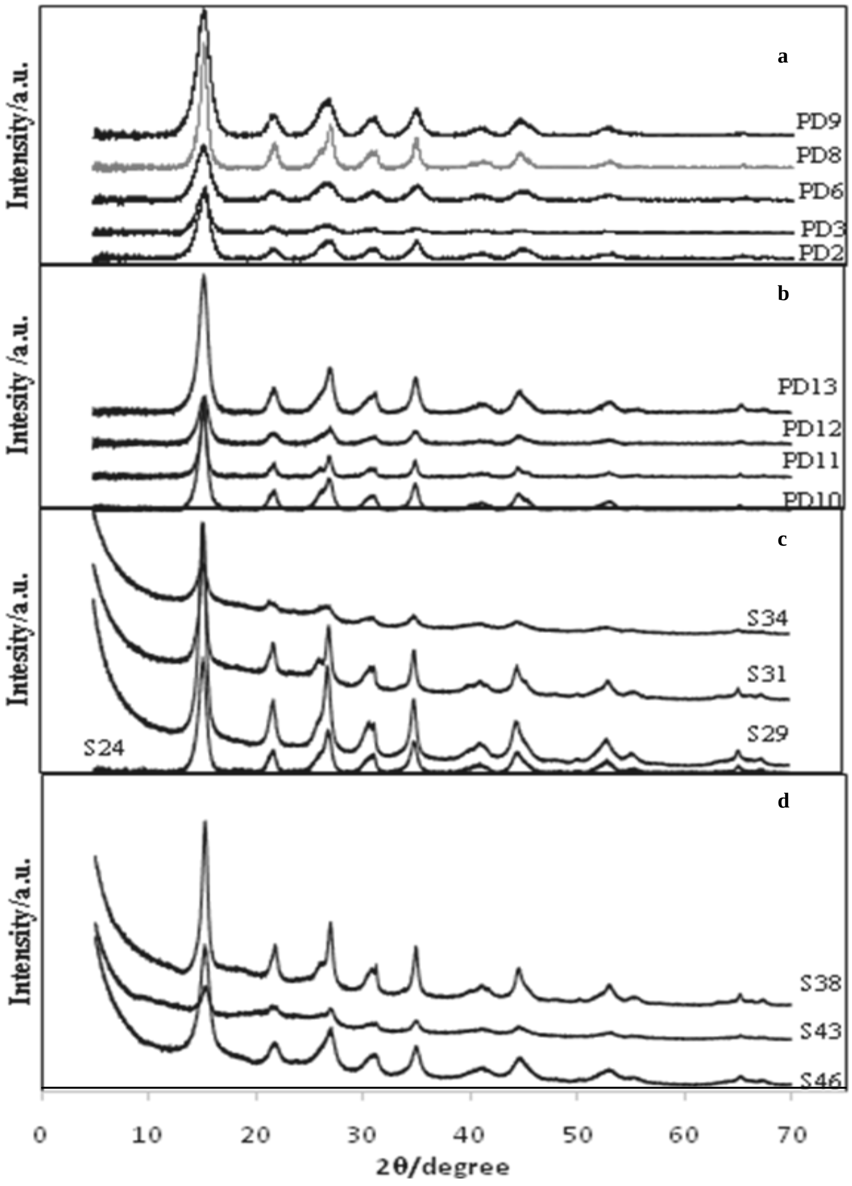

Fig2.5. X-ray diffraction spectra of NH4-Dawsonite at different process parameters: a - fix concentration (1.1M for basic solution versus 2M for acidic one, respectively) and modifying the flowrate; b – fix lowered values of concentration (0.55M for basic solution and 1M for acidic one) and modifying the flowrate; c – fix values of concentration with different ratio than experimented before (0.22m for basic solution and 2M for acidic one) and equal values for the flowrate modified step by step; d – fixed equal flowrates (20ml/min for both solutions) and decreasing the concentration till the limit of precipitating crystalline dawsonite (0.12M for basic solution versus 1.09M for acidic one). See also tables 2.2, 2.3 and 2.4.

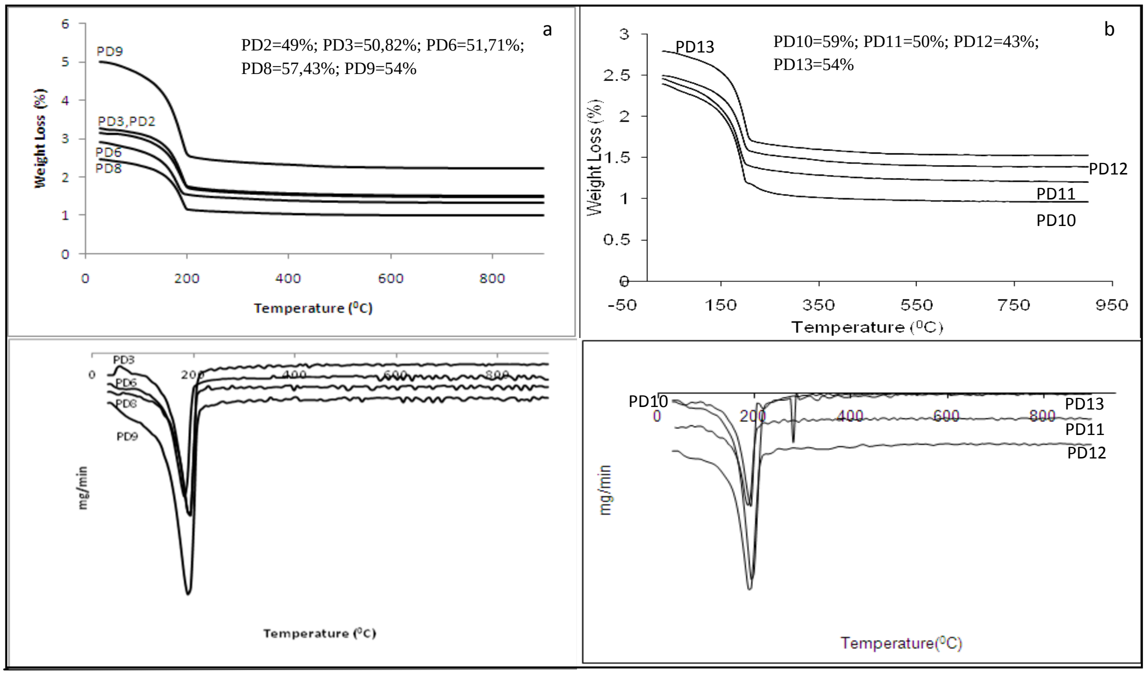

Fig2.6. Thermogravimetric analyses in synthetic air: a. Thermal decomposition profiles and thermal transitions steps of NH4-Dawsonite at fix concentration (1.1M for basic solution versus 2M for acidic one, respectively) and modified flowrate; b. Thermal decomposition profiles and thermal transitions steps of NH4-Dawsonite fix lowered values of concentration (0.55M for basic solution and 1M for acidic one) and modifying the flowrate.

An interesting correlation can be distinguished between aqueous solutions flow rate, concentration and particle size of the product. By decreasing the concentration of both solutions at fixed flow rate the average particle (aggregate) size of the precipitate obtained is decreasing too (Table 2.1 and Figure 2.9). SEM analysis confirms these observations (Figures 2.7 and 2.8). As micrographs show the morphological properties of the product obtained in these specific conditions, it presents the average size measured for aggregates and not for individual particles. The aggregation is probably formed after stirring for 3 h at 60^0C the slurry obtained by precipitation. Crystal growth was demonstrated to be dependent of the hydrodynamic effect that results from a faster solution velocity around larger crystals (analogous to the Bernoulli effect). The stirring effect increases the rate of crystal growth but does not confirm that the growth process would be constant for each of the crystals formed. Depending on the crystal geometrical shape the specific phenomena, which provoke the growth, could be advection or diffusion[9]. This might explain the different crystal size which led to the aggregation phenomenon found by SEM analyses.

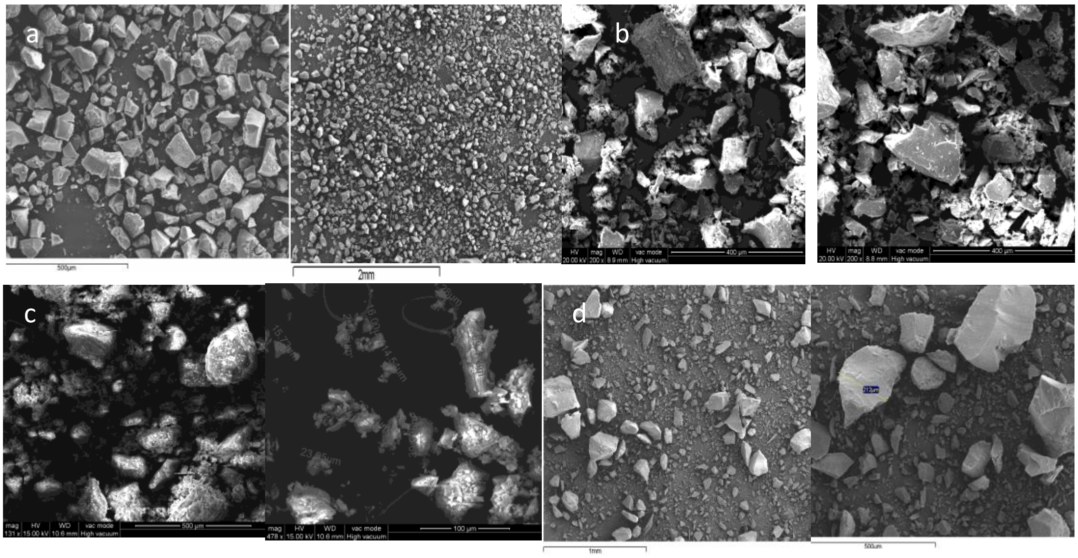

Fig.2.7: Scanning electron micrographs of crystalline N4-Dawsonite at different process parameters: a. Sample PD6 (average aggregate size of 193µm); b. Sample PD9 (average aggregate size of 111,04 µm); c. Sample PD10 (average aggregate size of 97.05µm); d. Sample PD11(average aggregate size of 132,3 µm). Detailed information on selected process parameters are presented in Table 2.1.

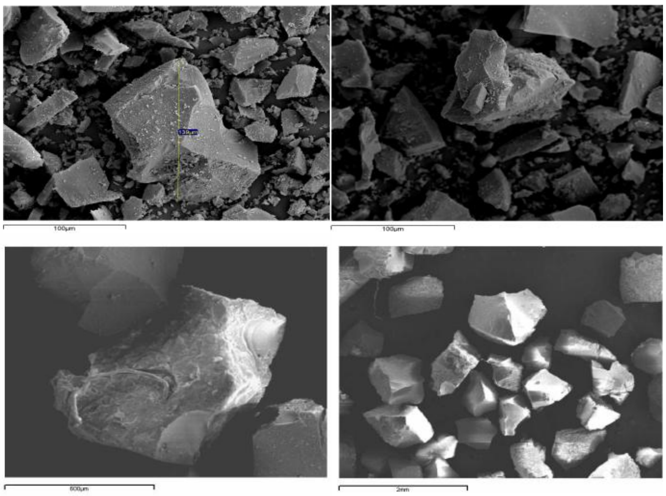

Fig.2.8: Scanning electron micrographs of crystalline N4-Dawsonite at different process parameters: a. Sample PD15 (average aggregate size of 50,718µm – process parameters: flowrate 4ml/min for aluminum solution (0,5M) and20ml/min for carbonate solution (0,91M)); b. Sample S29 (average aggregate size of 923,75µm – process parameters: flowrate 40ml/min for both aqueous solutions with increased concentration ratio regarding the carbonate excess);

The low values of the residence time within precipitation process, which differs for each experiment varying from 0.1 to 0.2 s, is a great advantage in terms of reaction speed and in controlling the particles formation comparing with the conventional process.

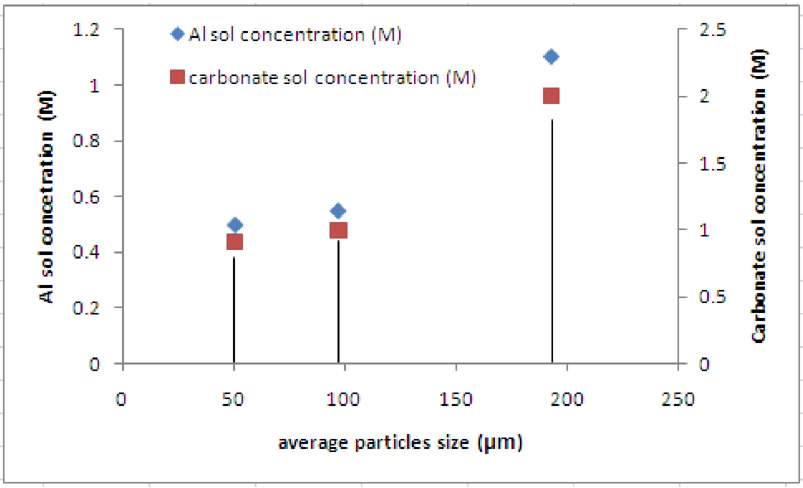

Fig.2.9: Concentration influence over the average aggregates size formation.

Accordingly with those lattered above further experimental work was needed at this point, in order to understand better the correlation between physical and chemical factors that could influence the kinetics of the precipitation process and crystal formation, how perfect mixing is influencing or has no influence on the formation of crystalline NH_4-dawsonite. Following the hypothesis of this doctoral work, in *Chapter 3*, new experimental conditions (pressurized system) were outlined and a new set-up was developed.

3. Conclusions

In this Chapter ammonium dawsonite was successfully prepared within the channel of IMM Caterpillar microreactor by precipitation reaction. The limited production time interval was increased by adjusting the flow rate and the concentration of the acidic and base solutions, reaching 18 minutes. Using XRD and TGA techniques the metal content, crystalline phase and purity of the product were illustrated. Large crystals were determined inside the catalyst and high purity interval (60-95%) was confirmed. SEM analysis characterized the morphology of the aggregates obtained by showing the shape and size, but in the same time opened new questions that have to be solved. In general terms, microreactor technology can be applied to synthesize ammonium based catalyst precursors but more research is needed in order to demonstrate the real advantages of this micro scale approach.

References

[1] Chatterjee K. K., 2007, Uses of Metals and Metallic Minerals, New Age Publications, ISBN: 8122420400 , 8122425119;

[2] Santen R.A., Leeuwen P.W.N.M., Averill J. A., 2000, Catalysis: An Integrated Approach, React.Kinet.Catal.Lett.,Vol.69, no.1, 199-200;

[3] Schütz F., Unger K., , 1997, Handbook of Heterogeneous Catalysis, Eds. G. Ertl, H. Knözinger, J. Weitkamp Wiley-VCH, Weinheim, Vol.2, 72-86;

[4] Santiago M., Yalfani M. S., Pérez-Ramírez J., 2006, In-line dispersion–precipitation method for the synthesis of metal-substituted dawsonites. Genesis of oxide materials with superior properties, J. Mater. Chem.16, 2886–2889; DOI: 10.1039/b607031k;

[5] Moore J., Adams M., Allis R., Lutz S., Rauzi S., 2003, CO2 Mobility in Natural Reservoirs Beneath the Colorado Plateau and Southern Rocky Mountains: An Example from the Springerville-St. Johns Field, Arizona and New Mexico, prod75-inter1.netl.doe.gov;

[6] Stoica G. and Pérez-Ramírez J., 2007, Reforming Dawsonite by Memory Effect of AACH-Derived Aluminas, Chem. Mater., 19 (19), pp 4783–4790;

[7] Stankiewicz A., 2007, On the Applications of Alternative Energy Forms and Transfer Mechanisms in Microprocessing Systems, Ind. Eng. Chem. Res., 46, 4232-4235;

[8] Patterson A. L.,1939,The Scherrer Formula for X-Ray Particle Size Determination, Physical Review, vol.56, 978-982;

[9] Kile E. D. and Eberl D.D, 2003, On the origin of size-dependent and size-independent crystal growth: Influence of advection and diffusion, American Mineralogist, vol.88, 1514-1521;

Chapter 2

NH_4-dawsonite production within a Caterpillar microcreactor

Chapter 3

Continuous synthesis of porous Ammonium Dawsonite within a new microstructured system

Based on practical advantages that microsystems are offering: better yield and selectivity, better heat and mass transfer which improve the product quality, running a chemical reaction close to the kinetic limits, controlled residence time and temperature which lead to a better conversion and increased product quantity, safer: the hold-up of the reactive species within the reactor volume is minimized, reducing the hot spots[6] etc., a new precipitation set-up was proposed and developed by our group. The multiple usage of NH_4-dawsonite: ingredient in antacids, stabilizer in polymer, dry extinguisher in fuel leak fire, additive in synthetic fertilizer and most important the production of very pure α-Al_2O_3 by thermal decomposition determine an increase interest for novel, faster, easier, risk reduced and more economical production technologies for present catalyst precursor.

The chapter deals with the preparation of nano-sized ammonium dawsonite ($NH_4Al(OH)_2CO_3$) with a substantially uniform size distribution and a substantially uniform pore size distribution by continuous precipitation in a stainless steel CPMM pressurized system at constant temperature, pH and residence time .

Chapter 3

Continuous synthesis of ammonium dawsonite within a new microstructured system

1. Introduction

Mixing ultra-small volumes of liquid in range of picoliters could be possible by using molecular diffusion, however mixing larger volumes in a laminar regime, where turbulences are absent, might require more than just diffusion phenomenon[1]. Within a microchannel, at low Reynolds numbers is difficult to achieve a perfect mixing and often is required combinations of both convection and diffusion to reduce processing times, path lengths, and pressure drops to acceptable levels. At the same time at low Reynolds number mixing is controlled by molecular diffusion, inducing the growth of vortices which stretch and fold fluid streams reducing the time and the length of channel required to mix the fluid components[2,5].

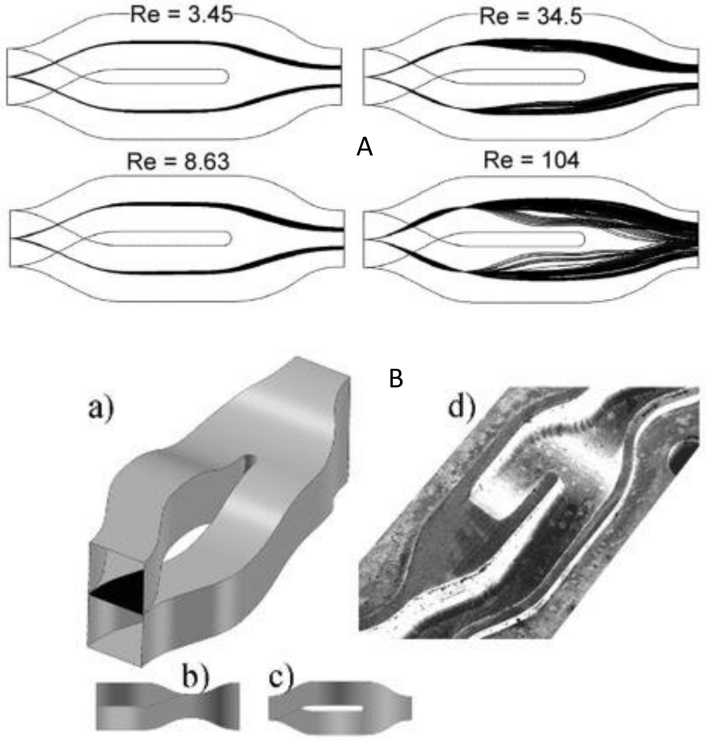

Fig. 3.1.A) Secondary flows appear in a split-and-recombine caterpillar microstructured mixer at high Re number, as imaged by particle tracking simulations. B) Left: geometry model of an optimised SAR mixer – a) slanted view with the splitting layer shown in black; b) side and c) top views. Right: scanning-electron micrograph of the lower channel part. The image shows one step of a SAR mixer made of stainless steel with a minimum channel cross section of 1 mm and a length of 6 mm. Source: *Schönfeld et al., 2004.*

The precipitation of NH_4-dawsonite was held inside the identical IMM Caterpillar micro-mixer with a split-recombine approach[7] performing multiple splitting and recombination of liquid component as reported in *Chapter 2*. The splitting approach of the flow streams inside a split and recombine (SAR) mixers is overlap by secondary recirculation flow at practical Reynolds numbers (Re) for most liquids which can be imaged, *i.g.*, by particle-tracking simulation which give “diffusive” patterns at high Re (See Figure 3.1A). The formation of the multi-lamellae within a SAR was shown to distinguish features of chaotic mixing due to exponential increase of chaotic stretching described by Lyapunov exponent (See Figure 3.1B)[3,5]. Studies regarding mixing inside both type of micromixers (passive and active one) reveal more and more characteristics that had to be taking into account when a synthesis starts. An important parameter that represents the key in calculating the dimensions of the micromixer capillary channel represents the pressure drop inside the channel. The pressure drop along the microchannel must be considered when designing micromixers as these devices are appointed for integration with other microfluidic components. For a straight microchannel with no obstructions, i.e. a conventional Y-type mixer, the pressure drop is ≈ 5.5 Pa mm^{-1} and the mixing very poor. For a channel presenting several angle types of obstructions the pressure drop increased substantially (≈ 61.7 Pa mm^{-1}) but the best mixing resulted[4].

Studies regarding the pressure drop inside the microchannel of the split-recombine Caterpillar micromixer were studied and published by Institut für Mikrotechnik Mainz GmbH and showed an exponential dependency between the pressure drop and flow rates used (see Figure 3.2). Higher the flow rate is higher the pressure drop inside the zigzag microchannel (certain angels for the obstructions) will be. As the micro-mixer used for NH_4-dawsonite production is represented by CPMM1200/8 (R1200 from Figure 3.2) and precipitation process was running into a laminar regime with a chaotic mixing approach, information regarding the pressure drop inside the microchannel was important to be taken into account.

The precipitation conditions described in *Chapter 2,* with the specification that the microsystem was developed to work at high pressures, were applied. Uniform size distribution and nano-sized ammonium dawsonite particles production was controlled by choosing an optimal flow rate for both mother solutions and increasing the system pressure at 1bar.

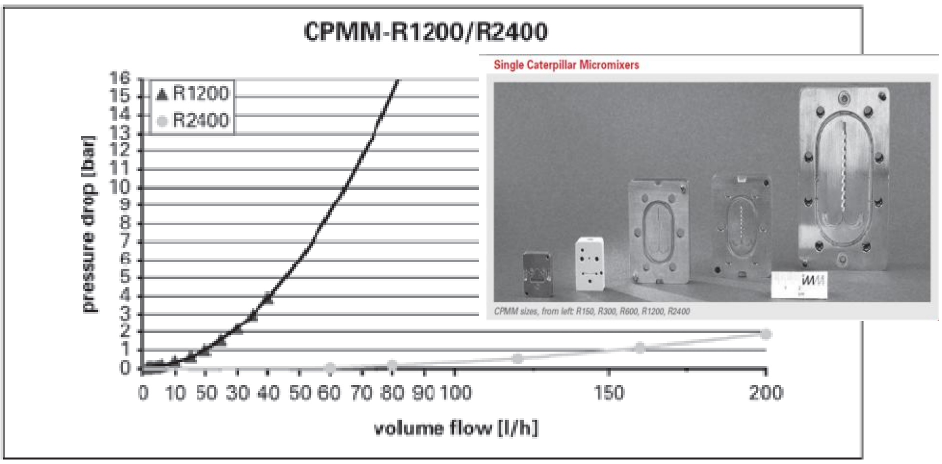

Fig. 3.2. Pressure drop as a function of the flow quantity streamed through both inlets

Crystallites having a size from 7nm to 20nm assembled into particles having a size till 70nm were found using XRD (X-Ray Diffraction) and TEM (Transition Electron Microscopy) techniques. Product purity was characterized by TGA (Thermogravimetric) techniques by comparing the weight loss values with the ideal one, 63% weight loss. The catalytic activity of the powder obtained was characterized by N_2-adsorption at 77K and higher BET surface area values were found regarding the values obtained for ammonium dawsonite synthesized by conventional batch precipitation (~300 m^2/g). The limiting production time was increased using pressurized system.

Experimental section

1.1. Metodology and materials

The reagents used for precipitation of NH_4-dawsonite within the new microsystem under-pressure were aluminum nitrate nonahydrated ($Al(NO_3)_3x9H_2O$) purchased from Chem-Lab NV. and ammonium carbonate ($(NH_4)_2CO_3$) from Fluka and J.T.Baker as presented in the previous chapter. Milli-Q water was used for aqueous phases in microfluidic system. The synthesis was carried out at constant pH (8) and temperature (60^0C) tuning the residence time as a function of flow rate (modified by the pressure applied). In this case the working regime was transformed more into a turbulent one by conducting the precipitation inside through active chaotic mixing.

The expected result was to increase the time of production by controlling the dawsonite crystal formation and to increase the yield of the process (increased the conversion into the wanted product). It is demonstrated in the literature that the yield of a reaction depends on the residence time[8] as shown in the Figure 3.3. Faster the reaction runs higher the conversion of the finite product is.

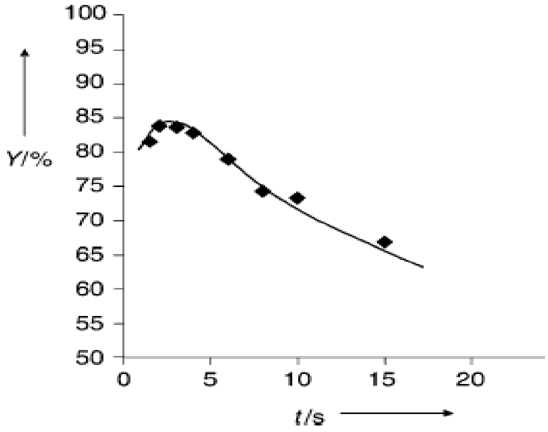

Fig.3.3: Dependence of yield (Y) on residence time (t) for a microstructured reactor at a reaction temperature of 50^0C. Source: Jähnisch et al. 2004

Considering the residence time as was calculated in *Chapter 2* (0.1s, 0.2s) and the knowledge lettered above, maintaining precipitation approach at microscale[7] as simple as possible, the optimization of the process parameters based on applied pressure was achieved within the new microstructured system proposed. The pressurized set-up is presented further (Figure 3.4). The system pressure was adjusted by the pressure dumper in such a way that the pressure drop inside the microreactor was reduced as much as possible. The acid and base solutions are continuously fed with metering pumps into the microreactor whereas the pressure inside the system is adjusted at 1 bar. Both metering pumps could reach up to 16 bars and the flow rates can be modified within the automatic software fixing the stoke length and stroke rate in the same time. The connection with the microreactor inlets was made by one meter compact stainless steel coil for each inlet (see Fig.3.4 a), in order to have a better control of heat transfer from inside-outside or/and vice versa and simultaneously enhance the reaction time.

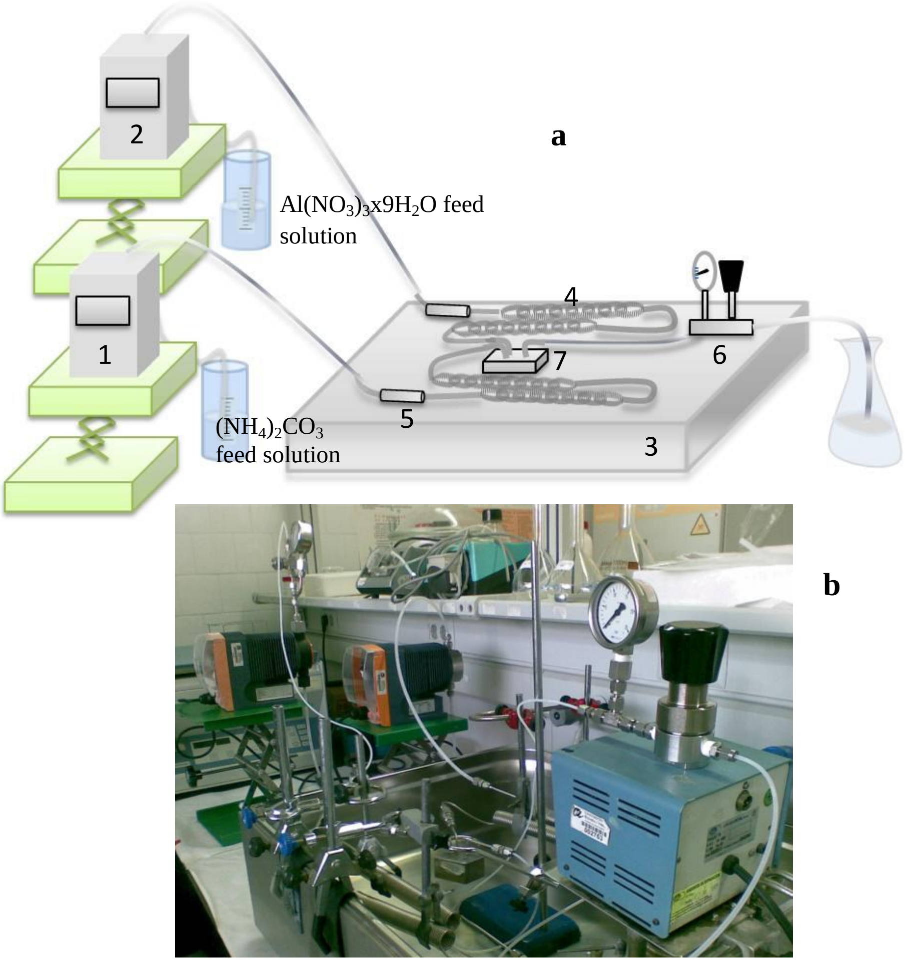

Fig.3.4: a) Microsystem set-up fitted for pressure 1 bar: 1 – Metering pump (for $(NH_4)_2CO_3$ initial solution), 2 – Metering pump (for $Al(NO_3)_3$ initial solution), 3 – Water bath, 4 – Stainless steel coil, 5 – Check valves, 6 – Pressure dumper, 7 – Caterpillar microreactor CPMM1200/8; b) Lab-scale microsystem set-up photo.

NH_4-dawsonite was first prepared by using four different concentrations of aqueous solutions of $Al(NO_3)_3x9H_2O$) and $(NH_4)_2CO_3$ which were mixed at 333K (60^{0}C) inside the precipitation channel. Syntheses were carried out at constant pH = 9 into a laminar regime mixed with a turbulent one (under the pressure influences). For comparative purposes dawsonite synthesis was held further at different value of flow rates of acid and base solution (see table 3.1). The resulting products were aged at 333 K (60^{0}C) for 3 h, followed by filtration, washing and drying at 333K (60^{0}C) for more than 12 h. The post-precipitation treatment stirring step at 60^{0}C for 2 or 3 hours (see ***Chapter 2)*** was skipped for avoiding the micro-sized crystals growth within the final product.

Table 3.1: Process parameters used within the both systems studied

Sample code	Aqueous solutions concentration (M)		Aqueous solutions flow rate (mL/min)	
	$Al(NO_3)_3x9H_2O$	$(NH_4)_2CO_3$	$Al(NO_3)_3x9H_2O$	$(NH_4)_2CO_3$
S13	1.1	2	10	20
S18	0.55	1	12	48
S24	0.22	2	20	20
S44	0.12	1.09	20	20

Also, the results were compared with those obtained for the same process parameters performed at atmospheric pressure[7], those listed in the literature[9] and the results obtained through the precipitation process at miliscale[10].

1.2. Characterization of NH_4-dawsonite at pressure 1 bar

The metal content of the dawsonite product was investigated by X-Ray Diffraction Technique (XRD) by using similar Siemens D5000 diffractometer for characterization of crystalline/amorphous phases that could appear for nonhydrated dawsonite ($NH_4Al(OH)_2CO_3$). Thermogravimetric analysis (TGA) performed within identical Mettler Toledo TGA/SDTA851e microbalance was to determine the purity of these products. Synthetic air and inert gas (N_2) flow were used for drawing the thermal curves, ramping temperature from 30 to 900^0C with 10^0C/min.

The morphological properties, particle size distribution and particle size values of NH_4-dawsonite were characterized by TEM (Transition Electron Microscopy) using a JEOL JEM-1011 microscope operated at 100 kV. The sample preparation for TEM analysis was following some specific determined steps: one or two droplets of the sample suspended in ethanol/acetone were placed on a carbon-coated copper grid (shining side) followed by evaporation at ambient conditions or for less than 2 minutes within an oven adjusting the temperature at 60^0C. The TEM images were processed by Image-J software. One of the most important characteristics of a catalyst is the porosity that leads to catalytic activity characterization. BET surface area value and micro and/or meso pores inside the product were analyzed by N_2-adsorpition at 77 K using a Micrometrics ASAP 2000 device.

2. Results and discussion

The pressure influence over the final product was investigated. Furthermore, the comparison between product obtained by using microsystem at atmospheric pressure and the product obtained with the system at 1bar gave us a better understanding regarding the precipitation process at microscale and also, about the optimal conditions that had to be applied in order to enhance the catalyst properties. First, the microsystem ran with the highest concentrations for both aqueous solutions ($Al(NO_3)_3$ – 1.1M and $(NH_4)_2CO_3$ – 2M) and their corresponding flow rates (10ml/min $Al(NO_3)_3$ and 20ml/min $(NH_4)_2CO_3$) at fixed 1bar of pressure. Step by step, all chosen process conditions followed the same procedure till were reached the minimum possible values (See Table 3.1) both for aqueous solution concentration and flow rates ($Al(NO_3)_3$, 0.12M, 20 ml/min and $(NH_4)_2CO_3$, 1.09M, 20 ml/min) which lead the precipitation to crystallites formation. A white solid precipitate was synthesized meanwhile the time of production was searched (See Table 3.2). Results shown in Table 3.2 confirm an increase up to 5 times in the time of production by running the precipitation at 1bar pressure and decreasing the concentration of both aqueous solutions.

Table 3.2. Time of production values at different process conditions.

Substance concentration (M)		Substance flow rate (ml/min)		Time of production (s)	
$Al(NO_3)_3$x $9H_20$	$(NH_4)_2CO_3$	$Al(NO_3)_3$x $9H_20$	$(NH_4)_2CO_3$	System at atmospheric pressure	System at pressure 1bar
1.1	2	10	20	40 (S13)	245 (S1-S4)
0.55	1	12	48	58 (S18)	260 (S5group)
0.22	2	20	20	109 (S24)	191 (S7group)
0.12	1.09	20	20	558 (S44)	371 (S8group)

S1-S4, S5group, S7group and S8group represents the experiments within the new set up.

The crystalline phase was analyzed for all samples obtained, under specific process conditions. Almost all experiments conducted at pressure 1bar showed lower crystallinity comparing with those obtained by the system at atmospheric pressure.

Traces of ammonium nitrate (NH_4NO_3) were found within trials experimented at high concentration of initial aqueous solutions (see Figure 3.5).

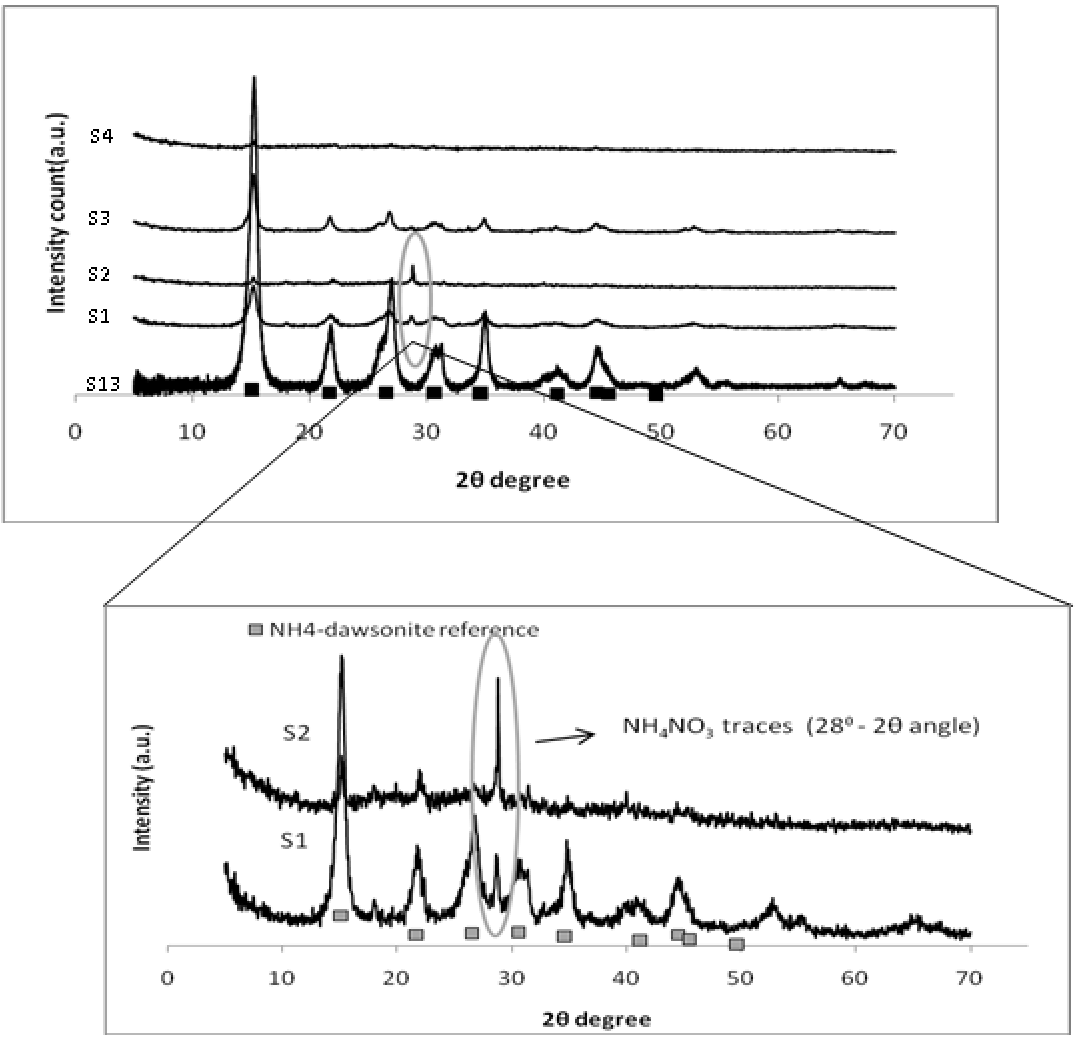

Fig.3.5: X-Ray Diffraction spectrum of crystalline and amorphous NH_4-dawsonite at specific process parameters (10-20 ml/min as flow rate and 1.1M-2M as concentration) and pressure 1 bar. Grey circle represents the traces of NH_4NO_3. All crystalline phases follow the NH_4-dawsonite reference pattern. The comparison was made with the XRD spectra obtained at the same process parameters but the microsystem was working at atmospheric pressure (S13)

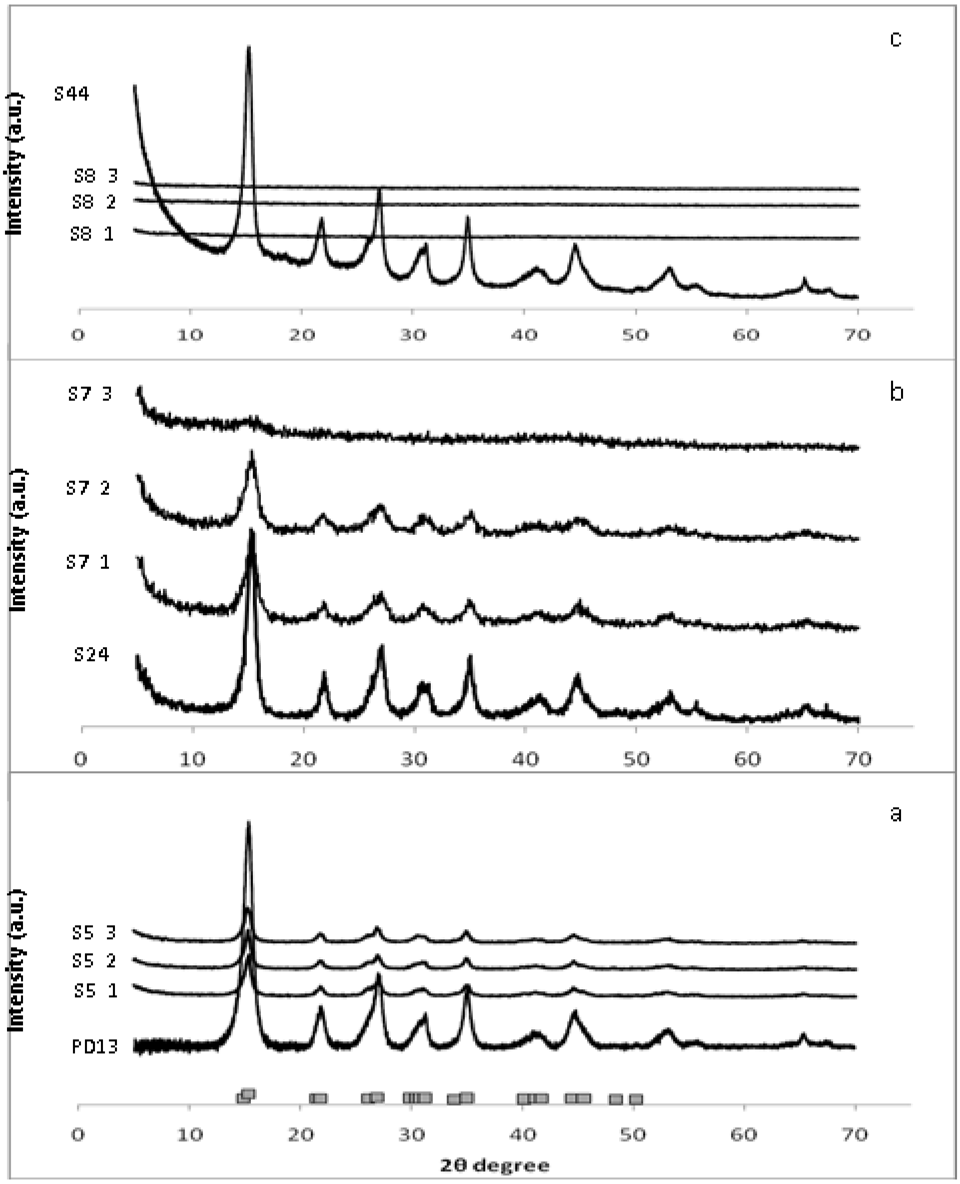

Fig.3.6: X-Ray Diffraction spectrum of crystalline and amorphous NH_4-dawsonite at specific process parameters and pressure 1 bar; a - XRD spectra for samples obtained at flow rate: 12-48 ml/min and concentration: 0.55M-1M for $Al(NO_3)_3x9H_2O$ and $(NH_4)_2CO_3$ aqueouse solution respectively) at both atmospheric pressure and 1 bar; b - XRD spectra for samples obtained at flow rate: 20-20 ml/min and concentration: 0.22M-2M for $Al(NO_3)_3x9H_2O$ and $(NH_4)_2CO_3$ aqueouse solution respectively) at both atmospheric pressure and 1 bar; c - XRD spectra for samples obtained at flow rate: 20-20 ml/min and concentration: 0.12M-1.09M for $Al(NO_3)_3x9H_2O$ and $(NH_4)_2CO_3$ aqueouse solution respectively) at both atmospheric pressure and 1 bar; All crystalline phases follow the NH_4-dawsonite reference pattern (grey dots).

This could be explained by means of partially reacted product or by the residence time inside the microreactor channel, that being reduces under 0.2 seconds and could affect the precipitation reaction. X-Ray Diffraction (XRD) spectra show low crystalline phase for samples S1-S4, S7group (S7_1 and S7_2) and S44 (atmospheric pressure precipitation) as shown in Figure 3.5 and 3.6. The NH_4NO_3 traces were presented within the samples S1 and S2 (See Figure 3.5).

High crystalline phase was determined for samples S13 and S24 obtained at atmospheric pressure and S5group produced applying pressure (1bar). Furthermore, amorphous phase appeared within the samples S7_3 and S8 obtained at pressure 1bar. The appearance of amorphous phase within the samples could be explained in terms of limiting values of concentration for both aqueous solutions which are able to be converted into crystalline NH_4-dawsonite. Presence of amorphous phase for all new S8group samples confirms that at minimum working concentration and equal flow rate the production of crystalline NH_4-dawsonite is only possible if adding a post treatment process of stirring in order to start the growth of crystals. Adjusting pressure at 1bar, the limiting time interval increased reaching the value of 260 seconds for specific process parameters: flow rate 12 ml/min for aluminum solution and 48 ml/min for carbonate one and concentrations of: 0.55M-1M for base and acid solution respectively (See table 3.2).

Table 3.3: Experimental characterization of all trials including time of production.

Sample code	Time of production		Process parameters	Analysis			
	System at atmospheric pressure	System at pressure 1bar		XRD	TGA* (%)	TEM* Particle size(nm)	BET* surface area (m^2/g)
S1-S4	40	245	1.1-2M; 10-20mL/min	LC	69	13.35	83.8278
S5 group	58	260	0.55-1M; 12-48mL/min	HC	62	12.55	508.6357
S7 group	109	191	0.22-2M; 20-20mL/min	LC (2 exp) A (1exp.)	56.2	6.105	516.8103
S8 group	558	371	0.12-1.09M; 20-20mL/min	A all	-	-	-

(M) – initial aqueouse solutions concentration; (ml/min) – flow rate used for each initial solution; HC – high crystalline phase; LC – low crystalline phase; A – amorphous phase; * – average values

The reproducibility of the system was proved to be robust during these experiments but low crystalline phase within the catalyst precursor was obtained and at lowest concentrations for the aqueous solutions significantly small crystals were able to be found in the slurry so that the XRD device was unable to detect them. This confirms that the minimum limit for the working concentration was found and under these values no detected crystalline phase will be analyzed. The pressure influence over the purity was characterized by using TGA and the percentage of weight loss in each sample was calculated. Both TGA and TGA derivative curves showed higher purity for the products obtained within the microsystem under pressure comparing with the product obtained at atmospheric pressure (See Table 3.3).The weight loss by thermal decomposition reached almost the ideal value (63%) for sample S13 (61%) produced within the microsystem at atmospheric pressure and sample S4 (61%) and S5group (62%), powders obtained within the microsystem 1bar.

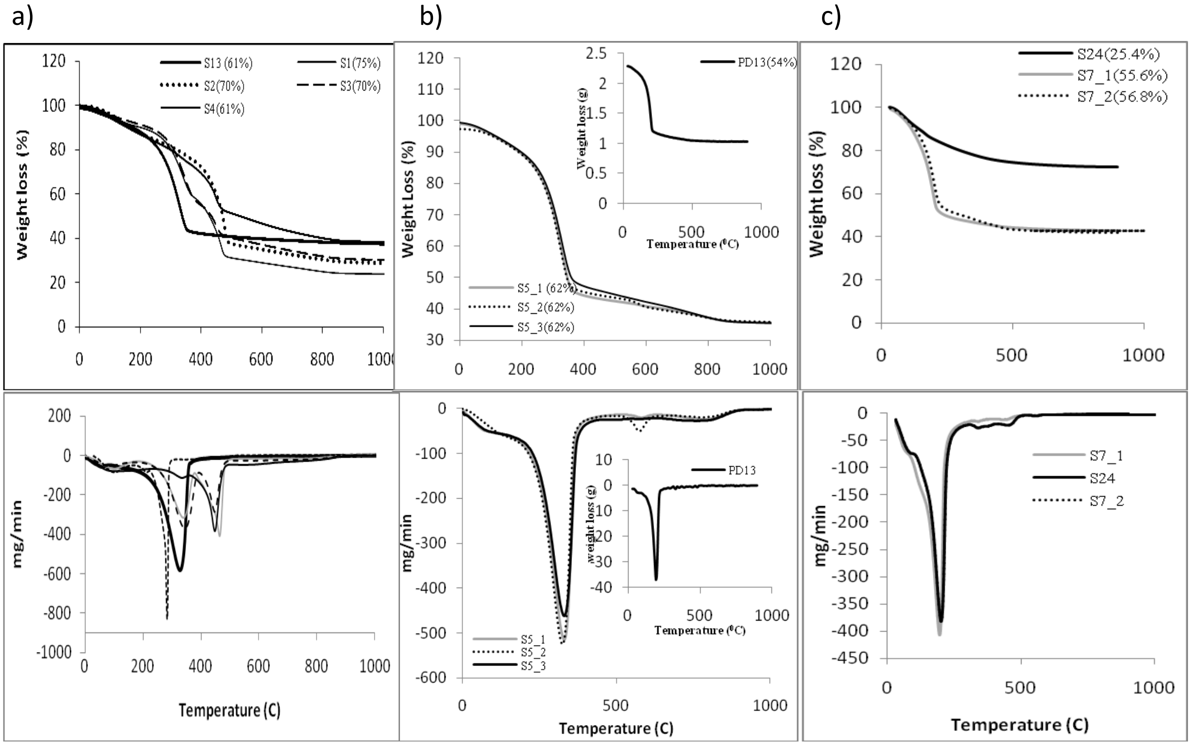

Fig. 3.7: (Top) Thermogravimetric profiles and (bottom) derivative curves of the weight loss of NH_4-dawsonite powder obtained at: a) flow rate: 10 ml/min for $Al(NO_3)_3x9H_2O$ aqueous solution and 20 ml/min for $(NH_4)_2CO_3$ aqueous solution, respectively and concentrations: 1.1M-2M for $Al(NO_3)_3x9H_2O$ and $(NH_4)_2CO_3$, respectively; b) 12-48 ml/min as flow rate for $Al(NO_3)_3x9H_2O$ with concentrations fixed at 0.55M and $(NH_4)_2CO_3$ with a concentration of 1M; c) 20-20 ml/min as flow rate and corresponding concentration values: 0.22M for $Al(NO_3)_3x9H_2O$ solution and 2M for $(NH_4)_2CO_3$ solution; and 1bar pressure.

A higher value of the weight loss during the thermal process was reached for samples S1 (75%), S2 (70%) and S3 (70%), value that overcame the theoretical one of 63%.

This could be explained by the presence of NH_4NO_3 traces inside these samples that decompose at different temperature during the thermal process. The rest of the samples showed less purity (PD13 – 54%, S7_1 – 55,6% and S7_2 – 56,8%, S24 – 25,4%) than those analyzed above but still better results were found comparing with the product obtained within the system at atmospheric pressure and at miliscale process[10] (weight loss approximately 50%). Both TGA and TGA derivative curves for crystalline NH_4-dawsonite are illustrated in Figure 3.7.

TGA derivative confirmed similar temperature transition (≈ 300^0C) for most of the samples and higher value (450^0C) for those containing traces of NH_4NO_3 (See figure 3.7a samples S1 and S3). The theoretical thermal transition that suggests pure ammonium dawsonite is 450^0C. Under this temperature the transition steps, which could appear can suggest the evacuation of the components step by step. There are 2 or/and 3 transitions of weight loss during the thermal process (between 200^0C and 450^0C) in most of the samples analyzed i.e. S1-S4 samples obtained at pressure 1bar or S7 group which show three transitions of weight loss during the thermal process (between 48^0C and 88^0C; 291^0C-340^0C and 404^0C-478^0C) (See Figure 3.7c). One step temperature transition was recorded for S5group (1bar pressure) powders at around 315^0C.

The results presented above confirm higher product purity prepared within the pressurized (1bar) microreactor system comparing to the results obtained for NH_4-dawsonite prepared within a milireactor[10] (weight loss – 50%) and an unpressurized microreactor system at different process parameters (S5group-PD13, See Figure 3.7b). Applying the pressure within the microsystem better results were found regarding the limiting time of production, crystallinity and product purity in comparison to the atmospheric pressure microsystem and ILDP milisystem[10].

Transmission electron microscopy (TEM) evidences the presence of nanometer (nm) particles size (Figure 3.8a,b,c) in contrast to micrometer (µm) aggregates size obtained within the old system at atmospheric pressure[7] (See Figure 3.8d). The aggregate components size was determined by TEM and was found in the range of nanometer scale (See Figure 3.8C).

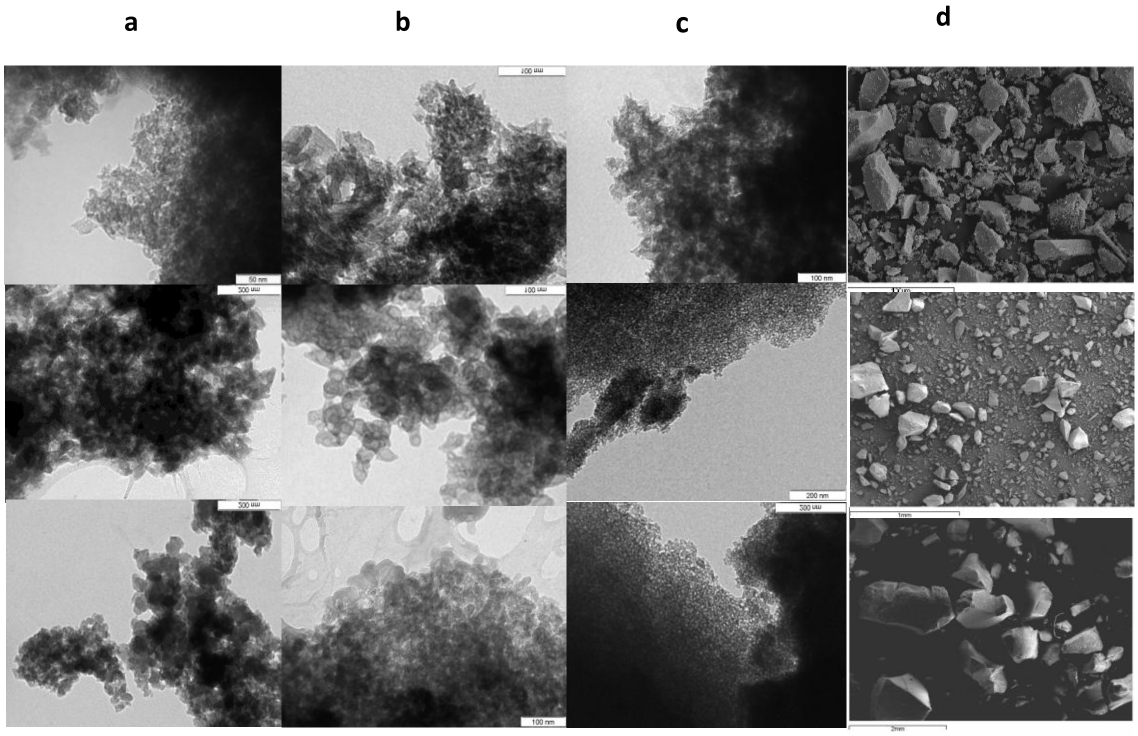

Fig.3.8 A. TEM micrographs of NH_4-Dawsonite powder obtained within the microsystem under pressure 1 bar, new set-up; Aa - represents the micrographs of samples obtained at following process parameters: flow rate (10-20ml/min for base and acidic solution respectively) and corresponding concentrations 1.1M-2M; Ab – micrographs of ammonium dawsonite powder obtained at 12-48 ml/min as flow rate for Aluminum aqueous solution and carbonate aqueous solution respectively and corresponding concentrations of 0.55M-1M; Ac - micrographs of ammonium dawsonite powder obtained at fixed flow rate: 20-20 ml/min for Aluminum aqueous solution and carbonate aqueous solution respectively and corresponding concentrations of 0.22M-2M; Ad - SEM micrographs of the same powder obtained within microsystem at atmospheric pressure, old set-up and same process parameters;

By applying pressure on the precipitation process we were able to obtain the particle size at the nanometer range (≤ 15nm sizes – 7nm and 20nm) and particle size distribution desired. Comparing with the results obtained in previous work[7] and those published for NH_4-dawsonite obtained at miliscale[10], working at pressure 1bar the results were much better and /or similar and the particle size distribution was better controlled. The textural properties of the solid were determined by adsorption of nitrogen at 77 K (Figure 3.9). Following IUPAC recommendations[11] the NH_4-dawsonite N_2 isotherm showed a combination of type II and IV isotherms (with H_1 hysteresis).

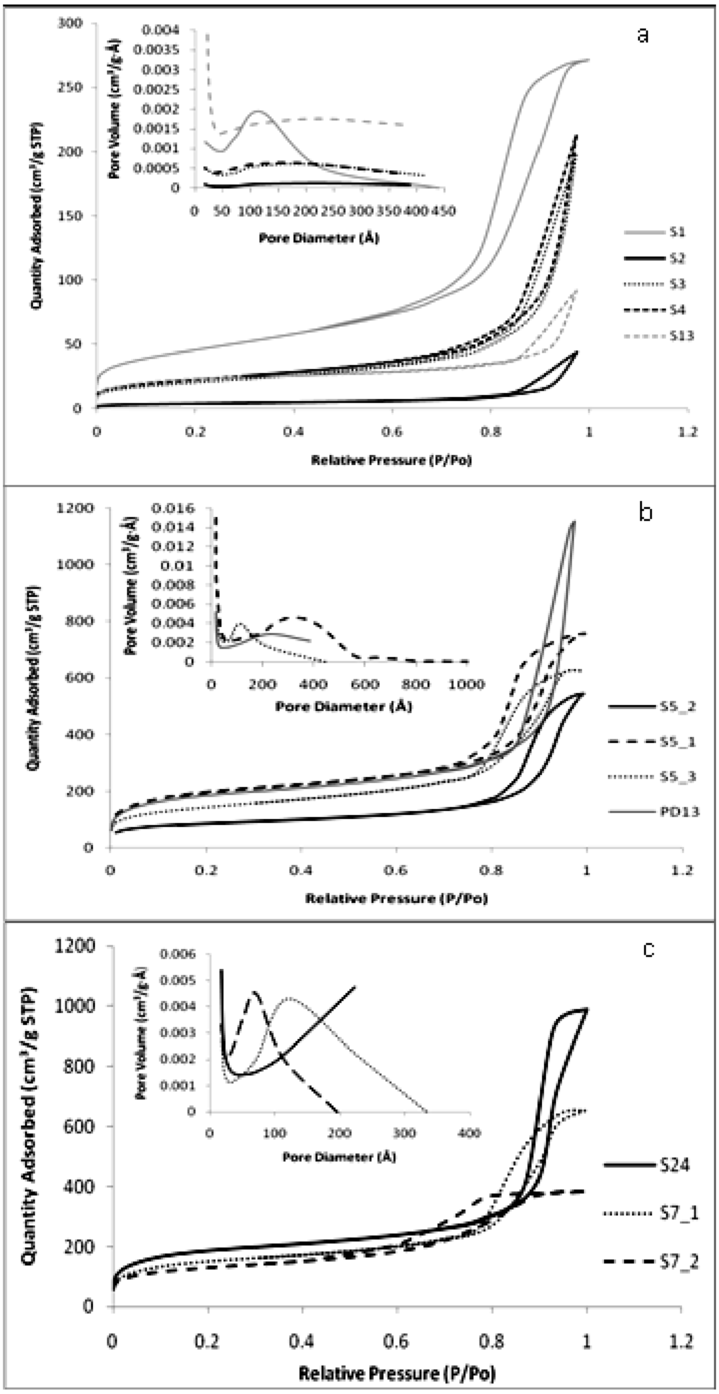

Fig.3.9: N_2 adsorption-desorption isotherms at 77 K of the NH_4-dawsonite samples obtained at 1 bar pressure and specific process parameters: a) flow rate: 10-20ml/min for $Al(NO_3)_3x9H_2O$ aqueous solution 1.1M and $(NH_4)_2CO_3$, 2M, respectively; b) flow rate: 12-48ml/min for $Al(NO_3)_3x9H_2O$ aqueous solution 0.55M and $(NH_4)_2CO_3$, 1M, respectively; c) flow rate: 20-20ml/min for $Al(NO_3)_3x9H_2O$ aqueous solution 0.22M and $(NH_4)_2CO_3$, 2M, respectively; Inset: corresponding BJH pore size distributions.

These fingerprints of type IV-like isotherm are characteristic for mesoporous materials with uniform pore size (See Figure 3.9 a,b,c), while type II – like isotherm is given by presence of micropores within the catalyst (See also Table 3.4).

The low quantity of adsorbed gas on the surface of the samples S2, S3 and S4 (Figure 3.9 a) indicates the formation of multilayers of adsorbed gas even though the samples pores were already saturated with N_2 gas. If saturation level for all samples obtained within the microsystem at pressure 1 bar (S2-S4, S5group and S7group) was almost 0, for sample obtained at atmospheric pressure (S13, PD13 and S24) was found around 0.18. Reaching the saturation level within the sample monolayer or/and multilayer of gas molecules start to be formed on the sample surface. This mono/multilayer approach is described very well by Langmuir theory and BET theory (more details in ***Chapter 4***). The latter statement is substantiated by the narrow pore size distribution in the samples, which is centered differently for each group analyzed (Figure 3.9.inset a,b,c). BJH pore size distribution shows a similar narrow distribution of mesopores centered between 100Å - 200Å for S1, S5_3 and S7_1, around 400 Å for S5_1 and less than 100Å the total pore distribution was addressed to sample S7_2. Mesoporosity was found inexistent within the samples S2-S4 (pressure 1bar) and S13 (atmospheric pressure). The total pore volume and specific surface area of the analogue mineral are in a direct correlation. The presence of *micro* and *meso* pores in the samples has a very high influence in changing the BET surface, lowering/rising it. As volume of micropore is decreasing BET Surface Area (S_{BET}) is decreasing i.e. total pore volume for sample S13 was calculated based on the micropores area and volume and the value reached 0.27 $cm^3\ g^{-1}$ (See also Table 3.4). This showed a BET surface area of about 836 $m^2\ g^{-1}$ which overcame the value obtained for NH_4-dawsonite prepared at miliscale (S_{BET} – ILDP process was 773 $m^2\ g^{-1}$)[10] and those obtained for the powder produced by using conventional processes (300 $m^2\ g^{-1}$). Applying t-plot method, the low content of micropores inside the samples was confirmed 0.008cm^3g-1 and 0.12cm^3g-1 (See Table 3.4). Modifying the process parameters by increasing the flow rate and decreasing the concentration for both aqueous solutions the BET surface area values were determine between 450m^2g^{-1} and 700m^2g^{-1} (Table 3.4). Analyses on the pore size distributions gives precise information about textural characterization of dawsonite analogue obtained through microsystem (applied pressure) but deeper research is needed in order to demonstrate the higher quality of the product and the advantages over conventional precipitation process and/or ILDP method[10].

Table 3.4: Textural characterization of the samples obtained within the microsystem under pressure 1bar

Sample code	V_{pore} (cm³/g)	$v_{micro}{}^{a}$ (cm³/g)	$S_{meso}{}^{a(*)}$ (m²/g)	$S_{BET}{}^{b}$ (m²/g)
PD8-S13	0,27406	0.124267	244.9909	835.6733
S1	0.0065047	0.005805	132.4698	164.4065
S2	0.0050065	0.000814	10.5819	14.6908
S3	0.023706	0.002431	59.1924	74.7194
S4	0.02701	0.003063	64.8965	81.4947
PD13-S18	0.187914	0.094584	218.2521	660.5951
S5_1	0.214281	0.081276	318.0671	706.7937
S5_2	0,092567	0.044437	108.9303	310.0645
S5_3	0.162355	0.059547	235.8449	509.0489
S24	0.1720	0.113955	140.2571	667.3279
S7_1	0.1350	0.078596	165.7252	532.2329
S7_2	0.1150	0.073785	123.5798	455.1904
S7_3	-	-	-	-
S44	-	-	-	-
S8 group	-	-	-	-

3. Conclusions

The limited time interval of NH_4-dawsonite production by using the pressurized microsystem (1bar) was increased between 2 and 6 times depending on the process parameters selected. The crystalline phase determined by using X-ray diffraction analysis (XRD) showed higher intensity for NH_4-dawsonite obtained with a larger ratio between flow rates (12ml/min – 48ml/min), base solution ($(NH_4)_2CO_3$) being in excess. The rest of the XRD results show a lower intensity/2θ degree diffractograms comparing to the XRD results obtained by using the first setup (setup at atmospheric pressure) for product precipitation. Some traces of ammonium nitrate were found during the analyses which can be explained by means of imperfect or superfast mixing inside the microchannel, giving the reaction no time to finish. TGA and DTGA analyses showed an increase of product purity in the case of present experiments. Similar BET area and uniform mesoporosity centered between 100Å-200Å were found for NH_4-dawsonite samples precipitated by handling an enhanced ratio between the flow rates of aqueous solution (S5 group, Sample PD13) and their respective concentration within both pressurized (1bar) and atmospheric pressure microsystems. The micrometer particle size of NH_4-dawsonite produced within the system at atmospheric pressure[7] decreased till nanometer size by applying pressure (between 7nm-20nm particle size).

The results presented above raised a new hypothesis due to the possibility of increasing the pressure within the microsystem and analyze its influence over NH_4-dawsonite crystallization process. A detailed theoretical and experimental work flashing above hypothesis is described in ***Chapter 4***.

References

[1] Ou J., Moss G. R., Rothstein J. P., 2007, Enhanced mixing in laminar flows using ultrahydrophobic surfaces, Physical Review 76, 016304;

[2] Fletcher P.D.I., Haswell S. J., Pombo-Villar E., Warrington B.H., Watts P., Stephanie Wong Y. F. and Zhang X., 2002, Micro reactors: principle and applications in organic synthesis, Tetrahedron, 58, 4735-4757;

[3] Hessel V., Löwe H., Schönfeld F., 2005, Micromixers—a review on passive and active mixing principles, Chemical Engineering Science 60, 2479 – 2501;

[4] Asgar A., Bhagat S., Papautsky I., 2008, Enhancing particle dispersion in a passive planar micromixer using rectangular obstacles, J. Micromech. Microeng. 18 (2008) 085005 (9pp);

[5] Schönfeld F., Hessel V., Hofmann C., 2004, An optimized split-and-recombine micro-mixer with uniform 'chaotic' mixing, The Royal Society of Chemistry, Lab Chip 4, 65-69, DOI: 10.1039/b310802c;

[6] Loewe H., 2009, Chemical Syntheses with Microstructured Reactors – Possibilities, Advantages, and Costs, MicroChem (Dalian) Co.Ltd (industrial report, www.microchem.com);

[7] Dubert D. C., Garcia-Valls R. and Pérez-Ramírez J., (2010), Dawsonite production with caterpillar microreactor, Chemical Engineering Transactions, 21, 1003-1008 DOI: 10.3303/CET1021168

[8] Jähnisch, K., Hessel, V., Löwe, H. and Baerns, M., 2004, Chemistry in Microstructured Reactors. Angewandte Chemie International Edition, 43: 406–446. doi: 10.1002/anie.200300577;

[9] Hernandez M.J., Ulibarri M.A., Cornejo J., Peña M.J., Serna C.J., 1985, Thermal stability of aluminium hydroxycarbonates with monovalent cations, Thermochim. Acta 94, 257-266;

[10] Stoica G. and Pérez-Ramírez J., 2007**,** Reforming Dawsonite by Memory Effect of AACH-Derived Aluminas, Chem. Mater., Vol.1, 4783-4790;

[11] Sing, K. S. W.; Everett, D. H.; Haul, R. A. W.; Moscou, L.; Pierotti, R. A.; Rouquerol, J. and Siemieniewska, T., 1985, Reporting physisorption data for gas/solid systems with special reference to the determination of surface area and porosity, Pure Appl. Chem., 57(4), 603–619;

Chapter 3

Continuous synthesis of ammonium dawsonite within a new microstructured system

Chapter 4

Influence of pressure over ammonium dawsonite continuous precipitation at microscale

As mentioned in *Chapter 3* pressure occupies an important place in the design of a micromixer by influencing the mixing, improving it. It is shown in the literature[14] that at higher pressure drop along the microchannel, developed *i.e.* by appearances of different obstructions within the channel or applying an extra pressure to the system, is generating an enhanced mixing results, therefore turbulent regime is induced (both convective and diffusive forces are intercepted) and better conversion of the product with distinguished qualities is obtained. Based on this information given above, this *Chapter* deals with the investigation of pressure influence over NH_4-dawsonite precipitation reaction and morphological and physical properties of the product analyzed. Nano-sized NH_4-dawsonite particles were provided by controlling the optimal flow rate for both mother solutions and by increasing the system pressure step by step. Different crystalline phase and crystallites size inside the samples were found by using X-ray Difraction Technique (XRD) and Sherrer theory. Higher purity and porosity properties were discovered after analyzing the powder by TGA and N_2-adsorption BET (Brunauer, Emmett, and Teller) techniques. Crystalline NH_4-dawsonite with decreased particle size was displayed by increasing the pressure within the microsystem, step by step.

Chapter 4

Influence of pressure over ammonium dawsonite continuous precipitation at microscale

1. Introduction

Typical residence times and pressure drop in micro-channels are significantly smaller than in macroscopic systems and allows higher external pressure to be applied if necessary[1]. Since the flow condition within microdevices allows for lower pressure drops and higher external pressure to be applied, the present *Chapter* describes in details the precipitation process of NH_4-dawsonite inside the Caterpillar micromixer (CPMM1200/8), at pH 9, temperature 60^0C and variable applied working pressure, within an interval started from 1bar up to 8bar. NH_4-dawsonite as a precursor for very pure alumina (aluminum oxide - Al_2O_3) production by thermal decomposition above 1173K[2] gained more and more ground over the decades and reached an important level in the field of alumina production.

The present chapter presents a deeper investigation regarding the influence of applied pressure over the continuous time of production and the characteristics of the product obtained: crystal formation, purity, catalytic properties (mesoporosity) and precipitation efficiency. Is a continuation of the experimental work conducted at 1bar (See ***Chapter 3***) with the aim of reaching the optimal process parameters for continuous NH_4-dawsonite production and enhanced product characteristics are expected. The results were compared with those presented in *Chapter 2* and *Chapter 3* and also with those published for the conventional processes of NH_4-dawsonite production. As mentioned in *Chapter 3***(***Section 1***)** the efficiency of the mixing increases proportionally with the miniaturization of the mixing channel. This involves smaller pressure drop inside the mixing channel and higher mixing efficiency[3]. For this reason applying an extra pressure within the system could induce better mixing of the aqueous solutions and enhanced control over the product particle formation reaching the optimal production time for industrial requirements.

2. Experimental section

2.1. Methodology and reagents

The precipitation process of NH_4-dawsonite took place within the microsystem at specific fixed parameters (pH = 9, temperature (60^0C)) and variable pressure (1bar-8bars). Two-phase flow process was selected by choosing a specific experiment with the optimal parameters presented in *Chapter 2* **(***Section 2.2***)** and *Chapter 3 (Section 2.1***)** based on the data published recently[4,5] in the literature. The initial aqueous solution concentration were fixed as followed: 0.55M for $Al(NO_3)_3x9H2O$ and 1M for $(NH_4)_2CO_3$ respectively with corresponding flow rates: 12 ml/min and 48 ml/min for each initial solution in this order.

The proposed set-up is identical to the microsystem presented in *Chapter 3***(***Section 2.1***)** and is reviewed in Figure 4.1. The pressure interval (1-8bar) was controlled by a pressure dumper. The acid and base solutions were pumped into the microreactor by using gamma/ L Solenoid metering pumps whereas the pressure at the inlet was adjusted for each experiment by modifying the pressure level within the pumps software. Both metering pumps could function at high pressure and the flow rates could be kept fixed within the automatic software by fixing the stroke length and stroke rate at the same time.

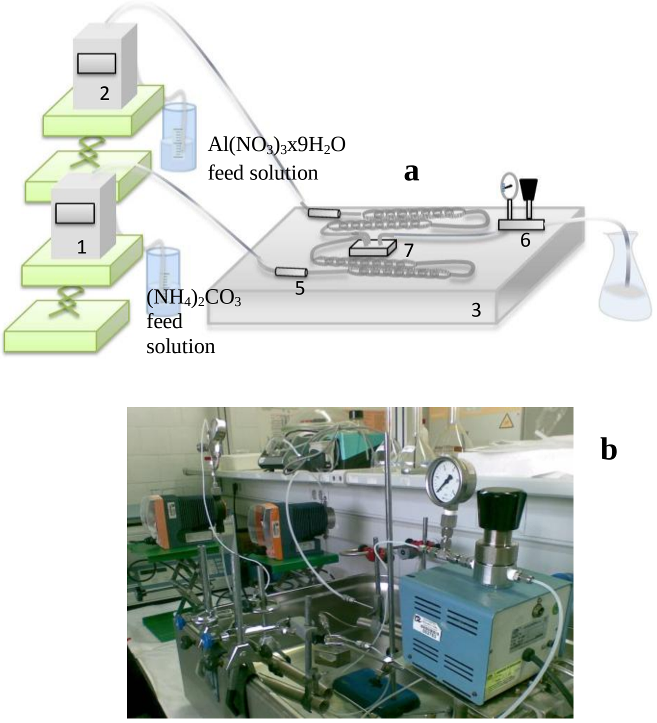

Fig.4.1: a) Microsystem set-up fitted for pressure ≥ 1 bar: 1 – gamma/ L Solenoid Metering Pump (for $(NH_4)_2CO_3$ initial solution), 2 – gamma/ L Solenoid Metering Pump (for $Al(NO_3)_3$ initial solution), 3 – Water bath, 4 – Stainless steel coil, 5 – Check valves, 6 – Pressure dumper, 7 – Caterpillar microreactor CPMM1200/8; b) Lab-scale microsystem set-up photo.

The connections with the microreactor inlets was established by one meter compact stainless steel coil for each inlet (see Figure 4.1 a), this allowed to have a better control of heat transfer from inside-outside or/and vice versa and in the same time to enhance the reaction time, respectively. An Erlenmeyer beaker was used to collect the white slurry with precipitated NH_4-dawsonite.

Temperature and pH were measured at the microreactor outlet to assure that they remained unchanged during the precipitation process. The post-precipitation treatment followed that same steps numbered in *Chapter 3* ***(****Section 2.1****)*** excluding the stirring step, as well. The results were compared to the ones obtained for the same process parameters ran at atmospheric pressure[4], with those listed in the literature[6] and the results obtained through the precipitation process at milliscale[2].

2.2. Product characterization

The characterization techniques: XRD, TGA TEM, N_2-adsorption with the BET method[7], to calculate the total surface area and the *t*-plot method[8] used to discriminate between micro- and mesoporosity were applied to investigated process efficiency and physical and morphological properties of the powder obtained at high pressure.

3. Results and discussion

Following the methodology already presented in *Section 2.1* the experimental results showed an improvement regarding the production time (increase up to 6 times comparing to the previous experimental results[4,5] if a higher pressure is applied within the mixing channel. This study confirms that the optimal pressure was 2bar. That increased dramatically the limiting production time and improved the process efficiency (See Table 4.1).The reproducibility of the system was proved by repeating the experiments at least three times.

Pressure influence on mixing efficiency is highlighted in Figure 4.1. It shows a proportional dependency; increasing the applied pressure within the microchannel the precipitation conversion increases, that confirms a better control of particle formation and better mixing. As Figure 4.2 shows the highest efficiency (54.3%) was reached by applying 6bar of pressure within the microchannel but less time of production was achieved (See Table 4.1) relating to the results obtained by applying 2bar working pressure.

Table 4.1: Summary of pressure influence over time of production and yield

Experimental parameters: Al $(NO_3)_3$x$9H_2O$ 0.55M, 12 ml/min $(NH_4)_2CO_3$ 1M, 48 ml/min			
Experiment code	Microsystem pressure (bar)	Average time of production (s)	Yield %
PD13	Atmospheric pressure	58	30.4
S1bar	1	186.6	26
S2bar	2	270	40
S4bar	4	203.5	38.6
S6bar	6	153	54.3
S8bar	8	200	50.33

Experimental parameters: Al $(NO_3)_3$x$9H_2O$ 0.55M, 12 ml/min and $(NH_4)_2CO_3$ 1M, 48 ml/min; *average time of production values for all trials at the same process parameters

Furthermore, the efficiency of the microsystem at atmospheric pressure was determined to be 30%, value that could satisfy the results at laboratory scale but a better conversion is needed in order to fulfill the industrial requirements. Even though, the highest yield was determined at high pressure (6 bars) no more than 2 bar were needed to increase the production time up to 6 times comparing to previous experimental work (See ***Chapter 2 and 3***).

Powder X-ray diffraction patterns of the produced samples (Figure 4.3) confirmed that dawsonite was the only crystalline phase in the precipitated product following the reference pattern of $NH_4AlCO_3(OH)_2$, (JCPDS 42-250). Eventhough, within the system under pressure the precipitate showed lower crystalinity balancing to the results presented by running the microsystem at atmosferic pressure; all spectra followed the reference trendline and no other traces were found.

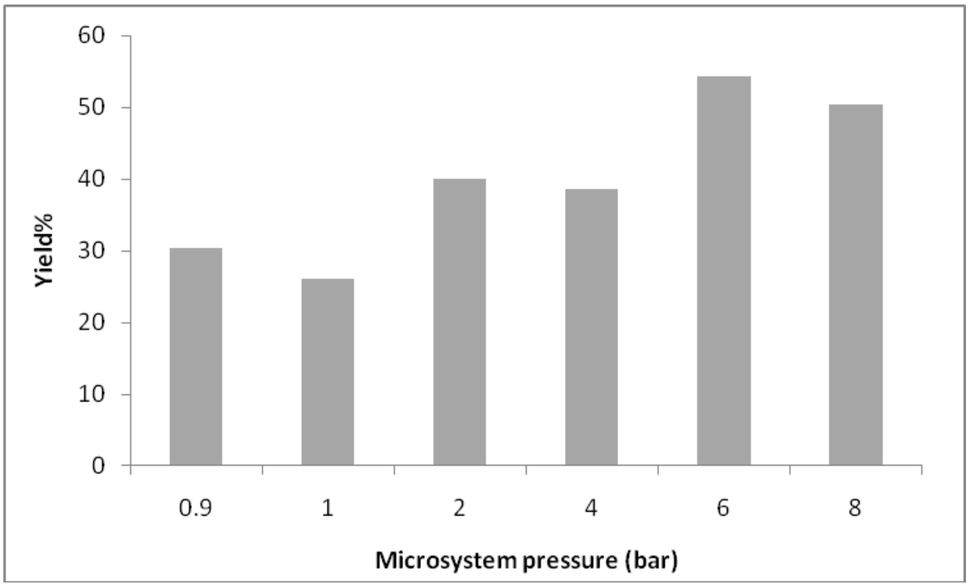

Fig.4.2: Microsystem pressure influence on the mixing efficiency at fixed process parameters: flow rate: 12-48 ml/min for base and acidic aqueous solution, respectively with the corresponding concentration: 0.55M and 1M.

The influence of high pressure within the system, on the crystallites size formed within powder was determined by using the Sherrer theory[9].

It is an approximate approach for calculating the cristal/crystallite size and gives information about the crystalline phase of a sample. Phase identification using X-ray diffraction relies mainly on the positions of the peaks in a diffraction profile and to some extent on the relative intensities of these peaks. The shapes of the peaks, however, contain additional and often valuable information. The shape, particularly the width, of the peak is a measure of the amplitude of thermal oscillations of the atoms at their regular lattice sites. It can also be a measure of the impurities. Crystallite size can also cause peak broadening. The Scherrer equation explains peak broadening in terms of incidence beam divergence which makes it possible to satisfy the Bragg condition for non-adjacent diffraction planes[9]. The instrument effects need to be excluded, then the crystallite size could be easily determined as a function of peak width (specified as the full width at half maximum peak intensity (FWHM)), peak position and wavelength. The Sherrer formula was used for the identification of average crystallite size (See eq. 1 and 2).

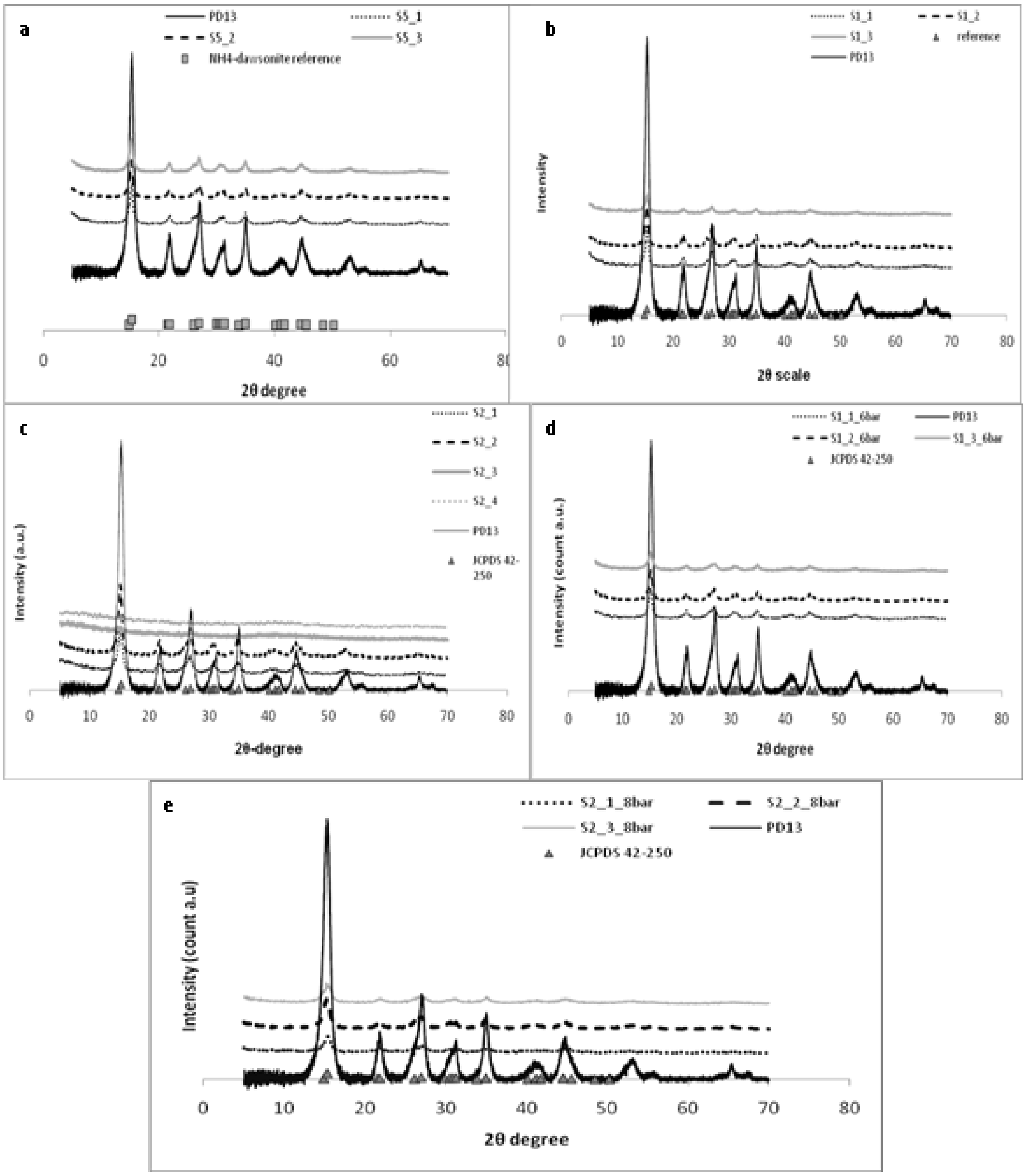

Fig.4.3: X-ray diffraction patterns of solid NH_4-dawsonite resulting from precipitation process at constant temperature and pH and preselected flow rate (12-48ml/min), concentration (0.55-1M) for aqueous initial solutions base and acidic one respectively and a) working pressure 1 bar, b) working pressure at 2bars, c) working pressure at 4 bars, d) working pressure at 6 bars and e) working pressure at 8 bars. Triangular pattern represents the reference data for pure NH4-dawsonite X-ray spectrum coded: JCPDS 42-250.

$$L_{vol} = \kappa\lambda / \beta_{1/2} \cos\theta_B \qquad \text{equation 1}$$

where L_{vol} is the volume-weighted size, *B* is the Bragg angle, λ is the wavelength of the x-ray and *k* is a unit cell geometry dependent constant whose value is typically between 0.85 and 0.99. $B_{½}$ is the full-width-half-max of the peak after correcting for peak broadening which is caused by the diffractometer. One way to represent $B_{½}$ is:

$$B^2_{1/2} = \mathbf{B}^2_{obs} - B^2_m \qquad \text{equation 2}$$

where B_{obs} is the measured peak width and B_m is the beak broadening due to the machine.

Table 4.2 showed similar behavior in crystal growth during the precipitation process under specific pressure conditions. The results confirmed the Sherrer theory that connects the broadening of the peak with the crystal size; the higher the crystallinity within a sample the smaller the crystallites size detected. Crystallite size could be different than the particle size due to the possibility of multiple crystallites accumulation within one particle of solid. This might reflect some inequalities between the two entities (See Table 4.2).

Table 4.2. Summerized values for particles and crystallites zise versus operating microsystem pressure

Experimental parameters: Al $(NO_3)_3$x$9H_2O$ 0.55M, 12 ml/min; $(NH_4)_2CO_3$ 1M, 48 ml/min

Experiment code	Microsystem pressure (bar)	[1]Average crystallite size (nm)	XRD	Average particle size (nm)
PD13	Atmospheric pressure	7.9055	HC*	13
S1bar	1	17.9	LC**	12.55
S2bar	2	17.92	LC	3.64
S4bar	4	13.405	LC	3.43
S6bar	6	17.92	LC	2.56
S8bar	8	10.04	LC	3.04

[1]Values calculated with Sherrer equation from XRD spectra of each sample analyzed. *HC – high crystallinity; **LC – low crystallinity

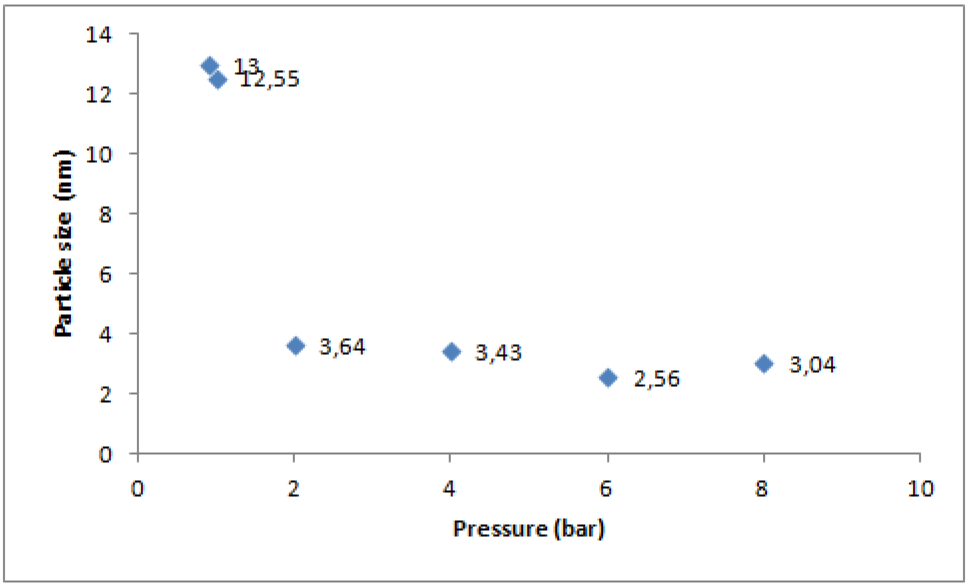

Fig.4.4: Pressure influence on particle size.

If the pressure influence over the crystallite growth was minimal comparing to the results recorded at atmospheric pressure, the influence on the particle size analyzed by TEM and processed by ImageJ software was found more interesting to be discussed further. The results are summarized in Table 4.2.

The particle formation tendency showed a direct dependency with the variation of the pressure inside the system (See Figure 4.4.) Increasing the working pressure smaller particle size was obtained and more controlled particle distribution was detected.

NH_4-dawsonite exhibited the characteristic aggregated spherical-like particles which were found different that the root-like particles obtained at atmospheric pressure (See PD13, Figure 4.5a) and fibrous K-dawsonite[6] particles presented in the literature (See also Figure 4.5h).

The NH_4-dawsonite particle morphology discovered through ILDP process at milliliter scale[10] showed similar shape with the powder particles obtained at 1-8bar (See Figure 4.5g).

Thermogravimetric analyses in air (Figure 4.6 a,b,c,d,e,f top) confirmed again the higher purity of the dawsonites comparing to milliliter scale production and batch one. The total weight losses of the NH_4-dawsonite samples amounted between 49% and 62% (average values between the trials at specific pressure), *i.e.* very close to the theoretical values based on the dawsonite formulas (63% for NH_4-dawsonite) the purity was reached for samples precipitated within the microsystem runing under 1bar and 4bar. A little lower purity was obtanined for NH_4-dawsonite synthesized at 2bar (See Figure 4.6c).

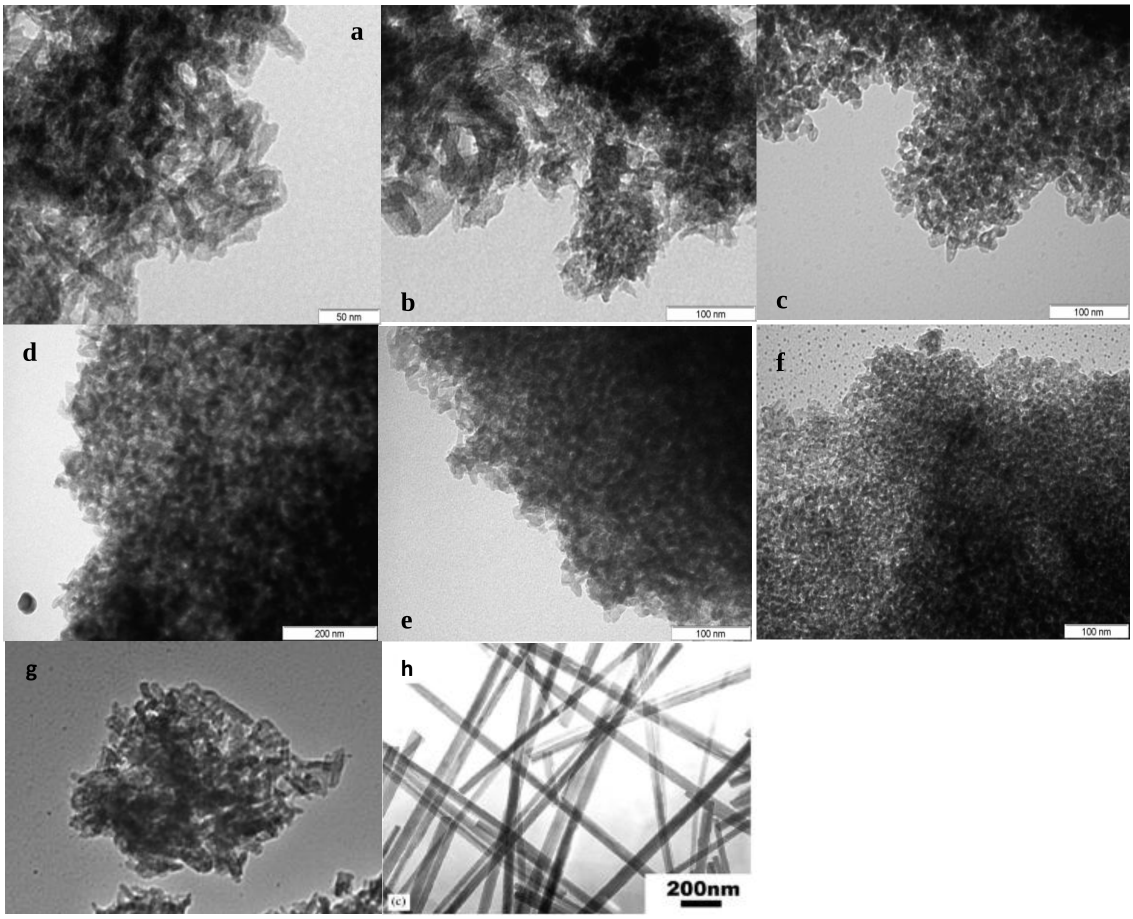

Fig. 4.5: Transition electron micrographs of NH_4-dawsonite synthesized within the microsystem working at pressure: a) atmospheric pressure, b) 1bar, c) 2 bars, d) 4bars, e) 6bars and f) 8bars and preselected flow rate (12ml/min and 49 ml/min for aluminum solution and carbonate solution respectively) and concentration(0.55M for aluminum solution and 1m for carbonate solution).g) TEM micrographs for NH_4-dawsonite prepared within a milireactor. Source: Stoica and Pérez-Ramírez (2007); h) K-dawsonite TEM micrographs prepared by conventional batch precipitation by using $KHCO_3$/Al ration of 16, pH of 9.5 and reaction time of about 24h. Source: Zhang et al. 2004.

Attending to the transition temperatures in Figure 4.6 (a,b,c,d,e,f bottom), the thermal stability of NH_4-dawsonite was found to be very similar for most of the samplses (*ca*. 320˚C) and a little shifted for samples obtained at atmospheric pressure and 2bar of pressure (PD13, Figure 4.6a and 2bar group, Figure 4.6c).

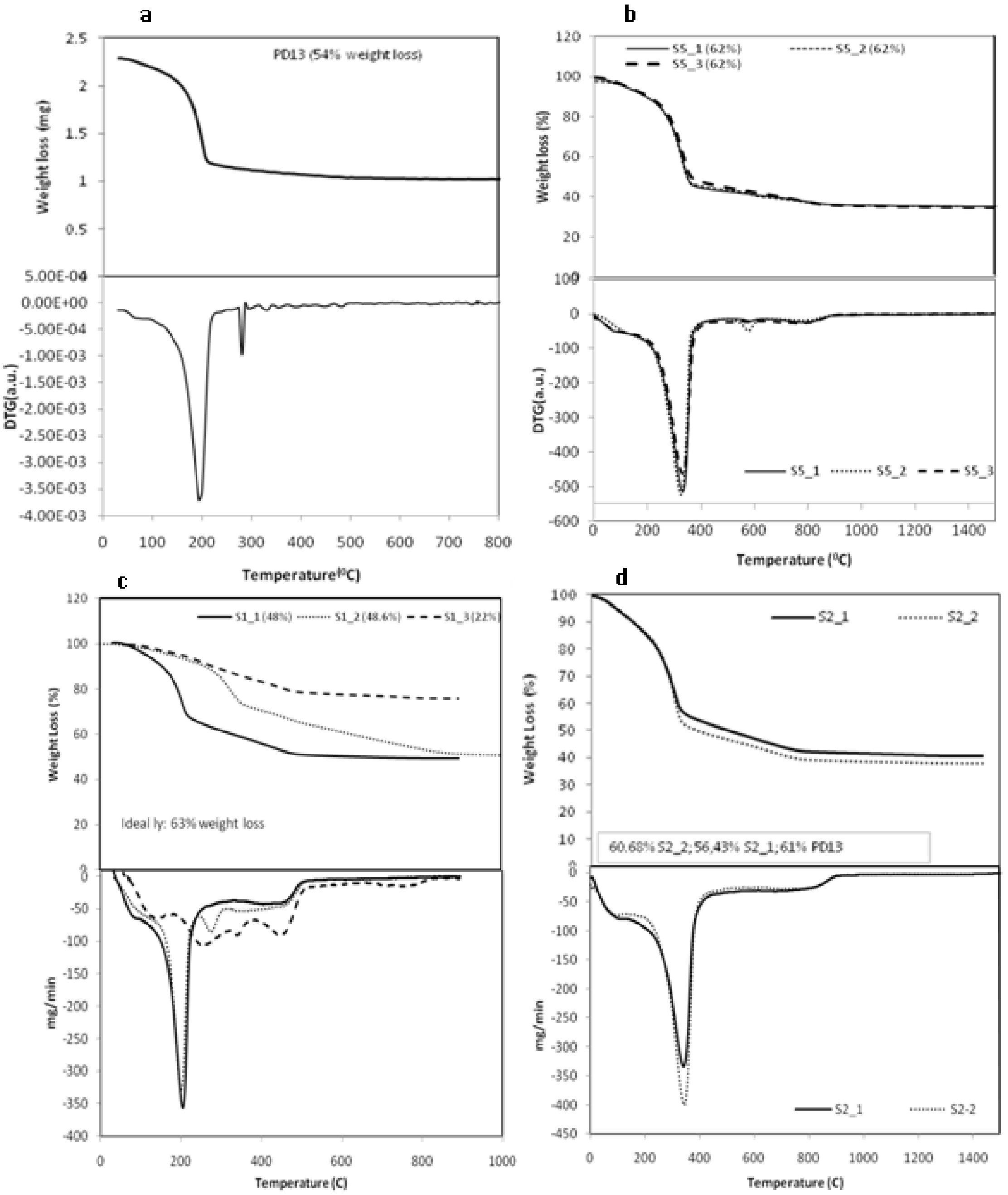

Fig. 4.6: (Top) Thermogravimetric profiles and (bottom) derivative curves of the weight loss of NH_4-dawsonite obtained within the system at: a) atmospheric pressure; b) 1bar; c) 2bar; d) 4bar; e) 6bar and f) 8 bar and preselected flow rate and concetrations for initial solutions: 12-48 ml/min, 0.55M-1M respectively.

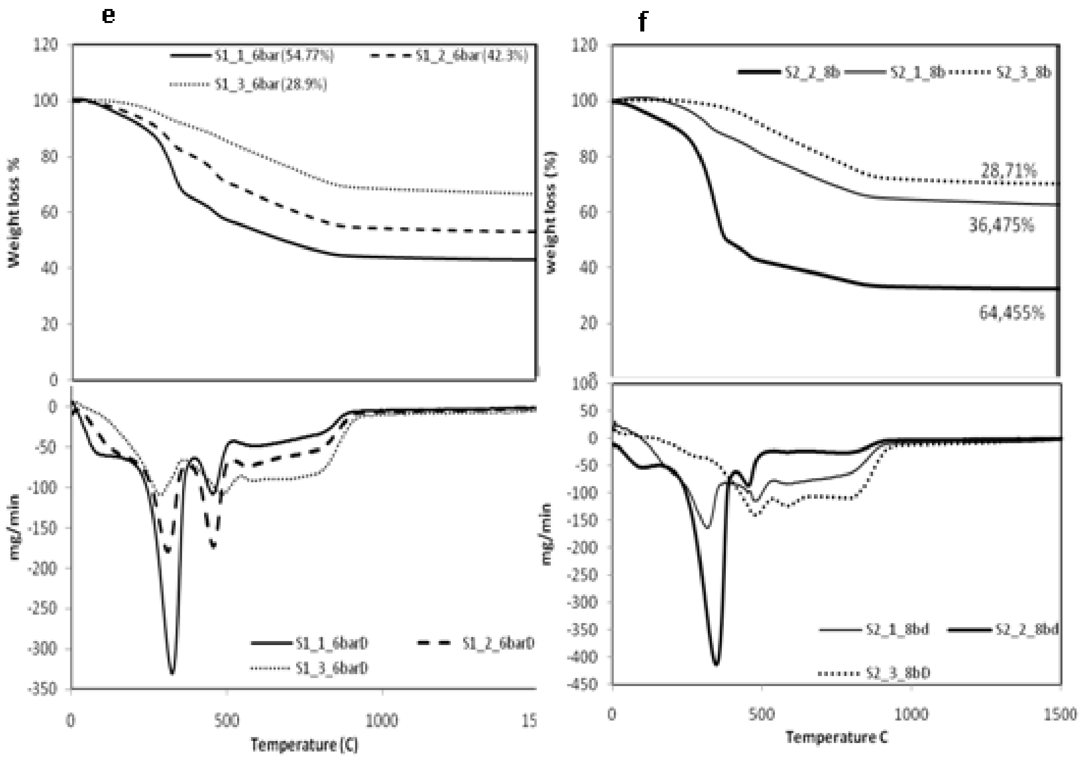

Fig. 4.6(continuation): (Top) Thermogravimetric profiles and (bottom) derivative curves of the weight loss of NH_4-dawsonite obtained within the system at: a) atmospheric pressure; b) 1bar; c) 2bar; d) 4bar; e) 6bar and f) 8 bar and preselected flow rate and concetrations for initial solutions: 12-48 ml/min, 0.55M-1M respectively.

These results are in good correspondence with those obtained at milliliter scale[10] and those reported for conventional processes[6]. Some extra thermal transition took place around value 450°C showing the complete thermal transformation of NH_4-dawsonite powder. The small particle and crystallite sizes determined by TEM and XRD, respectively, made it possible to anticipate a high degree of inter-particle porosity in the NH_4-dawsonite samples. The textural properties of the solid were determined by adsorption of nitrogen at 77 K (Figure 4.7). Following IUPAC recommendations[11] the N_2 isotherms of NH_4-dawsonite samples obtained within pressurized system could be classified as type IV with H_1 hysteresis and the isotherm of NH_4-dawsonite sample prepared at atmospheric pressure (PD13) as type II more than type IV. These fingerprints are characteristic of a purely mesoporous material with uniform pore size. The latter statement was substantiated by the narrow pore size distribution in the samples, which were centered between 10 nm and 30 nm (inset of Figure 4.7).

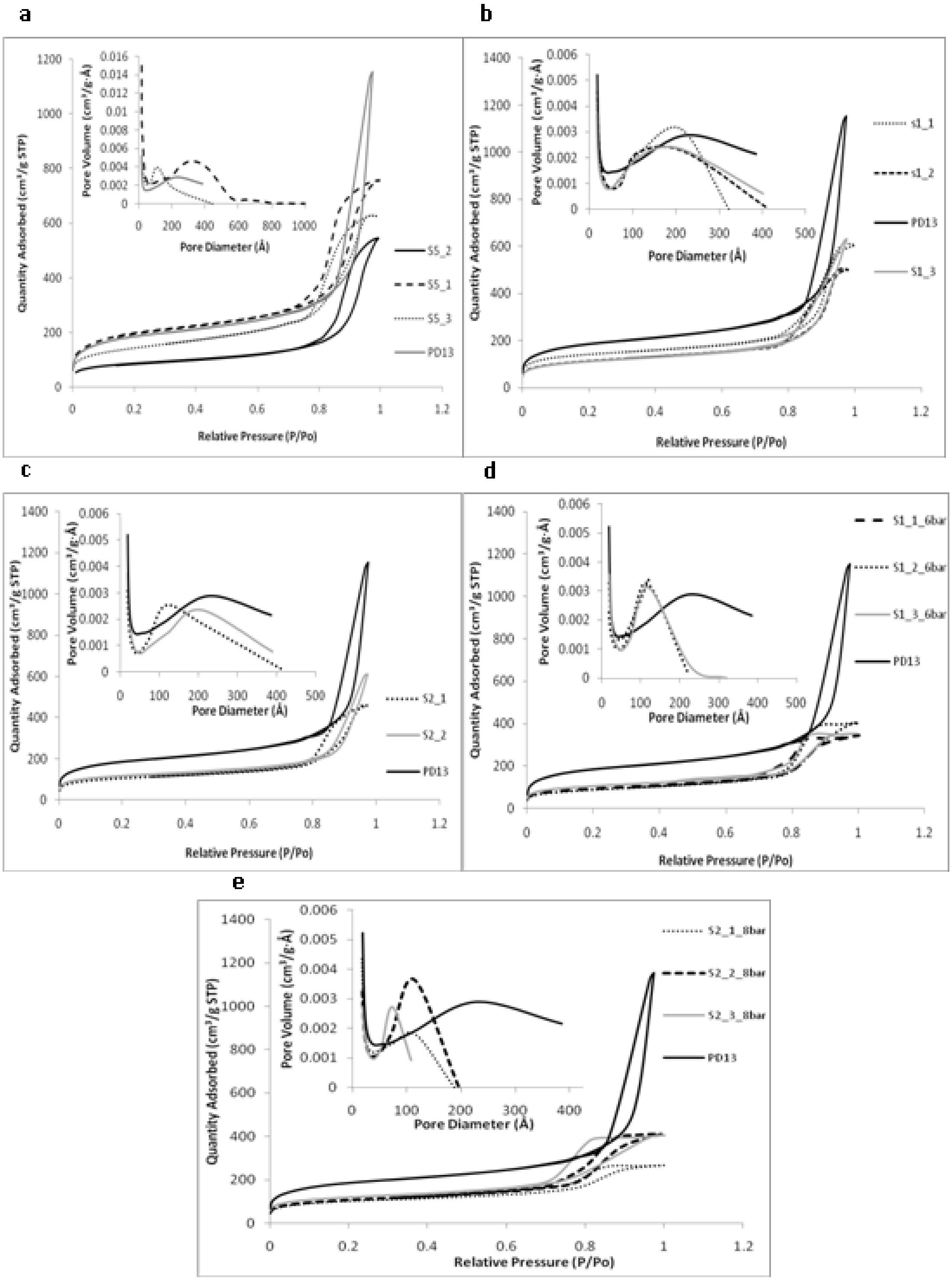

Fig. 4.7: N_2 isotherms at 77 K for NH_4-dawsonite samples obtained both at atmospferic pressure and varying the pressure inside the mysrosystem from a) 1 bar, b) 2bars, c) 4bars, d) 6bars and e) 8 bars. Inset: BJH mesopores size distributions within the each coresponded N_2 isotherms analyzed .

Table 4.3. Textural characterization of NH_4-dawsonite powder by N_2 adsorption

Sample code	V_{pore**} (cm³/g)	$v_{micro}{}^{a}$ (cm³/g)	$S_{meso}{}^{a(*)}$ (m²/g)	$S_{BET}{}^{b}$ (m²/g)
PD13	0.188	0.095	218	661
S1bar	0.214	0.081	318	509
S2bar	0.122	0.099	50	429
S4bar	0.097	0.066	76	388
S6bar	0.097	0.049	108	338
S8bar	0.094	0.064	69	382

*Value obtained by using the arithmetic average

The total pore volume and specific surface area of the powder analyzed were varying from 0.094 cm^3g^{-1} to 0.214 cm^3g^{-1}, S8bar sample, PD13 sample respectively (see Table 4.3). The more the pressure inside the microsystem increased the less the total volume of the pores inside the samples was obtained. This statement was confirmed also by the values of the specific surface area (BET) which varied from 338m^2g^{-1} to 661m^2g^{-1}(See Table 4.3).

The low quantity of microporosity was confirmed by application of the *t*-plot method.

Indeed the catalytic activity of micro-processed NH_4-dawsonite showed an analogy in terms of BET specific surface area with the respect of ILDP results by (total pore volume 1.6 cm^3g^{-1} and BET, 773 m^2g^{-1}, respectively)[10]and similarity regarding the results obtained by using microsystem at atmospheric pressure[4] and 1bar[5] (See Table 4.3 samples PD13, S1bar and S2bar). But the more the pressure increased inside the micosystem the lower the catalytic activity of the powder became. (See Table 4.3 samples S4bar, S6 and S8bar).Therefore, the precipitation of the crystalline synthetic mineral occurs in better conditions at lower values of the working pressure; in this case no need of extra energy consumption is required.

A summarized influence over time of production, textural and morphological characteristics of the powder obtained under pressure was showed in Table 4.4. It was determined an obvious influence on the time of production connected with the solid particle size and particle size distribution. The more the pressure is increased the longer time the process runs and smaller the particles obtained during the precipitation. Increasing the pressure within the microreactor lower influence over the porous properties was found, which put the microtechnology above the conventional processes regarding the safety and economical needs.

Table 4.4. Influence of pressure over time of production and powder characteristics

Sample code	Pressure (bar)	Average time of production (s)	Average particle size (nm)	S_{BET} (m^2/g)	Purity (weight loss/%)
PD13	0.987	58	13	661	54
S1bar	1	187	12	509	62
S2bar	2	270	4	429	49
S4bar	4	204	3	388	56
S6bar	6	153	3	338	55
S8bar	8	200	3	382	64

The optimal working pressures, useful for improving both the continuous time of production and catalytic (porosity) properties, were 1bar and 2bar. These results sustain and demonstrate once again the advantages of the miniaturization of the system through microreactor technology applications (See **Introduction** Section).

4. Conclusions

The influence of pressure on the precipitation process inside the split-recombine Caterpillar micromixer was studied. Increasing the pressure better control of the particle size and particle size distribution was found. An increase of limiting time of production was successfully determined (up to 6 times comparing to experiments made at atmospheric pressure and 1bar).

Lower sample crystallinity was detected, though, by applying pressure within the microsystem with respect to X-ray diffractograms drawn for NH_4-dawsonite prepared at atmospheric pressure[4].This could be explained in terms of reduced crystalline phase contained by the powder and smaller crystallites formed through the precipitation reaction. The broadened diffractograms found for samples precipitated at high pressure prove the sustained results. Higher purity was found for powder precipitated at pressure 1bar and 4bar opposing precipitation process at both milliliter scale[10] and industrial one. The weight loss calculated from TGA was closed to the theoretical one (63%) for experiments made at pressure 1bar and 4bar and decreased purity was determined for the rest specific parameters. Similar morphology of NH_4-dawsonite particles was determined comparing to those in the literature. Same aggregated spherical-type particles were discovered by transmission electron microscopy as was published by conventional processes[6]. Higher NH_4-dawsonite BET surface area was reached comparing to values of the powders prepared by the conventional precipitation (BET around 300 m^2g^{-1}) and similar characteristics with respect to the powder obtained by ILDP process[10] (between 500 m^2g-1 and 700m^2g-1).

The need of pressure within a microreactor was demonstrated to depend on the type of the reaction conducted, i.e. Diels-Alder reaction (2-furylmethanol and 3-furylmethanol with the maleimides) conducted within a capillary microreactor[12] or formation of benzylmethylcarbamic acid (γ) by reaction of N-benzyl methylamine (α) and CO_2 (β) reaching the pressure of 400bar[13] or NH_4-dawsonite precipitation within a split-recombine Caterpillar microreactor , which could be placed within low pressure (2bar) or/and atmospheric pressure microscale processes.

Microreactor technology under pressure has been most applied for organic synthesis or supercritical condition reactions and was demonstrated a higher efficiency comparing with the convectional processes. To have a better understanding on how solids need to be handled at micrometer scale the future work should be focused on different experimental process conditions conducted first within a simple T-junction in order to discover the influence of good/bad mixing on solid particle precipitation control and then within a straight channel poly (methyl methacrylate) microreactor delivered by IMM, Mainz, with the possibility of visualizing in all moments the mixing inside.

References

[1] Bothe D., Stemich C., Warnecke H. J., 2006, Fluidmixing in a T-shapedmicro-mixer, Chemical Engineering Science 61, 2950–2958;

[2] Stoica G., Pérez-Ramírez J., 2007, Reforming of dawsonite by memory effect of AACH-derived alumina Chem. Mater., *19*, 4783-4790;

[3] Fletcher P.D.I., Haswell S. J., Pombo-Villar E., Warrington B.H., Watts P., Stephanie Wong Y. F. and Zhang X., 2002, Micro reactors: principle and applications in organic synthesis, Tetrahedron, 58, 4735-4757;

[4] Dubert D. C., Garcia-Valls R. and Pérez-Ramírez J., 2010, Dawsonite production with caterpillar microreactor, Chemical Engineering Transactions, 21, 1003-1008 DOI: 10.3303/CET1021168;

[5] Dubert D.C., Pérez-Ramírez J. and Garcia-Valls R., 2011, Continuous synthesis of porous ammonium dawsonite within a new microstructured system, Chemical Engineering Transactions, 25, 231-236, DOI: 10.3303/CET1125039;

[6] Zhang X. and Wen Z., Gu Z., Xu X., Lin Z., 2004, Hydrothermal synthesis and thermodynamic analysis of dawsonite-type compounds, Journal of Solid State Chemistry 177, 849–855;

[7] Gu Z., Xu X., Lin Z., Brunauer S., Emmett P.P., Teller E., 1938, Adsorption of gases in multimolecular layer, J. Am. Chem. Soc. 60, 309;

[8] Lippens B. C. and de Boer J. H., 1965, Studies on pore systems in catalysts: V. The *t* method, Vol.4, Issue 3, 319-323;

[9] Meier M., 2004, Crystallite size measurement using X-Ray diffraction, Department of Chemical Engineering and Materials Science, University of California,Davis:(http://chms.engineering.ucdavis.edu/students/undergraduates/labs/files/XRD-CSize1.pdf);

[10] Stoica G. and Pérez-Ramírez J., 2007, Reforming of dawsonite by memory effect of AACH-derived alumina Chem. Mater., *19*, 4783-4790;

[11] Sing K. S. W., Everett D. H., Haul R. A. W., Moscou L., Pierotti R. A., Rouquerol J., Siemieniewska T., 1985, Reporting physisorption data for

gas/solid systems with special reference to the determination of surface area and porosity *Pure Appl. Chem.,* 57, 603;

[12] Verboom W., 2009, Selected Examples of High-Pressure Reactions in Glass Microreactors, Chem. Eng. Technol., 32, No. 11, 1695–1701;

[13] Tiggelaar R. M., Benito-López F., Hermes D. C., Rathgen H., Egberink R.J.M., Mugele F. G., Reinhoudt D. N., Albert van den Berg, Verboomb W., Gardeniers H. J.G.E., 2007, Fabrication, mechanical testing and application of high-pressure glass microreactor chips, Chemical Engineering Journal 131, 163–170;

[14] Elmabruk A. M., Mingxing Y., Yundong W. and Youyuan D., 2008, A State-of-the-Art Review of Mixing in Microfluidic Mixers, Chinese Journal of Chemical Engineering, 16(4) 503—516;

Chapter 4

Influence of pressure over ammonium dawsonite continuous precipitation at microscale

Chapter 4

Influence of pressure over ammonium dawsonite continuous precipitation at microscale

Chapter 5

Influence of imperfect mixing on NH_4-dawsonite particles formation within new types of micromixers

The present Chapter goes deeper in exploring the NH_4-dawsonite precipitation at microscale by investigating three types of microchannel geometry (T-shaped stainless steel, PMMA spilt-recombine and Y-shaped PMMA approaches) within two different mixing regimes (perfect (split-recombine)/imperfect (T/Y-shaped microsystem.)). All experimental analyses showed better results, from both quantitative and qualitative point of view, by applying simple microtechnology (straight channel microsystem) more than sophisticated one (split-recombine approach) on specific precipitation of ammonium dawsonite at micrometer scale comparing to milli/macrometer scale.

Influence of imperfect mixing on NH_4-dawsonite particles formation within a new types of micromixers

1. Introduction

Mixing in passive micromixers is controlled by two main approaches: multilamination and mixing by convection[1]. Multilamination mixing deals with shaping two or more liquid streams into smaller ones of alternative phases, so called lamellae[1], inducing an enhanced mixing inside the microchannel. A good description is given also, in *Chapter 1* (*Section 1.1.2*) of the thesis. Convective mixing combines two fluids by viscous-convective approach which leads to liquid lamellae of different composition with respect to the initial one[1]. Both approaches appear in the same characteristic laminar regime[1] which by the reduction of the length scale the Reynolds number decreases so much , Re <<1, that diffusion completely dominates the flow, unless other mechanisms are brought into play, as is the case of secondary flows or instabilities induced by elastic forces for non-Newtonian viscoelastic fluid flows[2]. One of the simplest types of this class of micromixers is T-shaped one (See Figure 5.1a) which exhibits the characteristic engulfment flow[1] depending on Reynolds number operated, i.e. engulfment flow at Re=186 (See Figure 5.1b) [4]. Many studies have been carried out to understand perfectly the mixing performance of the T-shaped micro-devise[2], because of its easy implementation in a complex microfluidic system[3]. A review of these studies is presented by Mansur et al.[3] where different mixing performance approaches are highlighted. As a basic design, the T-shaped channel is ideal for investigations of basic transport phenomena at the microscale, such as scaling laws or the effects of nonlinear forcing or fluid rheology[3]. Theoretical considerations regarding the scaling behavior sustain the advantages of micromixers technology, that support faster and exothermic reactions, as minimizing the scale better thermal control is reached. In case of a T-shaped micro-mixer, the secondary flow acts mainly in cross directions, i.e. perpendicular to the axial direction, and can be used to mix the two feed streams[4].

Even though, it was demonstrated that T-shaped microsystems pose as inefficient mixers when high mixing performance is needed, still its usage is required. Literature gives several important applications of T-shaped micromixers in gas and liquid flow, i.e. in extraction processes of ammonium salt with Palladium (Pd) catalyst recovery within the Butyl Cinnamate synthesis[5], for measuring a target analyte concentration by using the fluorescence intensity of the region where the analyte and the fluorescent indicator get in contact, study of rapid chemical reactions in solution with stopped-flow time resolved Fourier transform infrared spectroscopy (TR-FTIR), as a postcolumn reactor[6], for performing enzyme assays[7], as a tool for dispersing immiscible liquids and forming micro droplets[8] etc.

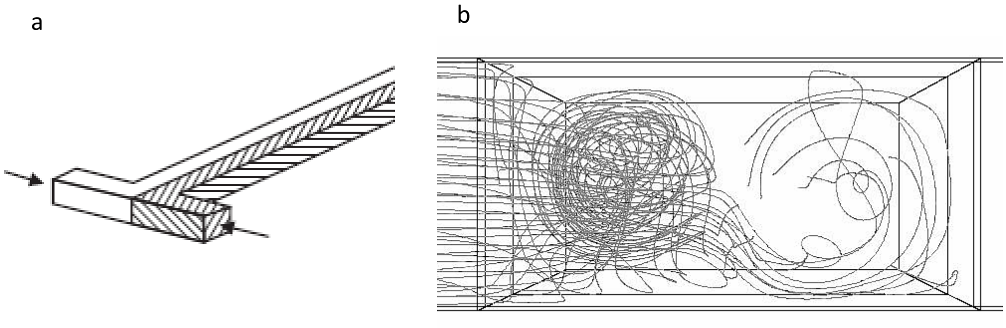

Fig.5.1: a) T -shaped micromixer basic design without pulsing, b) flow trajectories for engulfment flow (i.e. Re=186). Source: Nguyen and Wu (2005)[6]

Designing particle based materials was demonstrated to have better achievement by using continuous micro-scale processes rather than conventional ones[9]. T-shaped micromixers application in this field was the main type of microtechnological devices studied. Some exemplifications are lettered further: T-shaped mixer used to produce monodisperse sodium chloride aerosol particles[9]. An important review on bubble-liquid systems mechanism formation through a T-junction mixing channel and several others was reported in the literature with the aim of investigating the gas (i.g. air) bubble shape, size and formation mechanism[10]. They demonstrated that important quantitative and bubble length formation details were able to be obtained by using micro-flow devices (i.g. T-shaped mixer). In last decades, large efforts have been done for generating particles with different morphology because their vast range of industrial applications. Microtechnology was discovered to be the best alternative technique for generating emulsion droplets with enhanced properties. T-junction was adopted for generation of monodisperse magnetic emulsion droplets in different shapes: spheres, disks, and plugs[11] with higher magnetic properties than those synthesized by conventional processes (Figure 5.2). One of the most interesting applications of T-shaped micromixers developed recently was described by Kockmann et al. 2008[1] regarding the barium sulfate solid particles precipitation and their formation mechanism. Also they presented an extra usage of the T-junction to investigate azo coupling under industrial conditions.

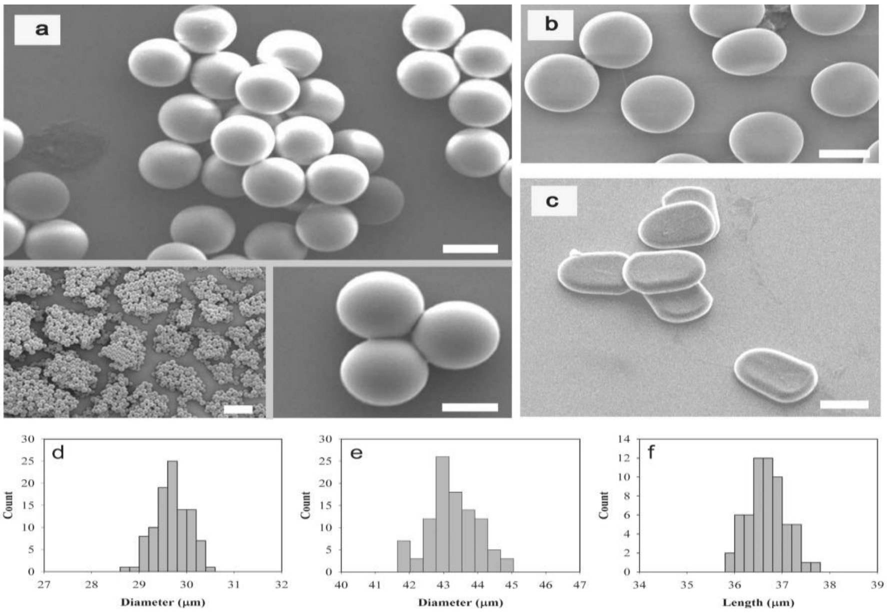

Fig.5.2. SEM images of magnetic microhydrogels: (a) spheres, (b) disks, and (c) plugs, and distribution of the diameter of (d) the spheres [(a) top, coefficient of variation CV = 1.2%], (e) the disks (CV = 1.6%), and (f) the long length of the plugs (CV = 1.3%). Source: Hwang et al. 2008.

The augmentation of all types of industries: pharmacy, analysis and biochemistry, chemistry, engineering, etc, for innovative and economic mixing technologies: effortless operation of highly exothermic/explosive chemical reactions has led to a greater development of new microfluidic systems material with enhanced chemical and physical properties. Metals, silicon, glass, and polymer are the main four types of materials used for microfluidic fabrication. Most of these are widely used in the industry but numerous limitations were established, namely: micromachining, opaque, absorption of biological molecules to silicon surface and electrically conducting properties which anticipate the restricted use of metal and silicon. Because of high costs of glass machining suppliers searched for other materials such as polymers which overcome the glass and silicon drawbacks by being optically clear, non-toxic and the cost is lowered substantially. Several types of polymers were suggested by the literature as fulfilling theses presented above: polycarbonate, polyethylene, polypropylene, polystyrene, poly (dimethylsiloxane) (PDMS), and poly (methyl methacrylate) (PMMA)[12]. Further, the focus will be set on PMMA material for T-shaped micromixer as the present work is based on its chemical and physical properties. PMMA is a synthetic polymer of methyl methacrylate, (See Figure 5.3.) used in both commercial dental and bone cement applications[13], and has the characteristics of a transparent thermoplastic material. Its commercial name is acrylic glass and represents the economical alternative to polycarbonate (PC) material. It is usually desired for its moderate properties , easy to handle and process and not last for its low cost. The usual industrial applications of acrylic resins, including here lattered PMMA are: adhesives, automotive signal lights, lenses, light fittings, medallions, neon signs, protective coatings, etc[15].

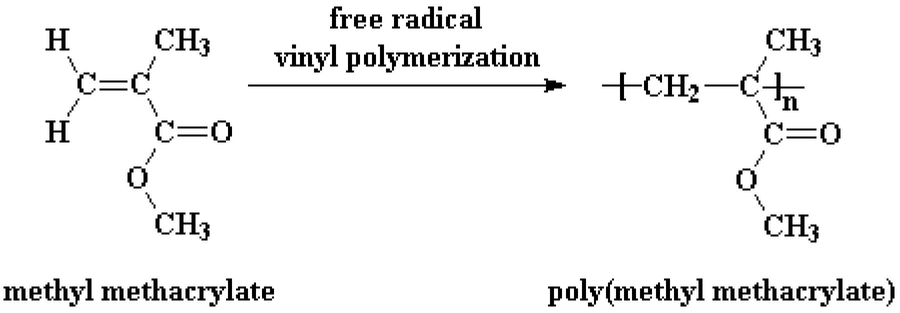

Fig.5.3. PMMA chemical structure and polymerization reaction.
Sourse:http://pslc.ws/macrogcss/maindir.html

Yu et al. extended PMMA applications in medical and environmental world by counting the important fields: DNA, amino acids, peptides and protein analysis, profiling saccharides, pollutants, nerve agents, and explosives screening, electrophoretic separation of ions, and detection of purines[16].

Based on the PMMA mater properties, the present chapter deals with a new application of PMMA-made microdevices in precipitation of porous material (ammonium dawsonite – NH_4-Dawsonite) and its chemical and physical characterization, with the aim of improving both the industrial process and quality market demands. As specified in previous chapters NH_4-Dawsonite principle application is as precursor of very pure Alumina (Al_2O_3) by thermal decomposition at temperature higher than 1100K which requires enhanced quality of the raw materials. Consider the advantages of PMMA – based material outlined above the present work experimented two types of microdevices PMMA-based for holding the NH_4-Dawsonite precipitation process seeking for novel useful information regarding the influence of different mixing within two different microchannel geometries on particle formation and crystal growth. PMMA split-recombine Caterpillar micromixer and PMMA Y-unction were proposed by the authors with respect of stainless steel T-junction approach used as preliminary mixing section.

The Chapter carry on the experimental work conducted at atmospheric pressure (See ***Chapter 2***) with the aim of reaching the optimal process parameters for continuous NH_4-dawsonite production and enhanced product characteristics, meanwhile the mixing and crystals growth inside the microchannels proposed were visualized and controlled. The results were compared with those presented in *Chapter 2*, with those published at milliliter (In Line Dispersion-Precipitation Technique) and batch scale for NH_4-dawsonite production.

2. Experimental section

2.1. Methodology and reagents

NH_4-dawsonite emulsion was synthesized following the exact methodology described in *Chapter 3* based on the same precipitation process parameters: constant pH (= 9) and temperature (60^0C) and variable flux and concentration for both mother solution used at atmospheric pressure, with the possibility of visualizing the first appearance of solid precipitate within the both channel geometries and the influence on solid deposition and growth by time. The set-up containing all approaches: PMMA split-recombine, T-junction cross-flow channels and Y-junction mixing device is pictured in Figure 5.4.A,B.

Table 5.1: Process parameters used within the both systems studied

Initial solutions concentration (M)		Initial solutions flow rate (mL/min)	
$Al(NO_3)_3x9H_2O$	$(NH_4)_2CO_3$	$Al(NO_3)_3x9H_2O$	$(NH_4)_2CO_3$
0.55	1	12	48
0.22	2	20	20
0.12	1.09	20	20
1.1	2	10	20

NH_4-dawsonite precipitate was first prepared by using four different concentrations of aqueous solutions of $Al(NO_3)_3x9H_2O$) and $(NH_4)_2CO_3$ which were mixed at 333K (60^0C) within the reaction channel. Syntheses were carried out at constant pH = 9 into a laminar regime at atmospheric pressure. For comparative purposes dawsonite synthesis was held further at different value of flow rates of acid and base solution (see table 5.1). The resulting products were collected into a beaker and then filtered under vacuum by using three types of filter paper: Whatman filter paper of 11µm, 7µm and 0.7µm pore size, followed by the washing step employing 250 mL distillated water for cleaning the CO_2 excess.

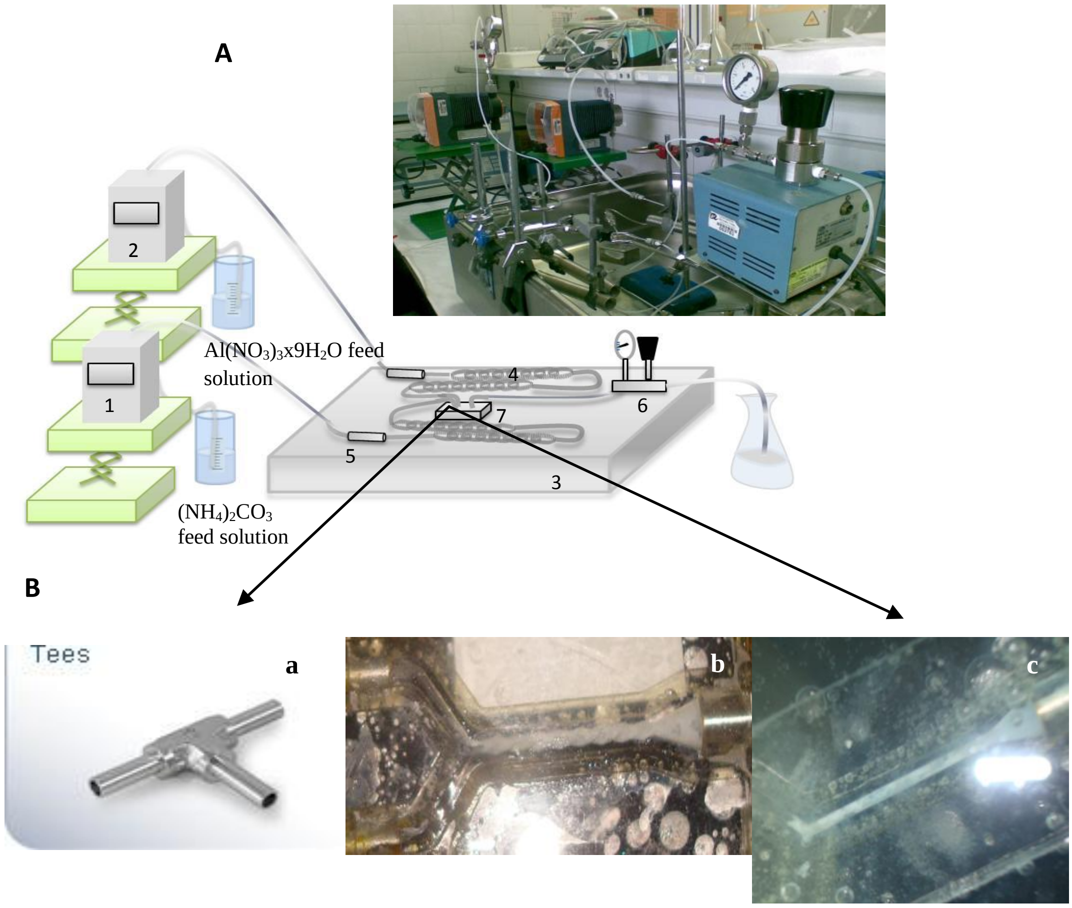

Fig.5.4: A) Microsystem set-up fitted for pressure atmospheric pressure: 1 – Metering pump (for $(NH_4)_2CO_3$ initial solution), 2 – Metering pump (for $Al(NO_3)_3$ initial solution), 3 – Water bath, 4 – Stainless steel coil, 5 – Check valves, 6 – Pressure dumper, 7 – Stainless Steel Caterpillar microreactor CPMM1200/8, Lab-scale microsystem set-up photo (inset), B) a – Stainless Steel T-junction 316L SS VOD/AOD. Sourse: www.ham-let.com, b – PMMA Caterpillar Micromixer CPMM-R1200/8-SO-PMMA-glued, c – Y-JUNCTION 1200 X 1200 PMMA;

The post-precipitation treatment: stirring step at 60^0C for 2 or 3 hours (see ***Chapter 2)*** was skipped for avoiding the microzise crystals growth within the final product. The specific process parameters listed above in Table 5.1 were chosen for optimizing the precipitation process based on geometry modification of inner channel and imaging the mixing inside it (See Figure 5.4 Aa,b,c). The results were compared with the ones obtained for the same process parameters carried at atmospheric pressure[17], with those listed in the literature[18] and the results obtained through the precipitation process at milliliter scale[19].

Further, the Chapter is structured following the three approaches listed earlier driving the conclusion simultaneously.

2.2. Powder characterization

Similar characterization techniques presented in the previous *Chapters* (*2,3 and 4*) were applied to investigate the chemical and physical properties of the precipitated dried NH_4-dawsonite. Porous properties of the material studied (BET specific surface area and mesopores distribution) were distinguished through BET method[20] and the *t*-plot method[21] respectively. Reaction channel geometry and different types of mixing at microscale were also studied with respect to the system efficiency.

3. Results and discussions

The experimental fragment followed the synthesis of NH_4-dawonite within different types of mixing based on microchannel geometry modification and its influence on the product quality and time of production. Furthermore, the comparison between product obtained on the microsystem at atmospheric pressure (first set-up, ***Chapter 2***) and the product obtained within all approaches discussed in *Section 2* of the present *Chapter* gave us a better understanding regarding the precipitation process at microscale and also, about the optimal conditions that had to be applied in order to enhance the catalyst properties. The optical visualization of the mixing inside both categories of microchannels could improve the knowledge searched in entire work regarding “How to handle solids at microscale” hence the industry to accept increasingly the microreactor technology. First, the microsystem ran with the highest concentrations for both aqueous solutions ($Al(NO_3)_3$ – 1.1M and $(NH_4)_2CO_3$ – 2M) and their corresponding flow rates (10mL/min $Al(NO_3)_3$ and 20mL/min $(NH_4)_2CO_3$) and step by step, all chosen process conditions followed the same procedure till was reached the minimum proposed values (See Table 5.1) both for aqueous solution concentration and flow rates ($Al(NO_3)_3$, 0.12M, 20 mL/min and $(NH_4)_2CO_3$, 1.09M, 20 ml/min). A white solid precipitate was synthesized meanwhile the time of production (See Table 5.2) and precipitate deposition spot were searched with the purpose to find the optimal parameters for preparing the mineral with the best quality and price. Figure 5.5 shows the different inside channel spots where the synthetic analogue started to attach on the walls inducing the solid aggregation phenomenon. Results shown in Table 5.2 confirm a significant increase in time of production for all three approaches by decreasing the concentration of both aqueous solutions. Depending on the specific geometry of the reaction channel used the production of NH_4-dawsonite completed in longer or shorter period, getting the optimal time by using the Y-junction approach.

Table 5.2: Time of production values at different process conditions for all three mixing geometries used

Substance concentration (M)		Substance flow rate (ml/min)		Time of production at atmospheric pressure (s)			
$Al(NO_3)_3$ x $9H_20$	$(NH_4)_2$ CO_3	$Al(NO_3)_3$x $9H_20$	$(NH_4)_2$ CO_3	*CPMM 1200/8*	*T-junction 316L SS VOD/AOD*	*CPMM-R1200/8-SO-PMMA-glued*	*Y-junction 1200 X 1200 PMMA*
1.1	2	10	20	40 (S13)	228(T7,T8)	232(S4_2)	499(S4Y)
0.55	1	12	48	58 (S18)	825(T1,T2)*	480(S3)	807(S3Y)
0.22	2	20	20	109 (S24)	340(T3,T4,T5)	1020(S2_1)	1176(S2Y)
0.12	1.09	20	20	558 (S44)	2461(T6)*	1190(S1)	1950(S1Y)**

*Average time of production calculated based on consumed volume of the initial solutions without interrupting the process till entire volume prepared initially ran out ; **Sample S1Y – amorphous;

For visualizing the precipitation process (Figure 5.5.b2) the increased time of production in Y-junction geometry might be explained by chaotic mixing appearance inside the straight channel, which could influence the distribution of the precipitate particles through the center of it and lowered the walls effect.

If the discussion is focused on PMMA Caterpillar micromixer with split-recombine approach which generates a perfect mixing the production time tendency is similar with that appeared within the Y-junction (See Table 5.2 and Figure 5.5.a). These two approaches have in common the same geometry for both inlets, regarding the distance between them and the angle of 120^0 (See Figure 5.6). The distinctive distance between the two inlets and the fluids contact angle (See Figure 5.6 red circle), showed to be critical for enhancing the precipitation process within microchannels. Experimental work showed larger production time concerning PMMA micromixers geometry comparing to that within the stainless steel mixers (See Table 5.2). Taking into account the information gathered the efficiency of the process was calculated further (Table 5.3).

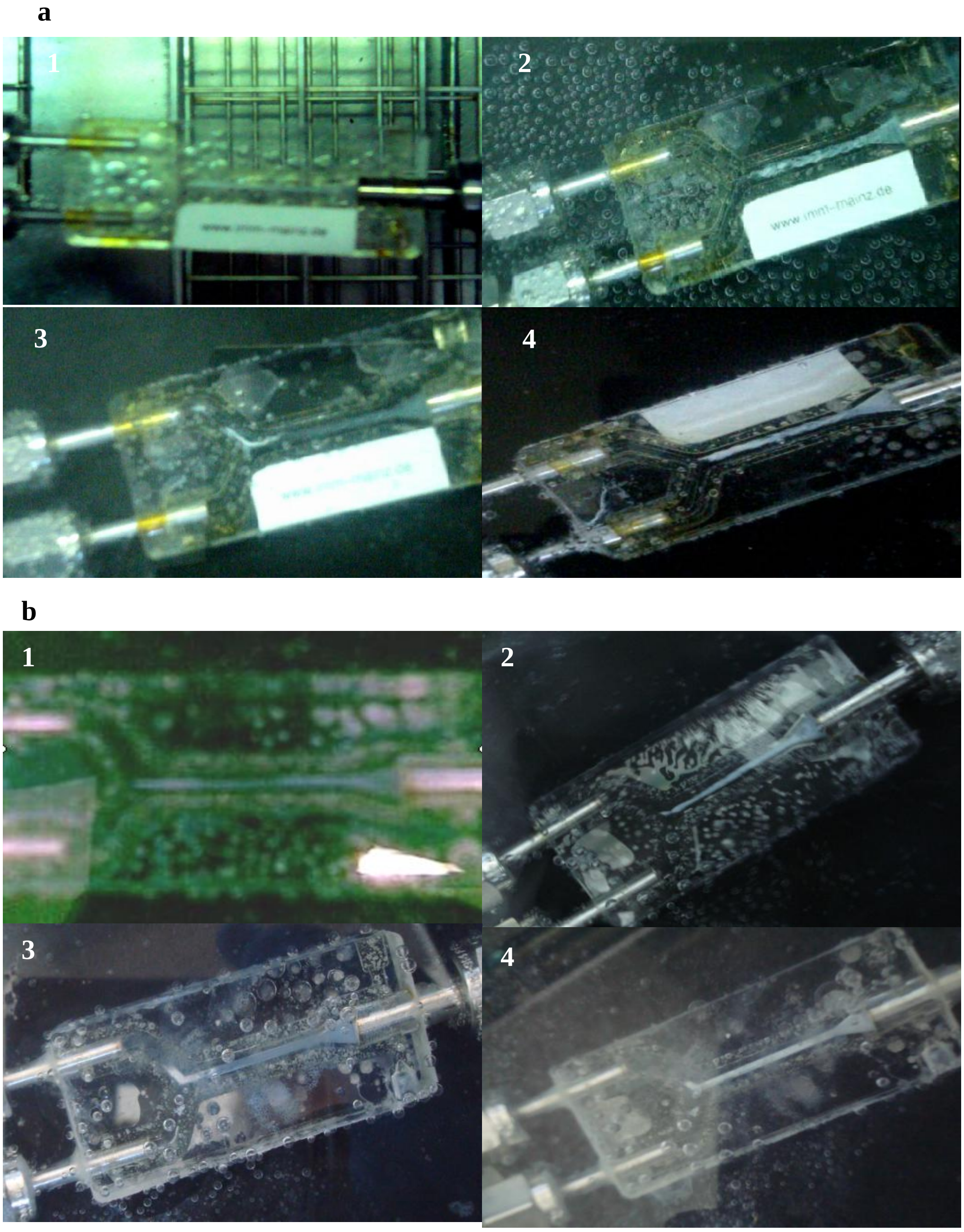

Fig.5.5: Visualization of different solid precipitate appearance inside both categories of mixing channel geometries: a) split-recombine channel – Caterpillar PMMA micromixer and b) straight channel – PMMA Y-junction; Powder precipitation pictured for variable process parameters: 1- initial solution concentrations: 0.12-1.09M (aq. sol. $Al(NO_3)_3x9H_2O$ and aq. sol. $(NH_4)_2CO_3$ respectively) with corresponding flow rates: 20-20 mL/min; 2- - initial solution concentrations: 0.22-2M (aq. sol. $Al(NO_3)_3x9H_2O$ and aq. sol. $(NH_4)_2CO_3$ respectively) with corresponding flow rates: 20-20 mL/min; 3 - initial solution concentrations:0.55-1M (aq. sol. $Al(NO_3)_3x9H_2O$ and aq. sol. $(NH_4)_2CO_3$ respectively) with corresponding flow rates: 12-48 mL/min; 4 - initial solution concentrations:1.1-2M (aq. sol. $Al(NO_3)_3x9H_2O$ and aq. sol. $(NH_4)_2CO_3$ respectively) with corresponding flow rates: 10-20 mL/min;

It was discovered an appealing dependency among all three mixing approach chosen; applying a chaotic mixing (characteristic to engulfment flow[1] in T,Y-junction microdevices) for precipitation reaction, the time of production increased proportionally with the yield which brought the conclusion that no perfect mixing is necessary to obtain a better and constant control of solid particle formation.

Table 5.3: Influence of different micromixer geometries over time of production and yield

Sample code	Time of production (s)			Yield (%)		
	T-junction 316L SS VOD/AOD	*CPMM-R1200/8-SO-PMMA-glued*	*Y-junction 1200 X 1200 PMMA*	*T-junction 316L SS VOD/AOD*	*CPMM-R1200/8-SO-PMMA-glued*	*Y-junction 1200 X 1200 PMMA*
(T7,T8); S4_2; S4Y	228	232	499	30	43	31
(T1,T2); S3; S3Y	825	480	807	15	38	58
(T3,T4,T5); S2_1; S2Y	340	1020	1176	52	54	65
T6; S1; S1Y	2461	1190	1950	72	47	56

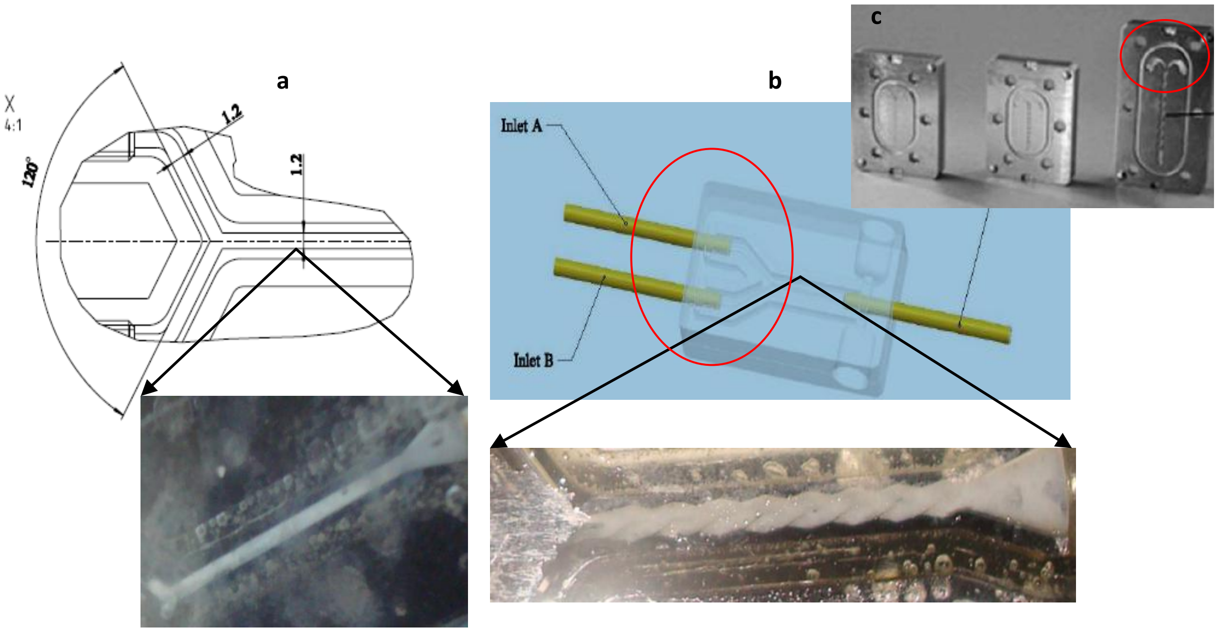

Fig. 5.6: a) PMMA Y-junction with straight channel sketch; b) PMMA split-recombine Caterpillar micromixer; c) Stainless steel split-recombine Caterpillar microreactor (CPMM 1200/8) – inside geometry.

As Figure 5.7 sketched a homogenous efficiency (constant increment of liquid conversion by time) was reached by applying a chaotic mixing within a Y-shaped with straight channel micromixer, attained almost 70% conversion.

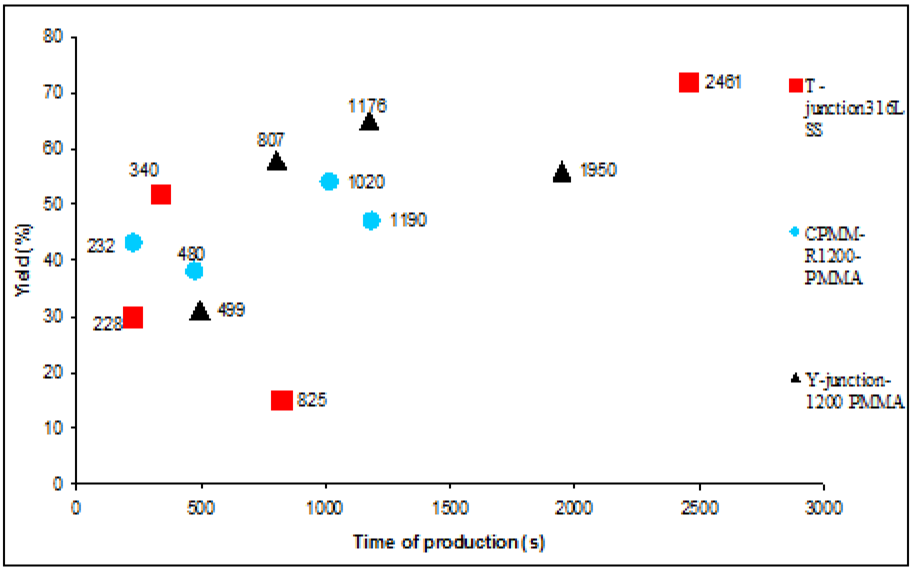

Fig.5.7: Mixing influence on NH_4-dawsonite time of production and precipitation process efficiency

Eventually, no perfect mixing is needed for synthesizing more solid quantity in less time. Furthermore, was also demonstrated that by using the straight channel approach with a specific position of the inlets the wall attraction forces were minimized substantially conducting to less particle attachment and implicit channel blocking exclusion. This sustains the microtechnology advantage referring to better control of the process, miniaturizing the amount of raw materials used and reaching faster transfer of research results into production which could easily satisfy the industry requirements of NH_4-dawsonite production.

Powder X-ray diffraction patterns of the produced samples (Figure 5.8) confirmed that dawsonite was the only crystalline phase in the precipitates NH_4-dawsonite ($NH_4AlCO_3(OH)_2$, JCPDS 42-250). The crystalline phase was analyzed for all samples obtained, under variable process conditions and all three mixing geometries. Amorphous phase was found for samples precipitated at lowest value for initial solution concentration and equal flow rates within straight microchannel of the Y-shaped geometry.

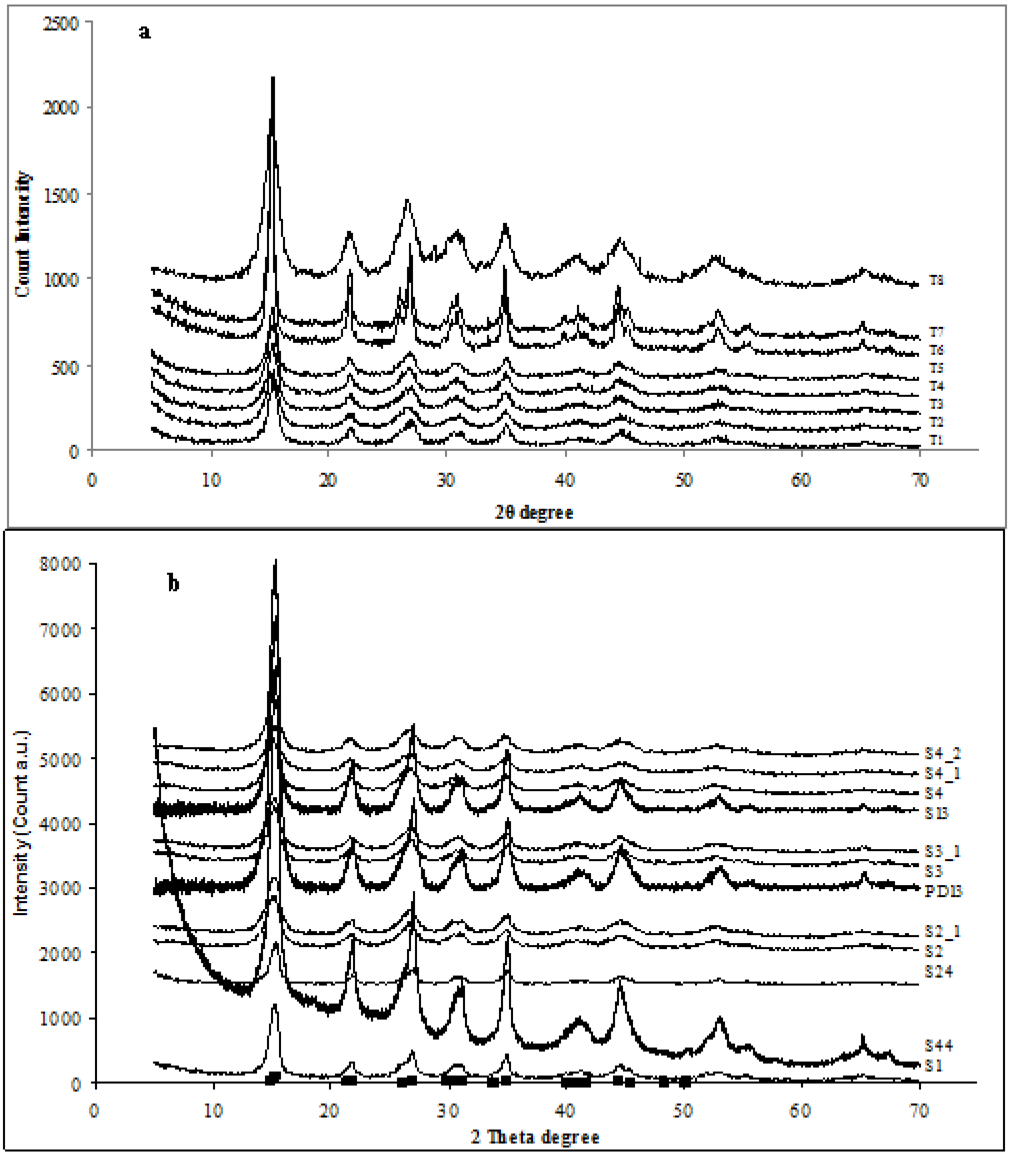

Fig.5.8: X-Ray Diffraction spectra of crystalline NH_4-dawsonite powder at specific temperature (60^0C), pressure (atmospheric pressure) and pH (9) and variable process parameters: solution concentration: 1.1-0.12M ($Al(NO_3)_3x9H_2O$) and 2-1M ($(NH_4)_2CO_3$) with corresponding flow rates: 10-20mL/min ($Al(NO_3)_3x9H_2O$) and 20-48mL/min ($(NH_4)_2CO_3$) for all three mixing geometries: a) T-junction 316L SS VOD/AOD, b) CPMM-R1200/8-SO-PMMA-glued and c) Y-junction 1200 X 1200 PMMA; Black bullets represents the $NH_4AlCO_3(OH)_2$, JCPDS 42-250 reference; S44, S24, PD13 and S13(PD8) picture the XRD spectra characterized for powder obtained within Stainless Steel Caterpillar micromixer(CPMM 1200/8 – old setup).

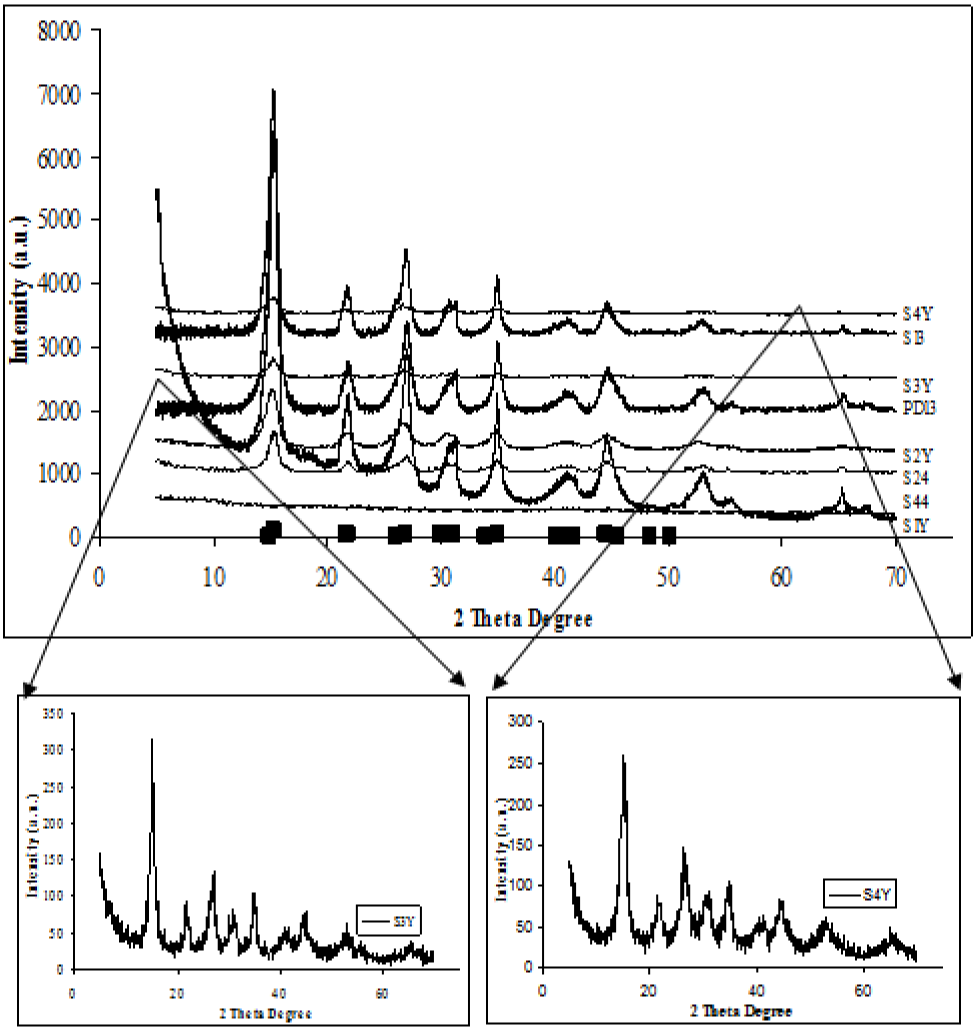

Fig.5.8: X-Ray Diffraction spectra of crystalline NH_4-dawsonite powder at specific temperature (60^0C), pressure (atmospheric pressure) and pH (9) and variable process parameters: solution concentration: 1.1-0.12M ($Al(NO_3)_3x9H_2O$) and 2-1M ($(NH_4)_2CO_3$) with corresponding flow rates: 10-20mL/min ($Al(NO_3)_3x9H_2O$) and 20-48mL/min ($(NH_4)_2CO_3$) for all three mixing geometries: a) T-junction 316L SS VOD/AOD, b) CPMM-R1200/8-SO-PMMA-glued and c) Y-junction 1200 X 1200 PMMA; Black bullets represents the $NH_4AlCO_3(OH)_2$, JCPDS 42-250 reference; S44, S24, PD13 and S13(PD8) picture the XRD spectra characterized for powder obtained within Stainless Steel Caterpillar micromixer(CPMM 1200/8 – old setup).

Lower crystalline phase was discovered in all three approaches comparing with the first set-up (CPMM R1200/8) experiments.

The presence of amorphous phase within trials experimented inside the Y-junction sustain once again, the limiting concentration variable for mother solution in order the precipitate and crystal growth to take place. As literature[1] showed T and Y-junction geometries are important for reducing the particle attachment and minimizing the channel clogging. Influence of different shapes of reaction chambers inside the microreactors used in this study on the crystallites size within the poweder obtained was also determine by using the Sherrer theory[22] (See also ***Chapter 4*** Section 3).

Analyzing table 5.4 a comparable particle size distribution and crystallites size values were reached for all combinations of process parameters used within the Y-shaped geometry. Larger difference was found within the T-junction approach comparing with both PMMA Caterpillar and Y-junction micro mixers, fact that demonstrate the crucial influence of reaction chamber geometry (straight /zig-zag channel or inlets angle position) over mixing regime and efficiency. Considering the results performed in table 5.4 insignificant difference was discovered regarding the two PMMA approaches: perfect mixing within Caterpillar micromixer and chaotic one within the Y-shaped micromixer, used for the precipitating the synthetic mineral.

Table 5.4:: Summerized values for particles and crystallites zise versus different operating geometries for precipitation process

Experiment code	[2]Average particle size (nm)				[1]Average crystallite size (nm)			
	CPMM 1200/8	*T-junction 316L SS VOD/AOD*	*CPMM-R1200/8-SO-PMMA-glued*	*Y-junction 1200 X 1200 PMMA*	*CPMM 1200/8*	*T-junction 316L SS VOD/AOD*	*CPMM-R1200/8-SO-PMMA-glued*	*Y-junction 1200 X 1200 PMMA*
S13; *(T7,T8); S4_2; S4Y	193 µm	-	6	2	13	10	4	5.5
S18; *(T1,T2); S3; S3Y	90 µm	2	3	3	8	6	5	7
S24; *(T3,T4,T5); S2_1; S2Y	896 µm	-	4	2	10	18	5	6
S44; T6; S1; S1Y	-	-	4	-	14	15	6	A

[1]Values calculated with Sherrer equation from XRD spectra of each sample analized. *For these samples the crystallite size was calculated by average arithmetic value. A – Amorphous phase; [2]Values calculated with ImageJ software.

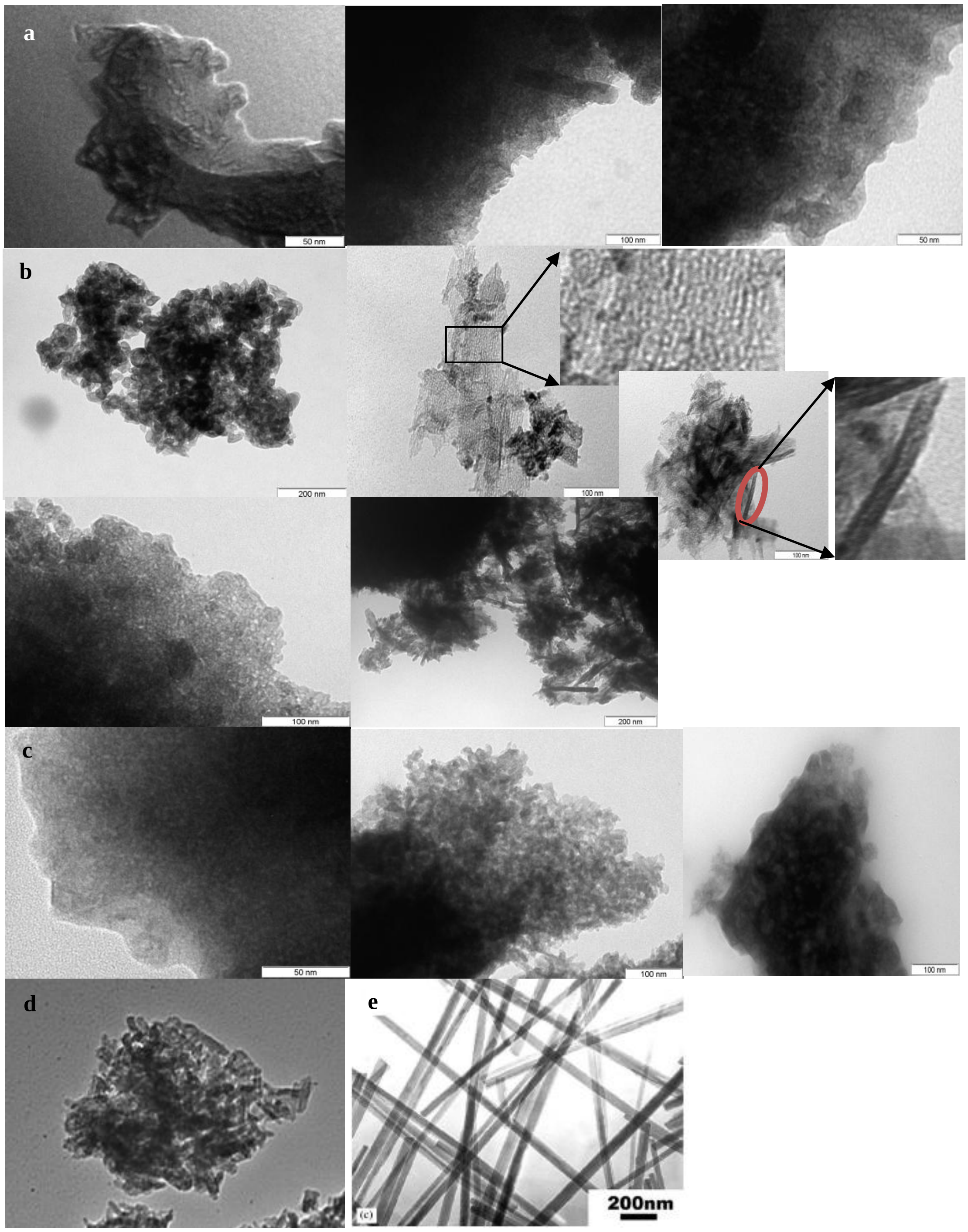

Fig. 5.9: Transition electron micrographs of NH_4-dawsonite synthesized powder at specific temperature (60^0C), pressure (atmospheric pressure) and pH (9) and variable process parameters for all three mixing geometries: a) T-junction 316L SS VOD/AOD (Samples T1,T2), b) CPMM-R1200/8-SO-PMMA-glued (Samples S1, S3, S4_1, S4_2) and c) Y-junction 1200 X 1200 PMMA (S2Y, S3Y, S4Y); d) TEM micrographs for NH_4-dawsonite prepared within a milireactor. Source: Stoica and Pérez-Ramírez (2007)[24]; e) K-dawsonite TEM micrographs prepared by conventional batch precipitation by using $KHCO_3$/Al ration of 16, pH of 9.5 and reaction time of about 24h. Source: Zhang et al. 2004[23].

The particles and crystallites size determined were very similar even though two opposite working regimes were induced fact that demonstrates the hypothesis: no perfect mixing is needed for handling better the solids production at micro scale. By this, Y-junction approach with some specific geometrical consideration could be used as an alternative for reducing channels blocking during solids precipitation. NH_4-dawsonite, in most of the experiments, exhibited the characteristic spherical-like particles which differ from the root-like particles obtained at atmospheric pressure within stainless steel split-recombine microreactor (See PD13, Figure 4.5a, ***Chapter 4***, Section 3) and fibrous K-dawsonite[23] particles presented in the literature (See also Figure 5.9e). Deviation from the present discovery represents the root-like particles for the powder synthesized by using PMMA split-recombine Caterpillar microreactor with inlets angle about 120^0 (Figure 5.9b) which illustrated similar morphology with solid NH_4-dawsinte precipitated within first set-up.

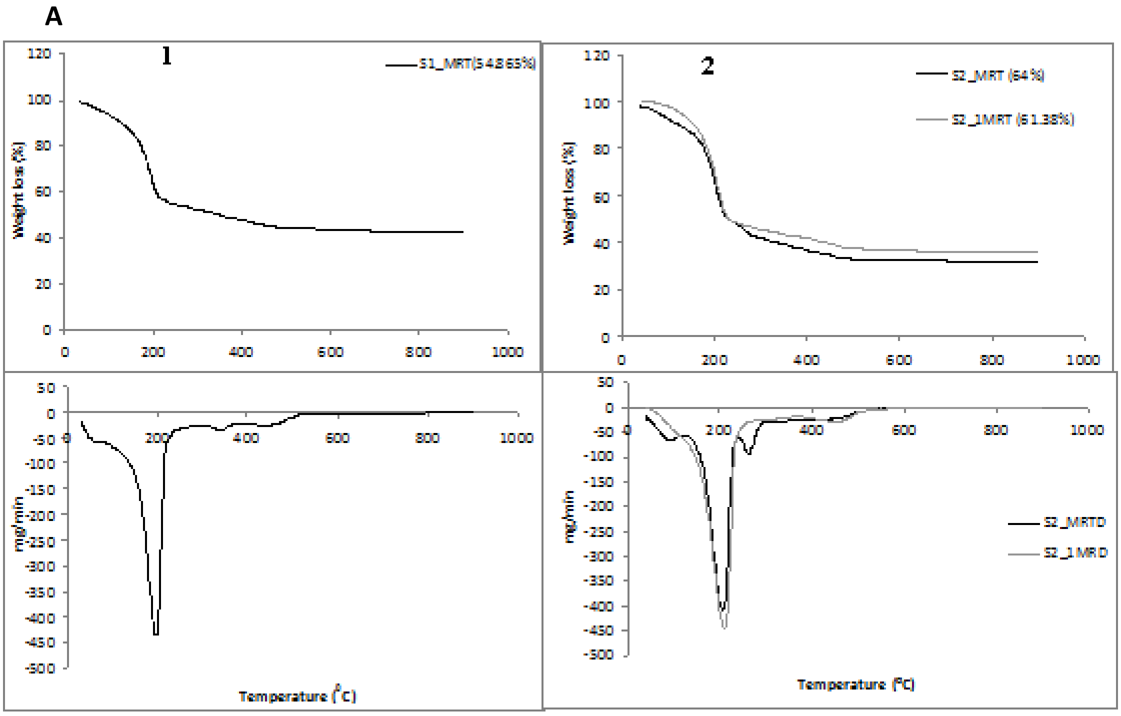

Fig. 5.10: (Top) Thermogravimetric profiles and (bottom) derivative curves of the weight loss of NH_4-dawsonite obtained within three different system geometries: A) CPMM-R1200/8-SO-PMMA-glued; B)) T-junction 316L SS VOD/AOD and C)) Y-junction 1200 X 1200 PMMA at fixed temperature (60^0C), pH (9) and atmospheric pressure and variable process parameters: 1-solutions concentration: 0.12-1.09M ($Al(NO_3)_3x9H_2O$ and $(NH_4)_2CO_3$ respectibely) and coresponding flow rates: 20-20 mL/min; 2- solutions concentration: 0.22-2M ($Al(NO_3)_3x9H_2O$ and $(NH_4)_2CO_3$ respectibely) and coresponding flow rates: 20-20 mL/min; 3- solutions concentration: 0.55-1M ($Al(NO_3)_3x9H_2O$ and $(NH_4)_2CO_3$ respectibely) and coresponding flow rates: 12-48 mL/min; 4- solutions concentration: 1.1-2M ($Al(NO_3)_3x9H_2O$ and $(NH_4)_2CO_3$ respectibely) and coresponding flow rates: 10-20 mL/min.

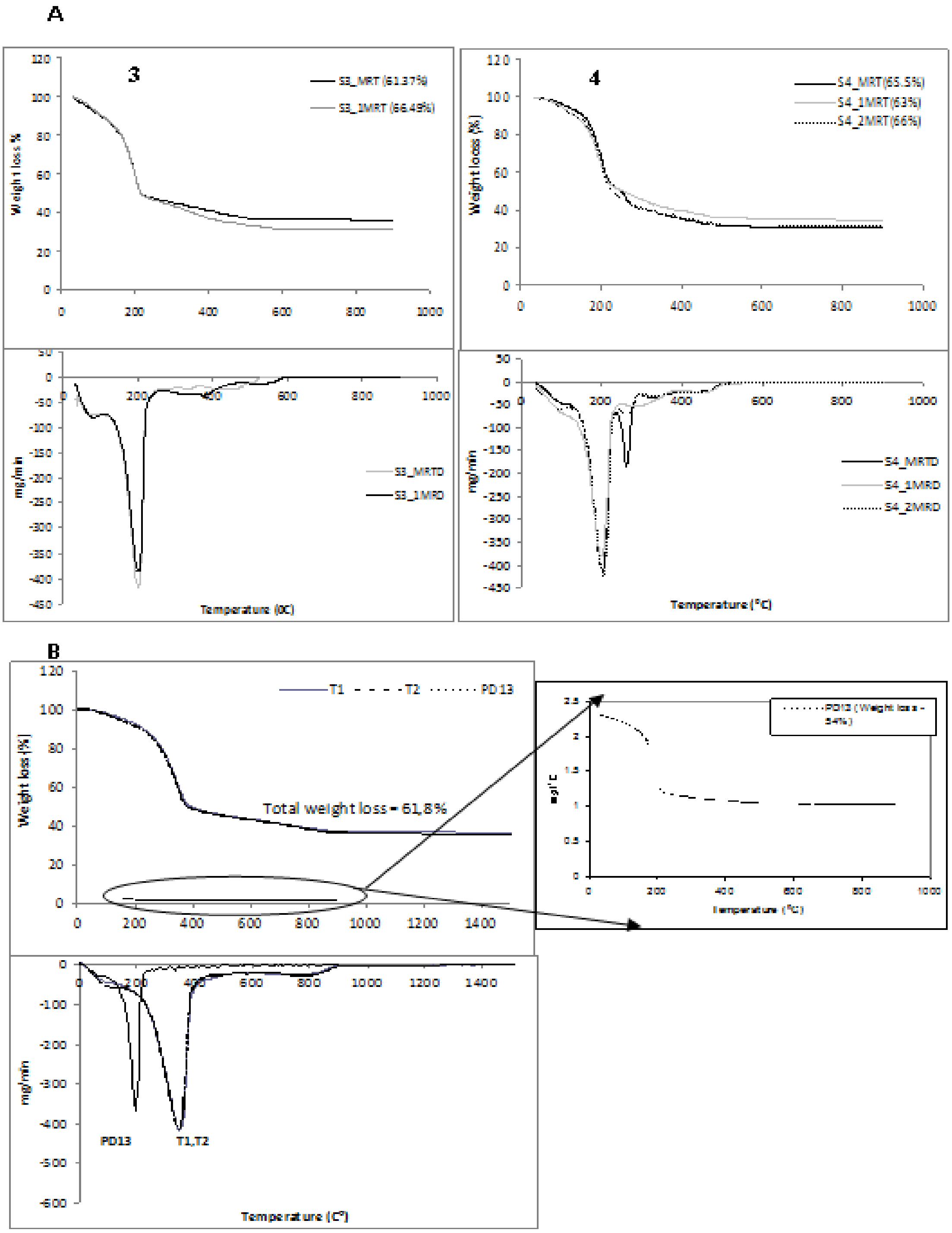

Fig. 5.10: (Top) Thermogravimetric profiles and (bottom) derivative curves of the weight loss of NH_4-dawsonite obtained within three different system geometries: A) CPMM-R1200/8-SO-PMMA-glued; B)) T-junction 316L SS VOD/AOD and C)) Y-junction 1200 X 1200 PMMA at fixed temperature (60^0C), pH (9) and atmospheric pressure and variable process parameters: 1-solutions concentration: 0.12-1.09M ($Al(NO_3)_3x9H_2O$ and $(NH_4)_2CO_3$ respectibely) and coresponding flow rates: 20-20 mL/min; 2- solutions concentration: 0.22-2M ($Al(NO_3)_3x9H_2O$ and $(NH_4)_2CO_3$ respectibely) and coresponding flow rates: 20-20 mL/min; 3- solutions concentration: 0.55-1M ($Al(NO_3)_3x9H_2O$ and $(NH_4)_2CO_3$ respectibely) and

coresponding flow rates: 12-48 mL/min; 4- solutions concentration: 1.1-2M ($Al(NO_3)_3x9H_2O$ and $(NH_4)_2CO_3$ respectibely) and coresponding flow rates: 10-20 mL/min.

The NH_4-dawsonite particle morphology discovered through ILDP process at miliscale[24] (Figure 5.9d) showed similar shape with the powder particles characterized for T,Y-junction and some specific parameters used within PMMA caterpillar microreactor (See Figure 5.9). Influence of channel geometry and inlets angle had higher effect on crystallite growth and particles formation for imperfect mixing comparing to the one experimented within the split-recombine approach. Beyond this, thermogravimetric analyses in air (Figure 5.10 top) confirmed again the increased purity of the dawsonites powder balancing to both milliliter scale and batch product. The total weight losses of the NH_4-dawsonite samples amounted between 54% and 66% (average values between the trials at specific process parameters and different mixing classes), *i.e.* similar and /or higher than the theoretical values based on the dawsonite formulas (63% for NH_4-dawsonite) the purity was reached for samples precipitated within all three approaches of microsystem experimented and almost in all cases for specific process parameters: lower ratio of concentration (0.55M-1M) and higher one for the flow rates (12-48 mL/min) the product reached the theoretical value for weight loss. Overcoming the ideal dawsonite purity could be affected by the device errors. Attending to the transition temperatures in Figure 5.10 (bottom), the thermal stability of NH_4-dawsonite was found to be very similar for most of the samples (*ca*. 300˚C) and some differences appeared for samples precipitated within T and Y-junction (Figure 5.10 B (samples T1,T2 and C (sample S4Y)) reaching the value aproximately 400^0C. These results are in good correspondence with those obtained at milliliter scale[24] and those reported for conventional processes[23] showing the complete thermal transformation of NH_4-dawsonite powder.

As was expected the T-junction and Y-junction had similar behaviour in product precipitation and its quality characteristics, being predominant in both approaches an engulfment regime and a chaotic mixing. Furthermore, we can conclude that mixing type provoked by different channel and inlets design has a great influence not only increasing the control over the solid particle size distribution but also enhancing significantly the purity of the finite powder.

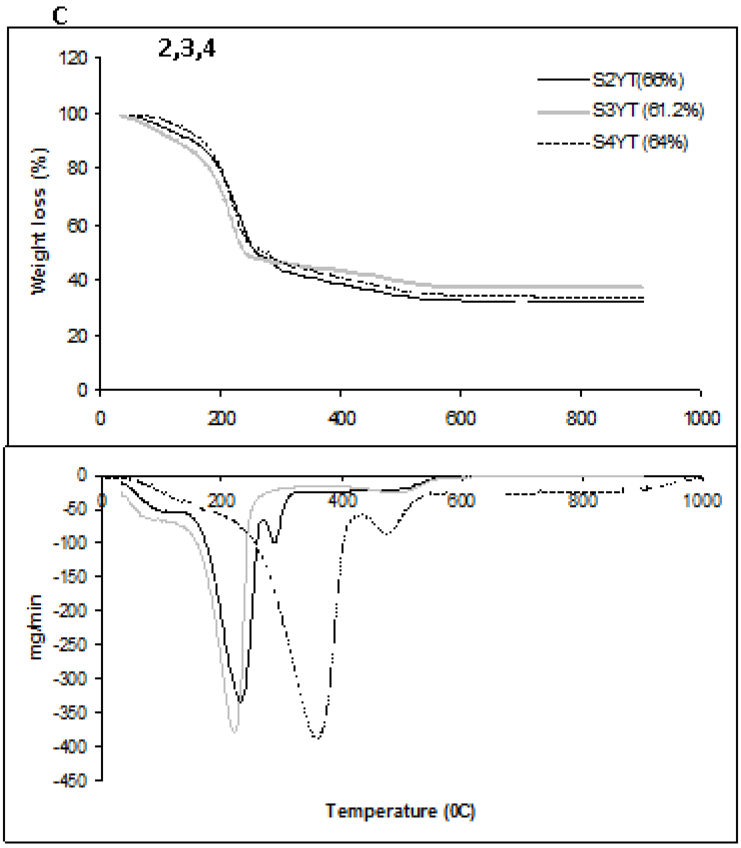

Fig. 5.10: (Top) Thermogravimetric profiles and (bottom) derivative curves of the weight loss of NH_4-dawsonite obtained within three different system geometries: A) CPMM-R1200/8-SO-PMMA-glued; B)) T-junction 316L SS VOD/AOD and C)) Y-junction 1200 X 1200 PMMA at fixed temperature (60^0C), pH (9) and atmospheric pressure and variable process parameters: 1-solutions concentration: 0.12-1.09M ($Al(NO_3)_3x9H_2O$ and $(NH_4)_2CO_3$ respectibely) and coresponding flow rates: 20-20 mL/min; 2- solutions concentration: 0.22-2M ($Al(NO_3)_3x9H_2O$ and $(NH_4)_2CO_3$ respectibely) and coresponding flow rates: 20-20 mL/min; 3- solutions concentration: 0.55-1M ($Al(NO_3)_3x9H_2O$ and $(NH_4)_2CO_3$ respectibely) and coresponding flow rates: 12-48 mL/min; 4- solutions concentration: 1.1-2M ($Al(NO_3)_3x9H_2O$ and $(NH_4)_2CO_3$ respectibely) and coresponding flow rates: 10-20 mL/min.

The small particle and crystallite sizes determined by TEM, XRD and thermal stability analyses, respectively, made it possible to anticipate a high degree of inter-particle porosity in the NH_4-dawsonite samples which showed similar mesopores distribution as showed in previous chapters. The textural properties of the solid were determined by adsorption of nitrogen at 77 K. Less BET specific surface area was calculated (some of the trials were involved) but more analyses are needed in order to exemplify without any error the higher/lower catalytic activity of NH_4-dawsonite for the industry requirements.

Summarized micromixer's different design applied influences over time of production, textural and morphological characteristics of the precipitate are highlighted in Table 5.5.

Table 5.5: Summarized geometry and mixing process influence on time of production, yield particle size (crystallite size) formation and product purity.

Substance concentration (M)		Substance flow rate (ml/min)		Time of production at atmospheric pressure (s)				Yield (%)			Average particle (crystallite size) (nm)				TGA (weight loss %)			
Al(NO$_3$)$_3$x 9H$_2$0	*(NH$_4$)$_2$CO$_3$*	*Al(NO$_3$)$_3$x 9H$_2$0*	*(NH$_4$)$_2$CO$_3$*	*CPMM 1200/8*	*T-junction 316L SS VOD/AOD*	*CPMM-R1200/8-SO-PMMA-glued*	*Y-junction 1200 X 1200 PMMA*	*T-junction 316L SS VOD/AOD*	*CPMM-R1200/8-SO-PMMA-glued*	*Y-junction 1200 X 1200 PMMA*	*CPMM 1200/8*	*T-junction 316L SS VOD/AOD*	*CPMM-R1200/8-SO-PMMA-glued*	*Y-junction 1200 X 1200 PMMA*	*CPMM 1200/8*	*T-junction 316L SS VOD/AOD*	*CPMM-R1200/8-SO-PMMA-glued*	*Y-junction 1200 X 1200 PMMA*
1.1	2	10	20	40 (S13)	228 (T7,T8)	232 (S4_2)	499 (S4Y)	30	43	31	193 µm (13nm)	- (10)	6 (4)	2 (5.5)	61	-	66	64
0.55	1	12	48	58 (S18)	825 (T1,T2)*	480 (S3)	807 (S3Y)	15	38	58	90 µm (8nm)	2 (6)	3 (5)	3 (7)	54	62	61	61
0.22	2	20	20	109 (S24)	340 (T3,T4, T5)	1020 (S2_1)	1176 (S2Y)	52	54	65	896 µm (10nm)	- (18)	4 (5)	2 (6)	25	-	61	66
0.12	1.09	20	20	558 (S44)	2461 (T6)	1190 (S1)	1950 (S1Y)	72	47	56	- (14nm)	- (15)	4 (6)	-	-	-	55	-

Note: All values presented in the table represent the average between all trials at similar experimental parameters.

A curios dependency was discovered interpreting the data for all three approaches: T-junction stainless steel, Y-junction PMMA and PMMA split-recombine application, chosen for analyses in this section in comparison with first microsystem (***Chapter 2***) and milliliter scale precipitation results. It is obvious in Table 5.5 a strong and constant improvement in time of production by applying PMMA Y-Junction geometry for all different levels of process parameters selected. Changing the type of mixing from perfect to chaotic and microchannel design from complicated: zig-zag to very simple: straight, the time of NH$_4$-dawsonite precipitation was significantly increased. This was confirmed by process efficiency calculated for each experiment conducted in all three designed geometries. Stronger influence over particle size distribution and crystallites formation was determined in case of Y-junction PMMA application reaching 2nm particle size and better control over the crystallization process was gained. In terms of product purity all three experimental designs had beneficial influence, by increasing it, in several cases reaching close to the theoretical purity value (63% weight loss) and in some of them overcoming it, comparing with the results collected from first set-up (stainless steel CPMM 1200/8)[17] and those published at milliliter scale precipitation process[19]. This important information led us to perform a future work plan for deeper knowledge and expertise regarding PMMA-Y-junction or T-junction usage for preventing clogging within microchannels and enhancing the process performance. In that case a clear understanding of crystallization reaction mechanism would be needed in order to perform a utile numerical simulation with the aim of adjusting the optimal process parameters which fulfill the industrial and market requirements.

4. Conclusions

Experimenting different types of microchannel design in solid NH_4-dawsonite precipitation gave us valuable information regarding the solid handling at micrometer scale. Significant increase in time of production was obtained by applying the simplest microreactor in terms of channel geometry and inlets angle (i.e. Y-shaped geometry). Perfect mixing was proved to be unnecessary for solid precipitation at micrometer scale; better product is possible to be synthesized through imperfect mixing too. The Y-junction approach might be used as an alternative for minimizing the particle deposition on channel's wall implying a better control in clogging phenomenon. Constant particle size distribution was reached for all specific process parameters within Y-shaped micromixer. Similar morphology (spherical-like particles) was obtained by using all three approaches. Some exceptions (root-like shaped particles) appeared within PMMA caterpillar split-recombine micromixer at lowest concentration of aqueous solutions and equal flow rate, information that demonstrated once again that microreactor technology has also its limitations. This was sustained also by the XRD analyses showing at specified above parameters the powder contained larger amorphous area than crystalline one. A possible explanation could refer to insufficient time for crystallite growth coming from limiting reagent quantity and high reaction rate. The type of mixing provoked by different channels and inlets design had a great influence not only increasing the control over the solid particle size distribution but also enhancing significantly the purity of the finite powder comparing with conventional dawsonite and that synthesized at milliliter scale (ILDP process[19]). The thermal stability of NH_4-dawsonite experimented in this work showed similar behavior with milli-scale powder. From this point of view the milliliter scale process (ILDP) could be miniaturized at micrometer scale successfully. Considering all these lattered a stronger collaboration with chemical and mechanical scientists should be tightened in order to get deeper and deeper in understanding both the precipitation of ammonium dawsonite and its chemistry.

References

[1] Kockmann N., Kastner J., Woias P., 2008, Reactive particle precipitation in liquid microchannel flow, Chemical Engineering Journal 135S, S110-S116;

[2] Correia A., Afonso A., Cavadas A., Oliveira M. S. N., Alves M. A. and. Pinho F. T., 2009, Numerical investigation of laminar flow in symmetric and asymmetric complex T-channels for micro-mixing, III Conferência Nacional em Mecânica de Fluidos, Termodinâmica e Energia (MEFTE - BRAGANÇA 09);

[3] Mansur E. A., Yun-dong W., You-yuan D., 2008, Computational Fluid Dynamic Simulation of Liquid−Liquid Mixing in a Static Double-T-shaped Micromixer, The Chinese Journal of Process Engineering, Vol.8, No.6, Article ID: 1009−606X(2008)06−1080−05;

[4] Bothe D., Stemich C., Warnecke H. J., 2005, Mixing in a T-shaped microreactor: scales and quality of mixing, Elsevier B.V./Ltd;

[5] Liu S., Fukuyama T., Sato M., Ryu I., 2004, Continuous Microflow Synthesis of Butyl Cinnamate by a Mizoroki-Heck Reaction Using a Low-Viscosity Ionic Liquid as the Recycling Reaction Medium, Organic Process Research & Development *8*, 477-481;

[6] Nguyen N.T. and Wu Z., 2005, Micromixers—a review, J. Micromech. Microeng. 15, R1–R16; doi:10.1088/0960-1317/15/2/R01;

[7] Beebe D. J., Mensing G. A., 2002, Walker G. M., Physics and applications of microfluidics in Biology, Annu. Rev. Biomed. Eng. 4, 261-286. Downloaded from arjournals.annualreviews.org;

[8] Haverkamp V., Ehrfeld W., Gebauer K., Hessel V., Löwe H., Richter T., Wille C., 1999, The potential of micromixers for contacting of disperse liquid phases Fresenius J. Anal. Chem. 364: 617–624;

[9] Heim M., Wengeler R., Nirschl H., Kasper G., 2006, Particle deposition from aerosol flow inside a T-shaped micro-mixer, J. Micromech. Microeng. 16, 70–76;

[10] Dietrich N., Poncin S., Li H. Z., 2008, Experimental Investigation of Bubble Formation in Micro-devices, CHISA 2008, Tcheque Republique, (HAL : hal-00366044, version 1);

[11] Hwang D. K., Dendukuri D., Doyle P. S., 2008, Microfluidic-based synthesis of non-spherical magnetic hydrogel microparticles, Lab Chip, 8, 1640–1647, DOI: 10.1039/b805176c;

[12] Mansur E. A., Mingxing Y., Yundong W., Youyuan D., 2008, A State-of-the-Art Review of Mixing in Microfluidic Mixers, Chinese Journal of Chemical Engineering, 16(4) 503—516;

[13] Sepideh R., 2011, A Microfluidics Approach to Novel Polymeric Microspheres Reinforced with n-TiO2 (Spin Title: Microfluidics-Novel polymeric microspheres-n-TiO2), Thesis Sepideh Rezvani 2011, http://www.engga.uwo.ca/people/pcharpentier/docs/Thesis%20Sepideh.pdf;

[14] Smith, William F.; Hashemi, Javad (2006). *Foundations of Materials Science and Engineering* (4th ed.). McGraw-Hill. ISBN 0-07-295358-6., Source: http://en.wikipedia.org/wiki/Polymethyl_methacrylate, View date: 23.08.2011;

[15] http://www.export911.com/ref/plasApp.htm, view date: 23.08.2011;

[16] Yu J., Webster P., Leung B., Mortimer K., Wright L., Processing of PMMA for microfluidic applications, Application notes Issue № AN1012IL02, Queen's University (http://www.ekspla.com/application-notes);

[17] Dubert D. C., Garcia-Valls R. and Pérez-Ramírez J., (2010), Dawsonite production with caterpillar microreactor, Chemical Engineering Transactions, 21, 1003-1008 DOI: 10.3303/CET1021168;

[18] Hernandez M.J., Ulibarri M.A., Cornejo J., Peña M.J., Serna C.J., 1985, Thermal stability of aluminium hydroxycarbonates with monovalent cations, Thermochim. Acta 94, 257-266;

[19] Stoica G. and Pérez-Ramírez J., 2007**,** Reforming Dawsonite by Memory Effect of AACH-Derived Aluminas, Chem. Mater., Vol.1, 4783-4790;

[20] Gu Z., Xu X., Lin Z., Brunauer S., Emmett P.P., Teller E., 1938, Adsorption of gases in multimolecular layer, J. Am. Chem. Soc. 60, 309;

[21] Lippens B. C. and de Boer J. H., 1965, Studies on pore systems in catalysts: V. The *t* method, Vol.4, Issue 3, 319-323;

[22] Meier M., 2004, Crystallite size measurement using X-Ray diffraction, Department of Chemical Engineering and Materials Science, University of California,Davis:(http://chms.engineering.ucdavis.edu/students/undergraduates/labs/files/XRD-CSize1.pdf);

[23] Zhang X. and Wen Z., Gu Z., Xu X., Lin Z., 2004, Hydrothermal synthesis and thermodynamic analysis of dawsonite-type compounds, Journal of Solid State Chemistry 177, 849–855;

[24] Stoica G. and Pérez-Ramírez J., 2007, Reforming of dawsonite by memory effect of AACH-derived alumina Chem. Mater., *19*, 4783-4790;

[25] Sing K. S. W., Everett D. H., Haul R. A. W., Moscou L., Pierotti R. A., Rouquerol J., Siemieniewska T., 1985, Reporting physisorption data for gas/solid systems with special reference to the determination of surface area and porosity *Pure Appl. Chem.*, 57, 603

Chapter 5

Influence of imperfect mixing on NH_4-dawsonite particles formation within a new types of micromixers

Chapter 6

Summary and outlook

The thesis presents a new approach regarding the application of microtechnology in production of catalysts, specifically NH_4-dawsonite [$NH_4AlCO_3(OH)_2$], using microreactor´s technology starting with the milliliter scale process, In-Line Dispersion Precipitation Method, which is a co-precipitation method applied for solids production (coded ILDP) patented by Javier Pérez-Ramírez group at ICIQ in 2007. Applying the microtechnology (or microreactor technology) the precipitation process will be safer, cleaner, environmentally friendly and economically worthy. The reduced and compact setup will generate more practical utility and space economy. The transferability from laboratory scale to industrial scale for most of the conventional processes adapts the scaling-up step which is time consuming because of the recalculation of the parameters for large scale, meanwhile the microreactor based processes need the numbering-up step which keep the same optimal parameters found and no recalculation would be needed. Different micromixer geometries were experimented in order to obtain a continuous precipitation reaction: stainless steel and Poly(methyl methacrylate) (PMMA) Caterpillar Microreactor, T (stainless steel) and Y (PMMA)-junction geometry all purchased from Institut für Mikrotechnik Mainz (coded IMM). The experimental precipitation began with the ILDP process parameters modifying them during the work hence the miniaturization of the process at microscale to be accomplished.

Chapter 6

Summary and Outlook

An overview regarding microtechnology field, its industrial applications and advantages together with dawsonite type materials state of the art are outlined. In order to enhance the knowledge regarding these topics and understand better the importance of both in developing the scientific research on synthetic minerals production the concept of micromixers (microfluidic systems) is detailed in *Chapter 1*. Microfluidics explains the fluid behavior within miniaturized systems which differs from conventional flow theory due to the small length scale of the systems. The main applications of microfluidic devices are counted further: medical diagnostics, genetic sequencing, chemistry production, drug discovery and proteomics (large-scale study – particularly their structures and functions). Most of these applications were well developed on continuous fluid flow synthesis but very few information were found regarding the continuous solid synthesis at microscale. Therefore, understanding the way of handling the solid synthesis within microfluidic devices would break the limits of the industrial process evolution.

Dawsonite-type compounds are crystalline double hydroxyl carboaluminates, analogues of the mineral dawsonite, $NaAlCO_3(OH)_2$. The interest on synthetic NH_4-dawsonite material increased in recent years because of its developing industrial applications: raw material for very pure alumina (aluminum oxide - Al_2O_3) production by thermal decomposition above 1173K, trapping carbon dioxide (CO_2) if the system maintain a high CO_2 pressures and remove greenhouse gases, pollutant gas remover from emissions of coal-fired boiler systems, flame retardant, component of a dry extinguisher of in-flight engine fuel leak fires, a stabilizer for chlorine-containing polymers, an effective ingredient in antacids, a parent material for transparent spinel and YAG14 ceramics, etc.

Encountering a safer, easer and rapider way of producing this kind of material represents an important developing in all technological fields.

This thesis deals with a totally new method of synthesizing ammonium-type dawsonite which first could overcome the drawbacks of conventional processes used for NH_4-dawsonite production and on the other hand should give better quantitatively and qualitatively properties of the product. NH_4-dawsonite precipitated by microreactor technology showed higher/similar purity and thermal stability comparing to the synthetic mineral obtained by In-Line Dispersion Precipitation (ILDP) process at milliliter scale and conventional processes. Similar enhanced porous and morphological properties were found in both micro and milli-scale with the observation that less quantity of reagent was consumed in the reaction and the efficiency rose till 70%. Depending on the type of geometry used for microdevices and implicit the type of mixing exerting inside the microchannel enhanced properties for solid dawsonite type materials are determined.

NH4-dawsinte production within a Caterpillar microreactor

Co-precipitation following the ILDP method of ammonium dawsonite (NH_4-dawsonite) catalyst precursor within the channel of an IMM Caterpillar micromixer was investigated in *Chapter 2*. Aluminum nitrate nonahydrate ($Al(NO_3)_3x9H_2O$) and ammonium carbonate ($(NH_4)_2CO_3$) were used as aqueous solutions for precipitating the catalyst within a microreactor set-up proposed. Associating the reagents flow rate and their corresponding concentrations in a right manner, enables the production time to be better controlled and to give certain information about the synthetic mineral properties. The most interesting correlation between the reagents flow rates and specific concentrations was achieved by modifying substantially the ratio between each of the specified parameters *i.e.* 0.12M for aluminum solution and 2M for carbonate one hence the excess of the $(NH_4)_2CO_3$ moles to rise approximately 16 times. Modifications were made for the flow rates too by equaling the ratio between them. Experiments carried out at these parameters showed significant increase in NH_4-dawsonite time of production, i.e. (***Chapter 2***, Table 2.4). The post-process treatment by stirring at 60^0C the slurry obtained increased the rate of crystal growth within the precipitate but could not confirm that the growth process would be constant for each of the crystals formed.

Continuous synthesis of porous Ammonium Dawsonite within a new microstructured system

Similar co-precipitation process parameters were used for synthesizing NH_4-dawsonite material inside the stainless steel Caterpillar Microreactor's zig-zag channel with the difference that the whole process was conducted at 1bar of pressure. A new microsystem was proposed and presented in *Chapter 3***.** Pressure influence over limiting time of production and product characteristics was investigated. High influence of pressure on time of production was discovered increasing the time by 6 times comparing to the previous experiments (See ***Chapter 2***). A significant dependency between pressure and crystalline phase formation within the dried powder was found for specific precipitation parameters characterized by a higher ratio between flow rates (12ml/min – 48ml/min), acidic solution ($(NH_4)_2CO_3$) being in excess. Some traces of ammonium nitrate were found during the analyses which can be explained by means of insufficient mixing or extremely low value of the residence time inside the microchannel, giving the reaction no time to finish.

Pressure influence on particle size formation was also an important approach for defining less than 10nm particles within the sample obtained. Well-developed mesoporosity was presented at this specific pressure and enhanced thermal stability and weight loss was analyzed comparing to both milliliter and micro-liter scale lattered previously. The results presented here sustain the hypothesis that a microsystem under pressure could give more benefits than a batch one or/and a milli-scale, nevertheless, deeper analyses are needed, especially if the aim leads to a continuous production with a higher flexibility in the industry. Even though, a small improvement of the precipitation process was detailed the advantages of the microreactor technology, placed already the objective on a higher level of interest.

Pressure influence over ammonium dawsonite continuous precipitation at microscale

The coresponding *Chapter* deals with a specific solid application of this microtechnology in the precipitation process of ammonium dawsonite (NH_4-dawsonite) inside the similar stainless steel Caterpillar micromixer (CPMM1200/8), at constant pH (9), constant temperature (60^0C) and variable applied working pressure, within an interval started from 1bar up to 8bar. This was possible, as the flow condition within microdevices allows for lower pressure drops and higher external pressure to be applied. More specifically, the pressure influence over the continuous time of production, precipitation efficiency and product characteristics: crystal formation, purity, catalytic properties is presented.
By increasing the pressure smaller particle size and lower crystalline phase within the solid were found. This suggests that the crystallites inside the powder are small and XRD diffractograms show more broadened peaks than previous found. Better results from thermal stability and mesoporosity point of view were determined at 1 and 4bar pressure. Increased time of production and catalytic activity was calculated for lower applied pressure (1bar, 2bar). The present section demonstrates a long and deeper understanding on how the applied pressure could influence the miniaturized precipitation process. Furthermore, depending on the type o application, high control on the pressure is requested in order to increase the efficiency of the process and product quality.

Imperfect mixing influence on NH_4-dawsonite particles formation by precipitation process within new types of micromixers

This last chapter deals with similar dawsonite precipitation conditions as presented in *Chapter 2* but in this case the process was carried out in three distinct types of microchannel geometry (T-shaped stainless steel, PMMA spilt-recombine and Y-shaped PMMA approaches) and at two different mixing regimes (perfect (spli-recombine)/imperfect (T/Y-shaped microsystems.)). Channel geometry and mixing influence over precipitation and powder production was studied. Significant increase in time of production was obtained by applying the simplest type of microreactor in terms of channel geometry and inlets angle (i.e. Y-shaped geometry) proving that solid NH_4-

dawsonite can be synthesized through imperfect mixing with better results connecting with the previous split-recombine Caterpillar microcreactor. The Y-junction approach might be used as an alternative for minimizing the particle deposition on channel's wall implying a better control in clogging phenomenon. Similar or better morphological and catalytic properties were characterized for samples precipitated within the straight channel (Y-junction from PMMA). The particle size and particle size distribution were improved reaching the size of 2nm particle. From above lettered can be stated that Y-junction –based microdevice with straight channel inside could be the appropriate design for a microreactor which might solve the well known clogging at microscale processes, when dealing with solid production. Further experimental work is necessary and a stronger collaboration with chemical scientists should be tightened in order to get deeper understanding regarding precipitation of ammonium dawsonite from crystallization process point of view. It is likely that the microtechnology will reach the industry and gain more benefice from its demonstrated advantages: fast transfer of research results into production, earlier start of production at lower costs, scale-up versus numbering-up approach, smaller plant size for distributed production, lower costs for transportation, materials and energy and more flexible response to market demands.

List of publications

Journals and Books

Dubert D.C., Garcia-Valls R., Pérez-Ramírez J., 2010,
Dawsonite production with Caterpillar microreactor, Chemical Engineering Transactions, Vol.21, 1003-1008, DOI: 10.3303/CET1021168;

Dubert D.C., Pérez-Ramírez J., Garcia-Valls R., 2011,

Continuous synthesis of porous ammonium dawsonite within a new microstructured system, Chemical Engineering Transactions, vol.25, 231-236, DOI: 10.3303/CET1125039;

Dubert D. C., Pérez-Ramírez J., Garcia-Valls R., 2011

Study of pressure influence over ammonium dawsonite continuous precipitation at microscale, *in process of submission.*

Dubert D. C., Pérez-Ramírez J., Garcia-Valls R., 2011,

Influence of imperfect mixing on NH_4-dawsonite particles formation within new types of microreactors (micromixers), *in preparation*.

Dubert D. C., Epple M., Garcia-Valls R., 2012,

NH_4-dawsonite crystallization process investigated at micrometer scale, *in preparation.*

Conferences

Dubert D.C., Garcia-Valls R., Pérez-Ramírez J.,
Dawsonite production with Caterpillar microreactor,
13th Conference on Process Integration, Modelling and Optimisation for Energy Saving and Pollution Reduction, Prague, Czech Republic, **2010**
- *poster presentation* (version complete)

Dubert D. C., Pérez-Ramírez J., Garcia-Valls R.,

Study of pressure influence over ammonium dawsonite continuous precipitation at microscale,
14th International Conference on Process Integration, Modelling and Optimisation for Energy Saving and Pollution Reduction, Florence, Italy, **2011**
- *poster presentation*

Dubert D.C., Garcia-Valls R., Pérez-Ramírez J.,
Dawsonite production with Caterpillar microreactor,
8th Edition of poster exhibition of Doctoral Program in Chemical Environmental and Process Engineering, Chemical Engineering Department, Rovira I Virgili University, Spain, **2010**
- poster presentation version 1

About the author

Diana Cristina Dubert was born on 10th of November, 1981 in Turda, Cluj, Romania. After completing the highschool in 2000 at Mihai Vitezu National College in Turda, she studied Biochemical Engineering from 2000-2005 at “Babes-Bolyai” University, Chemistry and Chemical Engineering Faculty from Cluj-Napoca. After graduation in 2005, she followed the Master in Environmental Science at “Babes-Bolyai” University, Environmental Science Faculty, Cluj-Napoca, from 2005- 2006. In the same time, she joined the Research Center in Physical Chemistry, AFM and STM Microscopy with Applications in Nanoscience and Biotechnology, investigating thin films (lecithin, collagen, gold nanoparticles) construction at liquid/gas interface by using Langmuir-Blodgette Technique. In 2006 she started the doctoral program at the same Research Center in Physical Chemistry, AFM and STM Microscopy with Applications in Nanoscience and Biotechnology, at Chemistry and Chemical Engineering Faculty, “Babes-Bolyai” University from Cluj-Napoca under the supervision of Prof. Dr. Maria Tomoaia-Cotisel. The main focus of the project was related with lecithin’s thin films deposition on solid support at air/water interface by applying Langmuir-Blodgett technique. In 2007, November, she received a Gencat scholarship at Rovira I Virgili University, School of Chemical Engineering,Tarragona, Spain for a European master research project in Environmental Science with the tuition in modeling the reverse osmosis process performance. After gaining the second master title in Environmental Science, in 2008, October, she started the full doctoral program at Rovira I Virgili University, School of Chemical Engineering, Chemical Engineering Department, Tarragona, Spain under the supervision of Dr. Ricard Garcia-Valls. The objective of the thesis was to apply the microtechnology in NH_4-dawsonite precipitation with the aim of adjusting the optimal process parameters for industry scale transfer. The most important results acquired during this research are enclosed in the present thesis.

The author is thankful for financial support of this project offered by IMPULSE (Integrated Multiscale Process Units with Locally Structured Elements) European consortium inside the frame of European Commission DG Research.

This PhD period will be followed by a post doctoral research at Rovira I Virgili University in collaboration with the Inorganic Chemistry Institute from University of Duisburg-Essen, Germany focused on determination of precipitation reaction kinetics for better understanding of the process itself. Concerning this continuous producton of solid ammonium dawsonite mught be accomplished. A strong collaboration with Mechanical Department from Rovira I Virgili University will be bond in order to restrict the research on the optimal process performance.

Chapter 6

Summary and Outlook